MS in Chemical Engineering

Modification and Characterization of Poly(Ethylene Glycol) Hydrolytically Degradable Hydrogels for Stem Cell Delivery

Master's Thesis

of

Helena Isabel da Silveira Gaifem

Developed within the discipline of Dissertation

conducted in

University of Maryland, Baltimore County

UMBC Advisor: **Dr. Jennie B. Leach**

FEUP Examiner: **Prof. Maria do Carmo Pereira**

Department of Chemical Engineering

July 2010

Mestrado Integrado em Engenharia Química

Modificação e Caracterização de Hidrogeis de Poli(etileno glicol) Hidroliticamente Degradáveis para Transporte de Células Estaminais

Tese de Mestrado

de

Helena Isabel da Silveira Gaifem

Desenvolvida no âmbito da disciplina de Dissertação

realizado em

University of Maryland, Baltimore County

UMBC
AN HONORS UNIVERSITY IN MARYLAND

Orientador na UMBC: **Dr. Jennie B. Leach**

Arguente FEUP: **Prof. Maria do Carmo Pereira**

Universidade do Porto
Faculdade de Engenharia
FEUP

Departamento de Engenharia Química

Julho de 2010

Acknowledgments

The execution of this project would not have been possible without the help of the many different people working in our lab.

First, I would like to thank Dr. Jennie B. Leach for all the suggestions and comments made to this work as well as for all the insight she provided to the completion of this project.

I would like to thank the PhD student Andreia Ribeiro for all the help, training and suggestions as well as for always trying to be an active presence in this project.

I would also like to thank Silviya Zustiak, PhD, for all the insight provided about the PEG gels and the best way to handle them in order to obtain the best results as well as for the training with some of the equipment in the lab.

Another thank you goes to the undergraduates Shelby Vargo and Dalton Hughes, for all the help provided in the realization of this project and for being such good lab mates; and to the undergraduates Stephanie Pubill and Rohan Durbal for all the knowledge about the PEG gels they willingly shared with me.

Finally I would like to thank Victor Fulda for getting the orders on time and all the other Leach lab group members for being such good colleagues.

Resumo

O tratamento de lesões cerebrais e espinal medula tem provado ser uma tarefa difícil devido à sua complexidade. Actualmente, a recuperação tanto cognitiva como funcional, do sistema nervoso central, consiste na substituição de células degeneradas por novas células viáveis no local da lesão. Deste modo, engenheiros de tecidos direccionaram os seus esforços para a combinação de células, materiais e biomoléculas para criar estruturas que permitam a regeneração de lesões no tecido nervoso.

Biomateriais sintéticos são bons candidatos para o desenvolvimento de estruturas tridimensionais para cultura e transplantação de células em engenharia dos tecidos. Estruturas tridimensionais não só são ideais para fornecer um ambiente biologicamente relevante às células durante a sua cultura e implantação, como também têm um grande potencial como sistemas de transporte de moléculas bioactivas para promover a formação de tecido (Dawson *e tal*, 2007).

A organização de tecido é altamente dependente das propriedades das estruturas de suporte às células, tais como degradação e integridade mecânica, portanto estas devem ser tidas em devida consideração. Contudo, ter conhecimento das propriedades mecânicas dos materiais antes da cultura celular não é suficiente pois é importante tomar conhecimento do efeito da incorporação de células nas propriedades desses materiais. Grande parte dos estudos em engenharia dos tecidos não tem em consideração a relação entre as células e os biomateriais e assumem que as propriedades do material medidas em caracterizações iniciais são aquelas a que as células serão expostas.

Neste projecto demonstramos que assumir que as propriedades iniciais do material são aquelas a que as células irão responder é falso e que cada caso deve ser avaliado individualmente. Nós demonstramos que a incorporação de células neuronais estaminais/progenitoras alteram dramaticamente as propriedades mecânicas dos géis de poli(etileno glicol). Também modificamos géis de poli(etileno glicol) com laminina e avaliamos as propriedades mecânicas dos géis antes da cultura celular, demonstrando que a incorporação de biomoléculas também altera as propriedades dos géis.

Estes resultados contribuem com novo conhecimento no design de biomateriais em engenharia de tecidos neuronal e irão definitivamente abrir novos horizontes relativamente à compreensão das interacções entre células, matérias e biomoléculas e ao desenvolvimento de melhores estratégias para a regeneração de tecidos.

Palavras Chave: Engenharia de Tecidos, Poli(Etileno Glicol), Materiais, Géis, Laminina
Células neuronais estaminais/progenitoras, Propriedades Mecânicas

Abstract

Finding successful ways to repair nerve damage has proven to be a hard task due to the complexity of brain and spinal cord injuries. Current approaches to achieve both cognitive and functional recovery of the damaged central nervous system focus on the replacement of degenerated cells by transplanting viable new cells into the injured site. Therefore neural tissue engineers are directing their efforts into combining cells, materials and biomolecules to create improved scaffolds that can enhance the regeneration of damaged nerve tissue.

Synthetic biomaterials are attractive candidates for the development of three dimensional (3D) scaffolds for cell culture and transplantation in tissue engineering. Three-dimensional scaffolds are ideal for providing a biologically relevant environment for cells during culture and implantation and have great potential as bioactive molecule delivery systems to promote tissue formation (Dawson *et al.*, 2007).

Tissue organization is highly dependent on scaffold properties such as degradation rate and mechanical integrity, so these must be taken into careful consideration. However, accounting the mechanical properties of the scaffolds prior to cell culture is not enough because it is important to acknowledge the effect of cellular incorporation in the properties of the 3D constructs. Most studies do not take into account the relationship between cells and biomaterials and assume that the properties of the scaffold measured in the initial characterization studies are the ones cells are sensing and being exposed to.

In this project we demonstrate that assuming that the initial properties of the scaffold as the ones being sensed by the cells is incorrect and each case should be evaluated individually. We have shown that incorporating neural stem/progenitor cells (NSPCs) dramatically change the mechanical properties of poly(ethylene glycol) (PEG) hydrogels. We have also modified PEG hydrogels with laminin and evaluated their mechanical properties prior to cell culture. We have shown that the incorporation of biomolecules also change the properties of the scaffolds.

These results contribute with breakthrough knowledge in the design of biomaterials in neural tissue engineering and will definitely open new horizons toward a better understanding of the individual interactions between cells, scaffolds and biomolecules and the development of improved strategies for tissue regeneration.

Key Words: Tissue Engineering, Poly(ethylene Glycol), Scaffolds, Hydrogels, Laminin, Neural Stem/Progenitor Cells, Mechanical Properties

Index

Index i

Figure Index iv

Table Index viii

Notation and Glossary iii

1. Introduction 1

1.1. Background and Presentation of the Project 1

1.1.1. Tissue Engineering 1

1.1.2. Natural and Synthetic Materials as Scaffolds 2

1.1.2.1. Natural Materials 3

1.1.2.2. Synthetic Materials 3

1.1.3. PEG Hydrogels 4

1.1.3.1. PEG Hydrogels in Neural Tissue Engineering 4

1.1.3.2. Development of Novel Hydrolitically Degradabel PEG Hydrogels 5

1.1.4. Laminin 7

1.1.5. Neural Stem/Progenitor Cells 9

1.2. Contributions of the Work 11

1.3. Organization of the Thesis 11

2. State of the Art 13

3. Technical Description 17

3.1. Preparing PEG Hydrogels 17

3.3.1. 10 kDa PEG-VS and PEG-SH 2 3.4 kDa 19

3.3.2. 10 kDa PEG-VS and PEG-SH 1 3.4 kDa 19

3.3.3. 20 kDa PEG-VS and PEG-SH 2 3.4 kDa 20

3.4. Procedure for the Swelling Experiments 20

3.5. Procedure for the Rheological Experiments 21

3.6. Procedure for the Diffusion Experiments 22

3.7. Cell Work....23
3.7.1. Preparing PEG Hydrogels with NSPCs....23
3.7.2. Analysis of PEG-Laminin Hydrogels as NSPCs Delivery Devices....24
3.7.3. Procedure for Swelling Experiments....25
3.7.4. Procedure for Rheological Experiments....25
3.8. Statistical Analysis....26
4 Discussion of Results....27
4.1. Physical Incorporation of Laminin in PEG Hydrogels....27
4.1.1. Rheological Experiments....27
4.1.1.1. Results for Hydrogels Synthesized with PEG-SH 2 3.4 kDa....28
4.1.2. Swelling Experiments....29
4.1.2.1. Results for Hydrogels Synthesized with PEG-SH 2 3.4 kDa....29
4.1.3. Bulk Diffusion Experiments....34
4.2. Incorporation of NSPCs Within the PEG Hydrogels....38
4.2.1. Rheological Experiments....42
4.2.2. Swelling Experiments....43
5. Conclusions....45
6. Evaluation of Work Conducted....46
6.1. Accomplished Objectives....46
6.2. Other Work Conducted....47
6.3. Journal Club....48
6.4. Limitations and Future Work....48
6.5. Final Comment....49
References....50
Appendix 1 Additional Protocols....59
Appendix 2 Preparation of Solutions....62
Appendix 3 Other Work Conducted....65
Appendix 4 Additional Information....71

Appendix 5 Journal Club Presentation 76

Figure Index

Figure 1: Tissue engineering approaches (Khademhosseini *et al.*, 2006). 1

Figure 2: Ideal properties of a neural scaffold (Subramanian *et al.*, 2009). 4

Figure 3: Schematic for PEG hydrogel cross-linking reaction. (a) Four-arm PEG-VS precursor polymer solution is mixed with (b) PEG-diesterdithiol cross-linker at a VS/SH molar ratio of 1:1 to give (c) a 3D hydrogel that is formed under physiological conditions. Where n is the number of the repeat PEG unit and m the number of methylene groups in PEG-SH (Zustiak and Leach, 2010). 7

Figure 4: Overview of the macromolecular organization of the ECM (Cell Biology, 2010). 8

Figure 5: Laminin structure (Sigma -Aldrich, 2010). 8

Figure 6: Differentiation and proliferation of neural stem cells (Scott, 2006). 10

Figure 7: Representation of surgical end-to-end reconnection (Schmidt and Leach, 2003). .. 13

Figure 8: Poly(L-lactic acid) foam nerve guidance channels. Porous biodegradable poly(L-lactic acid) conduits were synthesized using a solvent casting, extrusion and particulate leaching technique. (a) Nerve guidance channels from 10 mm to 22 mm in lengt h were used to repair transected rat sciatic nerves. (b) After 4 months the conduits remained intact, supported tissue infiltration and vascularization (Schmidt and Leach, 2003, Evans *et al.*, 2000). 15

Figure 9: (a) 4 arm PEG-VS, (b) PEG-diester-dithiol cross-linker, (c) 3D hydrogel formed by mixing (a) and (b) under physiological conditions (10% w/v, VS/HS=1, meaning that the number of thiol groups should be the same as the number of vinyl sulfone groups, pH>7 and at 37ºC) (Zustiak and Leach, 2010). 17

Figure 10: Schematic representation of the reaction between the 4 arm PEG-VS, laminin and the cross-linker PEG-SH. 17

Figure 11: Placement of the hydrogels on the glass slides: (A) 50 µL hydrogels and (B) 150 µL hydrogels. 18

Figure 12: Representation of the top and bottom plates of the rheometer and the placement of the gel. 21

Figure 13: Scheme of data collection from diffusion experiments in PEG hydrogels. 22

Figure 14: Representation of the migration of NSPCs as the hydrogels degrade. 24

Figure 15: Structure of PEG-diester-dithiol where m equals the number of methylene groups in the polymer and n is the number of the repeat PEG unit. 27

Figure 16: Representation of the storage modulus, G', of gels with 0%, 1% and 10% laminin. (*) denotes significant differences between the gels ($p<0.05$). Bars represent average ± standard deviation for $n \geq 3$ samples. 28

Figure 17: Representation of the swelling ratio of gels with 0%, 1% and 10% laminin. Bars represent average ± standard deviation for $n \geq 3$ samples. 30

Figure 18: Representation of the mesh size of gels with 0%, 1% and 10% laminin. Bars represent average ± standard deviation for $n \geq 3$ samples. 32

Figure 19: Representation of: (a) the hydrogel network and (b) laminin entrapped within hydrogel network. 33

Figure 20: Mass of laminin released in solution over time in gels with ~10% v/v of Laminin. 35

Figure 21: Standard curve used to determine the concentration of laminin in the release solution at each collection. 36

Figure 22: Fractional release of laminin versus the square root of time. 36

Figure 23: Initial mesh size and mesh size at approximately 75 degradation for gels with molecular weight of 3.4 kDa and with 2 methylene groups (Zustiak and Leach, 2010). 37

Figure 24: Phase contrast micrographs and overlay with DAPI of neural progenitor cells immobilized as neurospheres in the PEG hydrogels for 15 days: (a-c) 0% laminin PEG hydrogels and (d-f) 1% laminin PEG hydrogels. Cell nucleus is labeled with DAPI and is shown in blue. Scale bars, 10 μm. 39

Figure 25: After 15 days in culture, NSPCs remain undifferentiated and maintain the progenitor capacity (nestin-positive). (a) Phase contrast and (b) fluorescent images of immunostained NSPCs inside 0% laminin-PEG hydrogels. Cell nucleus is labeled with DAPI and is shown in blue. Scale bars, 10 μm. 39

Figure 26: Differentiation of the NSPCs delivered upon gel degradation. (a-c) Phase contrast and (d-e) fluorescent micrographs. Cell nucleus is labeled with DAPI and is shown in blue. Neurons are shown in red and astrocytes are shown in green. Scale bars, 10 μm. 40

Figure 27: Percentage of differentiated NSPCs into neurons and astrocytes in the 2D laminin controls and in the laminin-coated coverslips after release from the 3D PEG-laminin constructs. Bars represent average ± standard deviation for $n \geq 3$ samples. Symbols note statistical differences ($p<0.05$) between: * the 2D controls and + the 0% laminin-PEG gels... 40

Figure 28: Representation of storage modulus of gels with 0%, 1% and 10% v/v laminin, with and without NSPCs. (*) denotes significant difference between the gels ($p<0.05$). Bars represent average ± standard deviation for $n \geq 3$ samples. 42

Figure 29: Representation of swelling ratio of gels with 0%, 1% and 10% v/v laminin with and without NSPCs (controls). (*) denotes significant difference between the gels ($p<0.05$). Bars represent average ± standard deviation for $n \geq 3$ samples. 43

Figure 30: Representation of swelling ratio of gels with 0%, 1% and 10% v/v laminin with and without NSPCs (controls). (*) denotes significant difference between the gels ($p<0.05$). Bars represent average ± standard deviation for $n \geq 3$ samples. 44

Figure 31: Molecular structure of SATP. 59

Figure 32: Step 1 – reaction of SATA with a primary amine (present in the protein) (Pierce Biotechnology, Inc., 4/2004). 60

Figure 33: Step 2 – deprotection with hydroxylamine to generate free thiol groups (Pierce Biotechnology, Inc., 4/2004). 61

Figure 34: Representation of the storage modulus, G', of gels with 0%, 1% and 10% v/v laminin. Bars represent average ± standard deviation for $n \geq 3$ samples. 65

Figure 35: Representation of the swelling ratio of gels with 0%, 1% and 10% v/v laminin. Bars represent average ± standard deviation for $n \geq 3$ samples. 66

Figure 36: Representation of the mesh size of gels with 0%, 1% and 10% v/v laminin. Bars represent average ± standard deviation for $n \geq 3$ samples. 67

Figure 37: Pictures of (a) the type of rheometer used and (b,c) placement of the hydrogel on the bottom plate of the rheometer..... 71

Figure 38: Representation of G' and G'' versus angular frequency, for gels without laminin. 72

Figure 39: Representation of G' and G'' versus angular frequency, for gels with 1% v/v of laminin. 72

Figure 40: Representation of G' and G'' versus angular frequency, for gels with 10% v/v of laminin. 73

Figure 41: Representation of G' and G'' versus angular frequency, for gels without laminin. 73

Figure 42: Representation of G' and G'' versus angular frequency, for gels with 1% v/v of laminin. 74

Figure 43: Representation of G' and G'' versus angular frequency, for gels with 10% v/v of laminin. 74

Figure 44: Representation of G' and G'' versus angular frequency, for gels without laminin. 75

Figure 45: Representation of G' and G'' versus angular frequency, for gels with 1% v/v of laminin. 75

Figure 46: Representation of G' and G'' versus angular frequency, for gels with 10% v/v of laminin. 76

Figure 47: Pictures of (a) neurospheres inside PEG hydrogels with 1% v/v laminin and (b) NSPCs leaving a neurospehere inside PEG hydrogels with 1% laminin. 76

Table Index

Table 1: Results obtained for storage modulus (stiffness). 28

Table 2: Results obtained for swelling ratio. 30

Table 3: Results obtained for mesh size. 32

Table 4: Results obtained for storage modulus for hydrogels with NSPCs. 42

Table 5: Results obtained for swelling ratio and mesh size for hydrogels with NSPCs. 43

Table 6: Results obtained for storage modulus (stiffness). 65

Table 7: Results obtained for the different types of gels regarding swelling ratio. 66

Table 8: Results obtained for the different types of gels regarding mesh size. 67

Table 9: Results obtained for absorbance at 218 nm, to determine which fraction(s) contained the protein. 68

Table 10: Results obtained for absorbance at 412 nm step, to determine which fraction(s) contained the modified protein. 68

Table 11: Results obtained for the absorbance at 218 nm step, to see which fraction(s) contained the protein. 69

Table 12: Results obtained for the absorbance at 412 nm step, to see which fraction(s) contained the modified protein. 70

Notation and Glossary

G'	Storage modulus	Pa
G''	Loss modulus	Pa
Q_m	Swelling ratio	
M_S	Mass after swelling	g
M_D	Mass after drying	g
$\overline{M}_C$	Molecular weight between crosslinks	g/mol, Da
$\overline{M}_n$	Number average molecular weight of the uncrosslinked hydrogel	g/mol, Da
V_1	Solvent molar volume	cm^3/mol
υ_2	Polymer volume fraction in equilibrium swollen hydrogel	
Q_v	Volumetric swelling ratio	
ρ_p	Density of the dry polymer	g/cm^3
ρ_s	Density of the solvent	g/cm^3
$\overline{\upsilon}$	Specific volume of the polymer	
χ_1	Polymer-solvent interaction parameter	
ξ	Mesh size	nm
$\left(\overline{r_0^2}\right)^{1/2}$	Root-mean-square end-to-end distance of the polymer chain in the unperturbed state	nm
l	Average bond length	nm
C_n	Characteristic ratio of the polymer	
n	Number of moles	mol
M_r	Polymer molecular weight	g/mol, Da
D_e	Effective diffusivity	mm^2/min
c	Concentration of the solute inside the hydrogel	µg/mL
x	Position	mm
t	Time	min
δ	Half the hydrogel thickness	mm
c_0	Initial solute concentration	µg/mL
m_i	Mass at time i	µg
m_{inf}	Mass at the end of the experiment	µg
m_i / m_{inf}	Fractional mass of solute released at time i	
c_i	Concentration of solute in the release solution at time i	µg/mL
V	Volume	mL, L
V_S	Sample volume	mL
C_{NaCl}	Molar concentration of NaCl	M
m_{NaCl}	Mass of NaCl	g
M_{NaCl}	Molecular weight of NaCl	g/mol
n_{NaCl}	Number of moles of NaCl	mol
$C_{phosphate}$	Molar concentration of phosphate	M
$n_{phosphate}$	Number of moles of phosphate	mol
m_1	Mass of $Na_2HPO_4\,H_2O$	g

m_1	Mass of KH_2PO_4	g
C_{BSA}	Molar concentration of BSA	M
ρ_{BSA}	Density of the BSA	g/L
m_{BSA}	Mass of BSA	g
C_{EDTA}	Molar concentration of EDTA	M
V_{EDTA}	Volume of EDTA	mL

List of Acronyms

BSA	Bovine Serum Albumin
CNS	Central Nervous System
DMSO	Dimethylsulfoxide
DAPI	4',6-diamidino-2-phenylindole
ECM	Extracellular Matrix
EDTA	Ethylenediaminetetraacetate
GFAP	Glial Fibrillary Acidic Protein
hESC	Human Embryonic Stem Cell
MW	Molecular Weight
NSPC	Neural Stem/Progenitor Cell
PBS	Phosphate Buffer Saline
PEG	Poly(ethylene Glycol)
PLA	Poly(lactic Acid)
PNS	Peripheral Nervous System
SATA	N-Succinimidyl S-Acetylthioacetate
SATP	N-Succinimidyl S-Acetylthiopropionate
SCI	Spinal Cord Injury
SFB	Society for Biomaterials
SH	Sulfhydril
TEA	Triethanolamine
TUJ1	Neuron-specific class III beta-tubulin
VS	Vinyl Sulfone
2D	Two-dimensional
3D	Three-dimensional

1 Introduction

1.1. Background and Presentation of the Project

1.1.1. Tissue Engineering

Tissue engineering, also known as regenerative medicine, is an interdisciplinary science that makes use of biological and engineering principles to develop tissues, with or without synthetic components, to restore, maintain or enhance tissue and organ function. Restoration of tissue and organ function has traditionally been achieved by tissue and organ donation. However this type of approach is limited by a shortage in organ and tissue donors and immune rejection by the patients. Tissue engineering is an attractive solution for these problems as it will alleviate the shortage in organ and tissue donors and potentially eradicate immune rejection (Levenberg et. al, 2009).

Tissue engineering has three general approaches (Figure 1): (a) the use of isolated cells or cell substitutes to replace lost function, (b) the use of materials that are capable of inducing tissue regeneration, and (c) the use of scaffolds made of a combination between cells and materials (Khademhosseini *et al.*, 2006).

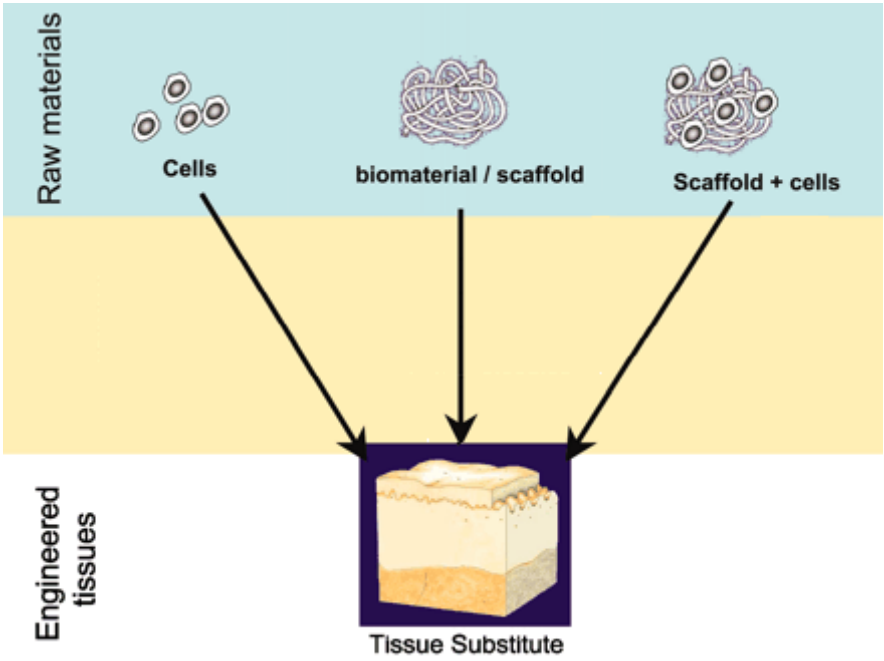

Figure 1: Tissue engineering approaches (Khademhosseini *et al.*, 2006).

To apply cells to replace lost function, the tissue can be developed inside the patient or outside the patient and then transplanted. To induce regeneration within a material, the scaffold is synthesized *in vitro* and then tested for several parameters such as toxicity and pathogenicity prior to *in vivo* testing (Khademhosseini *et al.*, 2006). In combination devices, the cells are incorporated within the scaffold, which contains biological molecules that provide cues for the cells to grow, proliferate and differentiate. Proper design of these cellular scaffolds involves not only the characterization of its mechanical properties but also analysis of cell behavior within the biomaterials. This *in vitro* characterization allows for the material optimization toward a desired cell fate, thus increasing the chances of successful tissue growth and repair *in vivo* (Ribeiro *et al.*, in prep. and Khademhosseini *et al.*, 2006).

Research in the area of neural tissue engineering has extensively used two-dimensional (2D) cell cultures and have allowed for great advances in the knowledge of cell-cell and cell-material interactions (Andressen et al., 2005, Jacques et al., 1998, Willits *et al.*, 2010). However, knowing that cells, including neural stem/progenitor cells (NSPCs), reside, proliferate and differentiate within complex 3D microenvironments *in vivo* (Namba *et al.*, 2009), neural tissue engineers are currently focusing their efforts in combining neurons, materials and biomolecules with the goal to create improved scaffolds that can enhance the regeneration of damaged nerve tissue. Thus, cell-biomaterial scaffolds have been used in neural tissue engineering applications. Three-dimensional (3D) biomaterials have been successful in improving regeneration of damaged peripheral and central nervous system (PNS and CNS) as not only they increase the survival of transplanted cells but also support the integration of neural processes (Namba et. al, 2009). Three-dimensional scaffolds are ideal for providing a biologically relevant environment for cells during culture and implantation and may also be used as bioactive molecule delivery systems during tissue formation (Dawson et. al, 2007).

1.1.2. Natural and Synthetic Materials as Scaffolds

Scaffolds provide an ideal platform for cell-cell and cell-material interactions and serve as bio-interactive structures that promote cell attachment, proliferation and organization; moreover, their geometry and properties can be engineered to suit most any human application (Dawson *et al.*, 2007). Thus, 3D scaffolds are useful culture systems as they mimic *in vivo* growth conditions more closely than monolayer cultures (Ribeiro *et al.*, in prep.).

Tissue organization is highly dependent on scaffold properties such as material degradation and mechanical integrity. These properties must be taken into careful consideration as they influence several cell responses such as adherence and differentiation. Therefore, prior to

seeding with cells, the scaffolds should be characterized. A variety of both natural and synthetic materials have been used to study the behavior of NSPCs (Dawson et. al, 2007).

1.1.2.1. Natural Materials

Natural materials, such as the components found in mammalian extracellular matrix (e.g., collagen, fibrinogen, laminin, hydroxyapatite), can be used to develop scaffolds for cell culture. Since they are obtained from nature, they have the advantage of being bioactive, biocompatible and having similar mechanical properties as native tissue. Natural biomaterials are also derived from plants, insects or animal components such as cellulose and silk fibroin, which provide a favorable microenvironment for NSPC culture (Schmidt and Leach, 2003).

Nonetheless natural materials have some disadvantages that are somewhat hard to overcome, which include limited control over physical and chemical properties, difficulty in modifying degradation rates, sterilization and purification as well as the potential for transmitting pathogens (Dawson et. al, 2007). Therefore, synthetic biomaterials are also attractive for the development of scaffolds for cell culture in tissue engineering.

1.1.2.2. Synthetic Materials

Synthetic materials are a promising alternative to natural materials as they have the advantage of being highly reproducible and controllable in terms of mechanical and chemical properties and degradation behavior. Moreover, their mechanical properties can be altered to mimic those of native tissues and allow cell and tissue ingrowth in short periods of time (Wnek and Bowlin, 2008).

Ideally, a synthetic scaffold should mimic both the physical and chemical properties of the native tissue, thus acting as a template and stimulating cell and tissue growth. Moreover, synthetic scaffolds should also be biocompatible and biodegradable. Biocompatibility will reduce adverse responses from the patient's immune system and biodegradability will permit the polymer to degrade inside the patient into nontoxic products. In addition synthetic materials should have highly interconnected porous networks with pore sizes large enough for cell migration, fluid exchange and tissue ingrowth (Jones, 2006). In the design of biomaterials for neural tissue engineering applications one also has to focus on the scaffold ability to allow for growth factor delivery and neurite outgrowth. Figure 2 presents the ideal properties of a neural scaffold.

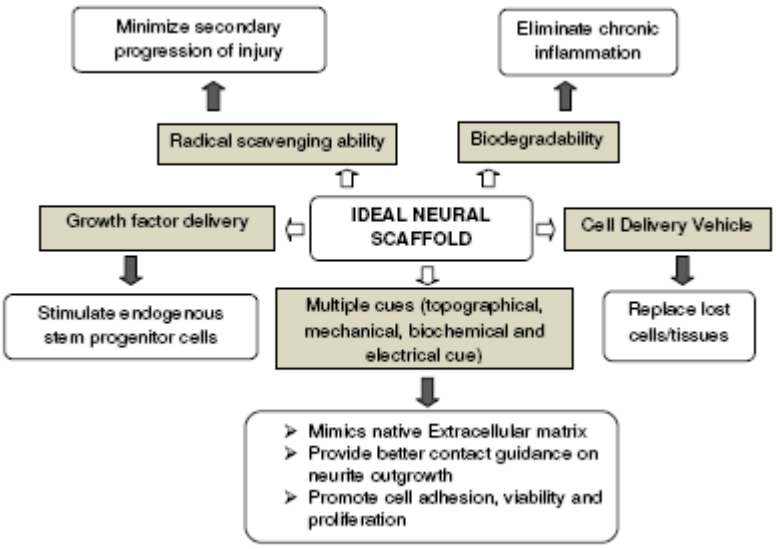

Figure 2: Ideal properties of a neural scaffold (Subramanian *et al.*, 2009).

1.1.3. PEG Hydrogels

Poly(ethylene glycol) (PEG) hydrogels have been one of the most studied synthetic materials in tissue engineering (Krsko and Libera, 2005), because PEG is an inert (adheres weakly to proteins and cells), biocompatible, nontoxic, nonimmunogenic, and water soluble polymer (Shalaby and Burg, 2004). This polymer is a neutral polyether, available in a variety of molecular weights and has been a subject of interest in the biotechnical and biomedical communities for its unique properties and for being approved by the United States Food and Drug Administration (FDA) (Harris, 1992).

1.1.3.1. PEG Hydrogels in Neural Tissue Engineering

PEG hydrogels and PEG gel solutions have been successfully used in nerve repair applications. Lore *et al.* have shown that PEG solutions can permanently reestablish functional and morphological continuity *in vivo* between severed ends of mammalian PNS and CNS axons (Lore *et al.*, 1999). PEG solutions have also been shown, by Nisbet and coworkers, to prevent nerve cells from rupturing, subsequent to administration 72 h after spinal cord injury, and prevented paralysis in three out of four animals tested (Nisbet *et al.*, 2007). Laverty *et al.* demonstrated that PEG can also anatomically and physiologically restore damaged axons in adult guinea pig spinal cord white mater (Laverty *et al.*, 2004).

PEG hydrogels have also been functionalized in order to improve them as scaffolds for neural tissue engineering. They have been functionalized with adhesive peptides, resulting in the extension of longer neurites (Mahoney and Anseth, 2006), as well as polypeptides, such as

poly-L-lysine, resulting in NSPC survival and differentiation into mature phenotypes (Hynes *et al.*, 2007). They have also been crosslinked with biodegradable peptide sequences which allowed improved cellular viability, increased cellular migration, and enhanced axon regeneration after spinal cord injury (SCI) in rats (Raeber *et al.*, 2005 and Piantino *et al.*, 2006).

Despite of these successful achievements, PEG based therapies have been shown to be effective only for small nerve injuries, therefore this type of therapy is not yet optimized for large nerve defects (Lore et al., 1999). Additionally, scaffold quality has been under-defined by their capability of promoting cell survival, proliferation and neurite extension, disregarding the effect of cell incorporation in the properties of the material. This leads to a poor understanding in how neurons interact with their extracellular environment and consequently to a delay in neuronal tissue engineering progression. Therefore we are focusing our efforts in developing an *in vitro* platform that can be used for studying specific cell-material interactions, and later on be optimized towards the delivery of neural stem/progenitor cells into injury sites.

1.1.3.2. Development of Novel Hydrolytically Degradable PEG Hydrogels

Tissue engineering efforts are now focused on the development of new biodegradable, biocompatible and nontoxic synthetic materials to use as scaffolds.

In order to create insoluble networks, PEG has to be end-functionalized with crosslinking groups. Some of the most common developed chemistries include the addition of acrylate, thiol, amine, maleimide or vinyl sulfone (VS) reactive groups (Veronese and Pasut, 2005). However, as crosslinked networks, these PEG-based hydrogels are nondegradable under physiological conditions.

In the interest of facilitating degradation of PEG-based hydrogels a few strategies have been established which make use of degradable block-copolymer components (e.g. poly(lactic acid), PLA). The copolymer PLA-*b*-PEG-*a*-PLA is a type of PEG-based hydrogel that has been successfully applied for many tissue engineering applications (Lu and Anseth, 2000, Mason et al., 2001, Lim and Park, 2000, Molina *et al.*, 2001 and Metters et al., 2000). However, some drawbacks have been associated with this material such as protein denaturation resulting from the PLA hydrophobicity, inflammation caused by acidic degradation byproducts of PLA (e.g. lactic acid and poly(acrylic acid)) (Metters et al., 1999) and the use of ultraviolet irradiation for the crosslinking reaction, which could be detrimental to cells (Bryant et al., 2000). Another hydrolytically degradable PEG-based hydrogel, that has been used for protein delivery, is multiarm PEG-amine crosslinked with an ester-containing amine (Zhao and Harris,

1998). This material is fully hydrophilic; however its application has been restricted by the fact that the amine reaction allows covalent binding of encapsulated proteins to the polymer network during crosslinking. This issue was surpassed by the use of PEG-multiacrylates and PEG-dithiols to form fully hydrophilic hydrogels with selective cross-linking chemistry (Elbert et al., 2001). Nonetheless, the crosslinking reaction can take up to one hour and this may have a negative effect on some cell types that are encapsulated prior to crosslinking. Additionally, it has been shown that when crosslinking PEG-multiacrylates with PEG-dithiols, low acrylate concentrations favored intramolecular reactions that lead to network nonideality (Metters and Hubbell, 2005).

To overcome these issues, Lutolf and Hubbell functionalized PEG with VS groups for tissue engineering applications (Hubbell and Lutolf, 2003). PEG-VS has the particularity of reacting specifically with free thiols (e.g. peptides terminated with cysteine residues) (Morpurgo et al., 1996), and considering that cysteines are rarely present on exposed surfaces of cells and proteins, this crosslinking approach allows a high degree of control over reaction specificity and rate.

Our group has therefore adapted the PEG-VS approach to yield a fully hydrophilic and inert hydrogel with rapid and highly specific crosslinking chemistry (Figure 3) (Zustiak and Leach, 2010). A new class of crosslinkers specific for PEG-VS, PEG-diester-dithiols, were synthesized and after reacting with each other these polymers formed stable, biocompatible and hydrolytically degradable PEG hydrogels under physiological conditions. These new PEG hydrogels possess tunable rates of degradation and mechanical properties, and by keeping the basic structure of the hydrogel constant but altering parameters such as molecular weight, polymer density, and distance between thiol and ester group in the crosslinker, the hydrogel properties can be controlled while maintaining crosslinking and degradation conditions that are compatible for cell and protein encapsulation. Thus this material has potential as scaffold for tissue engineering applications. Still, the influence of biomolecules on the mechanical properties of the hydrogels as well as relationships between hydrogel properties and cell responses has to be determined.

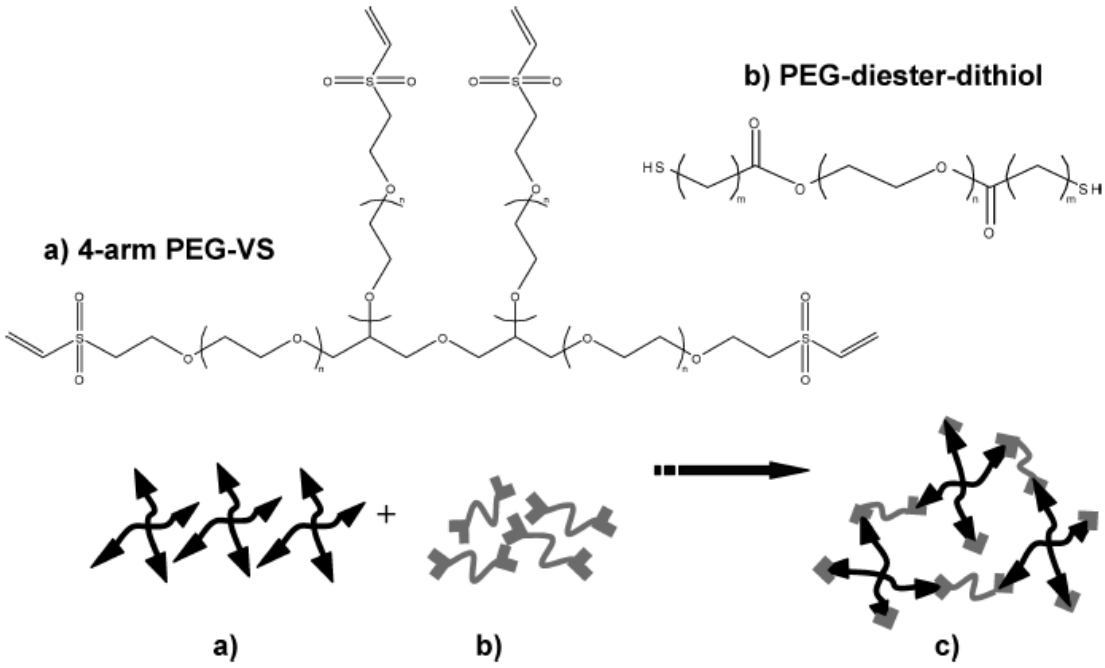

Figure 3: Schematic for PEG hydrogel cross-linking reaction. (a) Four-arm PEG-VS precursor polymer solution is mixed with (b) PEG-diesterdithiol cross-linker at a VS/SH molar ratio of 1:1 to give (c) a 3D hydrogel that is formed under physiological conditions. Where n is the number of the repeat PEG unit and m the number of methylene groups in PEG-SH (Zustiak and Leach, 2010).

1.1.4. Laminin

The extracellular matrix (ECM, Figure 4) provides structural support and a microenvironment to cells by offering cues for cellular development. The interaction between cells and the ECM is important for cell growth, proliferation and differentiation. One type of ECM is the basement membrane, which is comprised of several glycoproteins, such as collagen type IV and laminins, fibronectin and other proteins. Basement membranes are present in many stem cell niches, including skin, suggesting a key role for laminins in the regulation of stem cells (Lathia *et al.*, 2007).

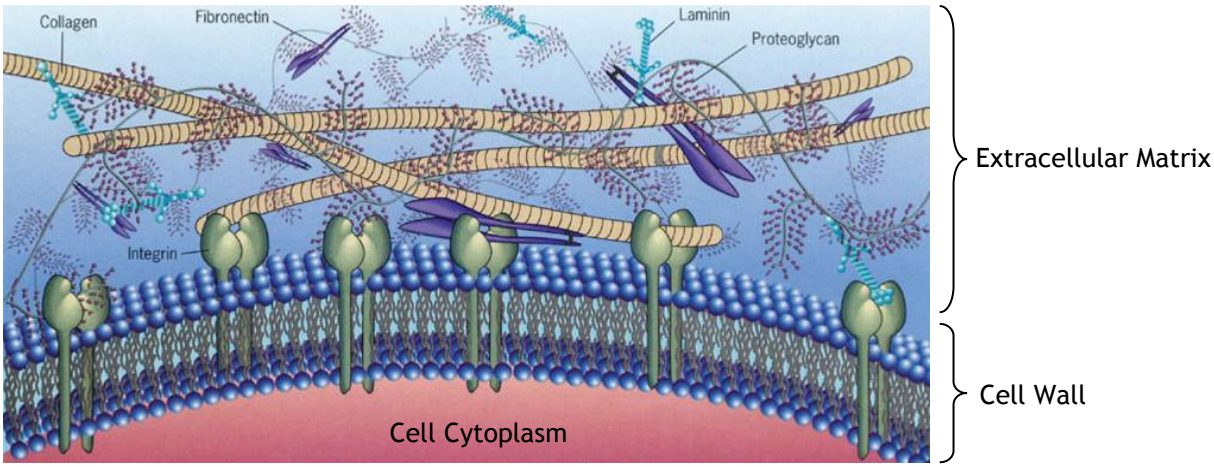

Figure 4: Overview of the macromolecular organization of the ECM (Cell Biology, 2010).

Laminins are important signaling molecules within stem cell niches, and are constituted by α, β, and γ chains. They are large proteins, ranging from 800 to 900 kDa, with a cross-like shape and with a mean arm size of 37 nm, for the identical three short arms, and 75 nm, for the longest arm (Figure 5) (Lathia *et al.*, 2007 and Rao *et al.*, 1982).

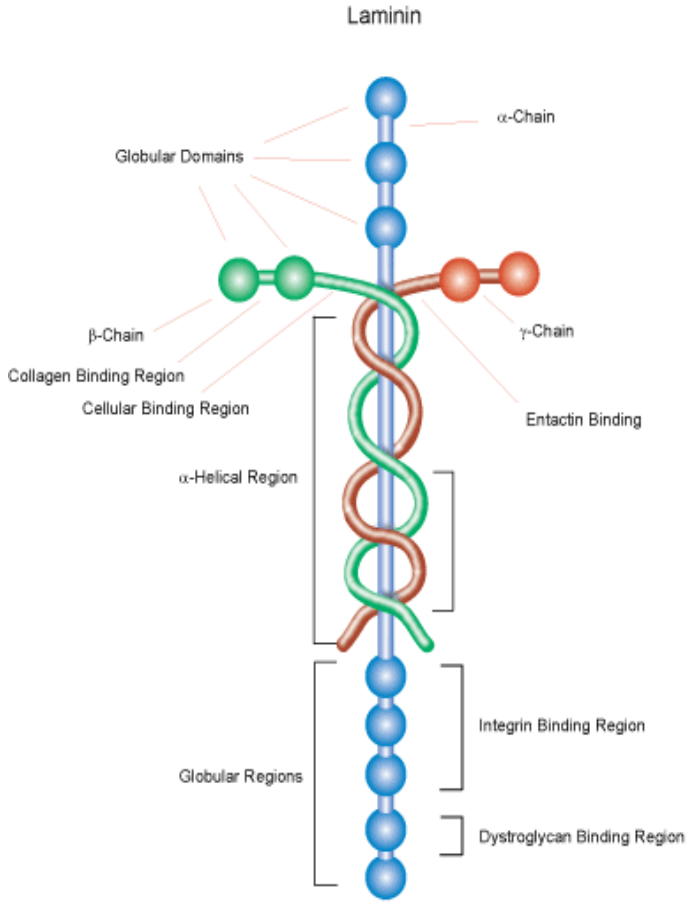

Figure 5: Laminin structure (Sigma -Aldrich, 2010).

Laminin has been shown to take part in guiding axonal outgrowth in numerous developing central and peripheral neural tissues. It has been suggested to act as an "anti-adhesive" agent promoting axon extension, since it acts by increasing growth cone motility rather than adhesion. Laminin has also been shown to be capable of initiating and sustaining neurite extension (Clark *et al.*, 1993).

Lathia and coworkers suggest that laminin/integrin signaling play an important role in the regulation of NSPCs fate. They have shown that laminin is present in the embryonic ventricular zone, the regions that give rise to the cerebral cortex, and that NSPCs express at least three classes of laminin receptors: integrins, dystroglycan and syndecans. Both $\alpha 6$ and $\beta 1$ integrin subunits (which together comprise the $\alpha 6\beta 1$ laminin receptor) are expressed at high levels on NSPC cell bodies within the ventricular zone at all embryonic stages examined. This suggests that laminin/integrin interactions could regulate the migration, survival and differentiation of NSPCs (Lathia *et al.*, 2007). Tavaloki and coworkers have demonstrated that laminin is a key ECM molecule that enhances neural progenitor generation, expansion and differentiation into neurons from human embryonic stem cells (hESCs). They performed tests with other components besides laminin (poly-D-lysine, fibronectin, collagen and matrigel), and verified that hESC-derived neural progenitor expansion, migration and differentiation into neurons were significantly greater on laminin than on other substrates. They have also shown that laminin/ $\alpha 6\beta 1$integrin signaling plays an important role in the directed differentiation of hESCs (Tavaloki *et al.*, 2008).

Laminin has therefore been shown to play an important role in regulating NSPC behavior suggesting the incorporation of this molecule in engineered scaffolds as a step forward in the design of biomaterials for neural tissue engineering applications.

1.1.5. Neural Stem/Progenitor Cells

Neural stem/progenitor cells have been subject of intensive investigation due to their potential therapeutic use in neurodegenerative disorders. They pose as a promising type of treatment, transplantation therapy, for incurable diseases such as Parkinson's disease (Andersson *et al.*, 2006) and spinal cord injury (Zigova *et al.*, 2003). NSPCs are multipotent cells capable of self renewal through cell division (proliferation), and differentiate into neurons and two types of glial cells, astrocytes and oligodendrocytes (Figure 6).

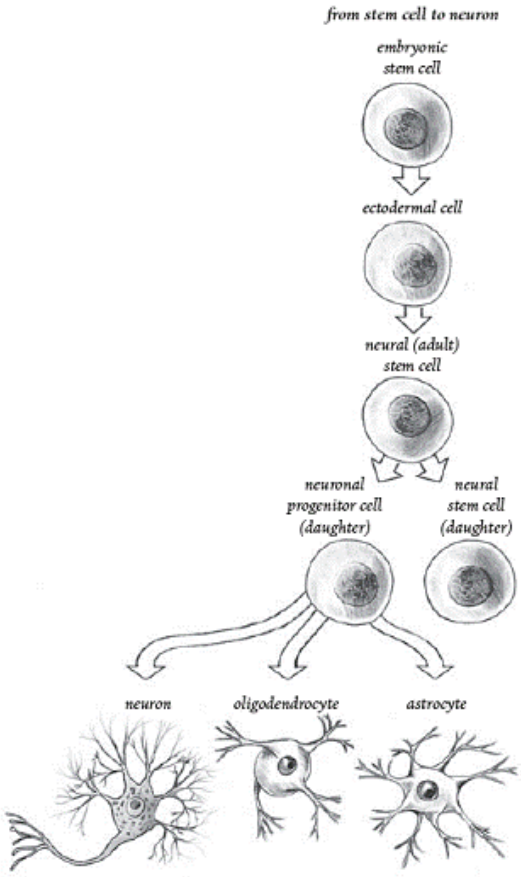

Figure 6: Differentiation and proliferation of neural stem cells (Scott, 2006).

NSPCs can be isolated from various regions of the CNS, including embryonic and adult spinal cord. In addition they have been isolated from rodent brain, spinal cord, skeletal muscle and bone marrow. They have been used in various applications, such as therapeutic platforms for tumor-targeted drug delivery (Zao *et al.*, 2008 and Aboody *et al.*, 2008) and as transplantation models for Parkinson's disease (Svendsen *et al.*, 1997) and SCI (Iwanami *et al.*, 2005 and Nakamura *et al.*, 2005).

Studies have shown that NSPCs when implanted in severed rat spinal cord have survived, and differentiated into neurons, astrocytes and oligodendrocytes, and were associated with improved functional recovery (Schmidt and Leach, 2003). University of California-Irvine scientists have shown that NSPCs are able to rescue memory in mice with advanced Alzheimer's disease (Blurton-Jones *et al.*, 2009). They are also among the first to demonstrate that NSPCs may be able to restore memory after brain damage (Yamasaki *et al.*, 2007).

NSPCs have also been proven to be valuable in tissue engineering efforts to repair brain and spinal cord injuries, due to their ability to generate neurons and glial cells. However, successful neurotransplantation currently faces limitations such as short term survival of

NSPCs, tumor formation and failure to integrate with host tissue (Kulbatski *et al.*, 2005 and Lepore *et al.*, 2006). To overcome these challenges, NSPCs have been combined with polymer scaffolds to generate functional neural and glial constructs that mimic mammalian brain or spinal cord structure, making them useful as nerve tissue replacements for brain or spinal cord injury (Ma *et al.*, 2004, Martinez-Ramos *et al.*, 2008 and Ma *et al.*, 2008).

Further studies in neural stem/progenitor cells biology combined with improved engineered NSPC scaffolds will certainly present rewards in the near future, including the development of more effective therapies for neurological disorders.

1.2. Contributions of the Work

Modified PEG hydrogels were synthesized. Hydrolytically degradable PEG hydrogels were physically incorporated with laminin and their mechanical properties determined. Through these studies we confirmed that the mechanical properties of these hydrogels are influenced by the addition of biomolecules, as significant differences were observed when compared with plain gels. Therefore, we have demonstrated that our PEG hydrogels are highly tunable and offer the opportunity of modifying both biological and mechanical properties, either by the incorporation of biomolecules or by altering the degradable crosslinker.

Neural stem/progenitor cells were incorporated within the modified PEG hydrogels. The behavior of NSPCs within the gels was observed. We observed that NSPCs cultured within the 3D environments tested in this study differentiated more into neurons than the cells that were initially cultured on top of the 2D laminin controls. Hence, we have shown that our novel hydrolytically degradable PEG hydrogels are promising as transplantable materials as they have potential to be customized and used as carriers of NSPCs into injury sites.

1.3. Organization of Thesis

This thesis is organized in several sections.

In the first section an introduction to the project is presented. Tissue engineering, 3D scaffolding and NSPCs are introduced as well as important aspects related to laminin. As these subjects are described the importance, interest and purpose of the work conducted is also presented.

The following section is the State of the Art, where all the advances in 3D scaffolding and cell culturing are presented.

The next section is the technical description of the work conducted. Here all the methods and protocols used are described in detail, including the preparation of the PEG hydrogels incorporated with laminin, the procedures to determine their mechanical properties and the incorporation of NSPCs within the hydrogels. The procedures to determine the properties of the hydrogels incorporated with NSPCs are also presented in detail.

Following is the Results and Discussion section, which is one of the most important sections of this thesis, as it is where the results obtained from the experiments conducted are presented and discussed.

The main conclusions of this project are then presented in the next section, followed by a general evaluation of the work conducted which includes a commentary on the objectives accomplished as well as some suggestions for future work to be performed under the field of this project.

In the appendixes additional information can be found. In these last sections the procedures to prepare the solutions used throughout the work are presented, as well as additional information related to the experiments conducted. There is also a section where other work conducted during the time of this project is described (having been introduced in the section of Evaluation of Work Conducted) and another section, being this the last one, that contains de presentation showed in the Journal Club held in our group meetings (being this also introduced in the section of Evaluation of Work Conducted).

2 State of the Art

Brain and spinal cord injuries are very hard to repair as they are very complex and the CNS has little capacity for self-repair.

Current clinical approaches to repair peripheral nerves include direct end-to-end reconnection of the damaged nerve ends (Figure 7) or the use of a nerve graft derived from a different location in the body of the patient. Direct end-to-end reconnection is used to repair small defects. However, when large defects are to be repaired this approach is not desired as any interference could inhibit nerve regeneration. Thus, a nerve autograph, which is tissue collected from another site of the body, poses as a good choice for large nerve repair. However, this technique may lead to loss of function and the need for multiple surgeries. There are now some FDA approved devices for small defects repair, including Integra Neurosciences Type I collagen tube (NeuraGen Nerve Guide) and SaluMedica's SaluBridge Nerve Cuff (Schmidt and Leach, 2003).

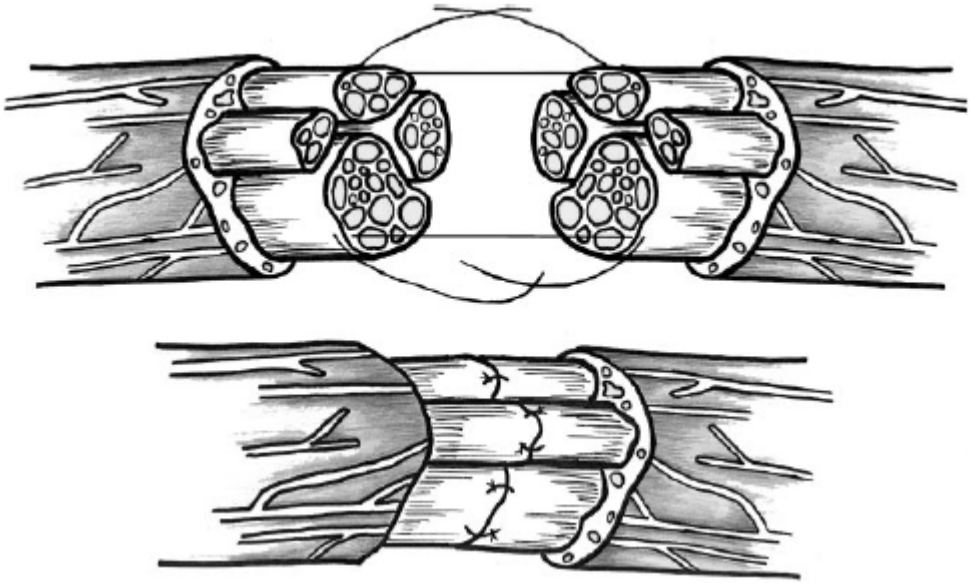

Figure 7: Representation of surgical end-to-end reconnection (Schmidt and Leach, 2003).

Therefore efforts in neural tissue engineering are directed toward the development of new strategies for nerve repair, which consists in combining NSPCs with 3D constructs for cell transplantation.

Currently a variety of both natural and synthetic scaffolds have been tested for NSPC behavior.

Natural materials, such as purified ECM proteins, have been extensively studied for their potential capability to serve as scaffolds for tissue regeneration. These materials have been shown to have influence over axonal development and repair (Rutishauser, 1993, Grimpe and Silver, 2002). Also, other constituents of the ECM can modulate neural activity and neurite extensions. Therefore some of these ECM materials have been used in nerve repair applications.

Silicone tubes filled with laminin, fibronectin, and collagen improved regeneration over a 10 mm rat sciatic nerve gap (compared to silicone controls) (Chen *et al.*, 2000). Oriented strands of fibronectin were used to bridge 10 mm nerve defects in rats (Whitworth *et al.*, 1995) and collagen filaments were used to guide regenerating axons across 20-30 mm defects in rats (Yoshii and Oka, 2001, Yoshii *et al.*, 2002). Studies have shown that oriented fibers of collagen, aligned with magnetic fields, constitute an improved template for neurite extension over randomly oriented collagen fibers (Ceballos *et al.*, 1999, Dubey *et al.*, 1999). Neural stem progenitor cells dissociated from embryonic cortical and subcortical regions were cultured in 3D collagen gels and retained their ability to proliferate and differentiate into neurons, astrocytes and oligodendrocytes (Ma *et al.*, 2004). Fibrin scaffolds have been studied to promote differentiation of neural progenitor cells into neurons and oligodendrocytes (Willerth *et al.*, 2006 and Willerth *et al.*, 2007). Agarose and alginate have also been used as natural scaffolds for neural tissue engineering studies, showing that these promote cell growth and proliferation as well (Ando *et al.*, 2007, Moriyatsu *et al.*, 2006, Prang *et al.*, 2006, Ashton *et al.*, 2007).

However, these results involve either the study of the behavior of cells within the scaffolds or the successful repair of small nerve defects. The interaction between the scaffolds and cells has yet to be evaluated and the capability of these scaffolds for regeneration of large tissue defects has yet to be improved. Additionally, these materials have disadvantages that are somewhat hard to overcome, including limited control over physical and chemical properties, difficulty in modifying degradation rates, sterilization and purification as well as the potential for transmitting pathogens (Dawson et. al, 2007).

Synthetic materials have also been studied for tissue engineering applications, as alternatives to natural material constructs. Poly(esters) such as poly(glycolic acid), poly(lactic acid) and poly(lactic-co-glycolic acid) were among the first synthetic materials to be studied due to their availability, ease of processing, biodegradation characteristics and approval by FDA (Schmidt and Leach, 2003). These materials continue to be studied and have also been processed into foams to repair transected rat sciatic nerves, a model used to study peripheral nerve regeneration (Figure 8). Materials like biodegradable poly(urethane) (Soldani *et al.*, 1998), poly(organo phosphazene) (Nicoli *et al.*, 2000), methacrylate-based hydrogels (Dalton

et al., 2002), and poly(3-hydroxybutyrate) (Young *et al.*, 2002) have capability for guiding regeneration.

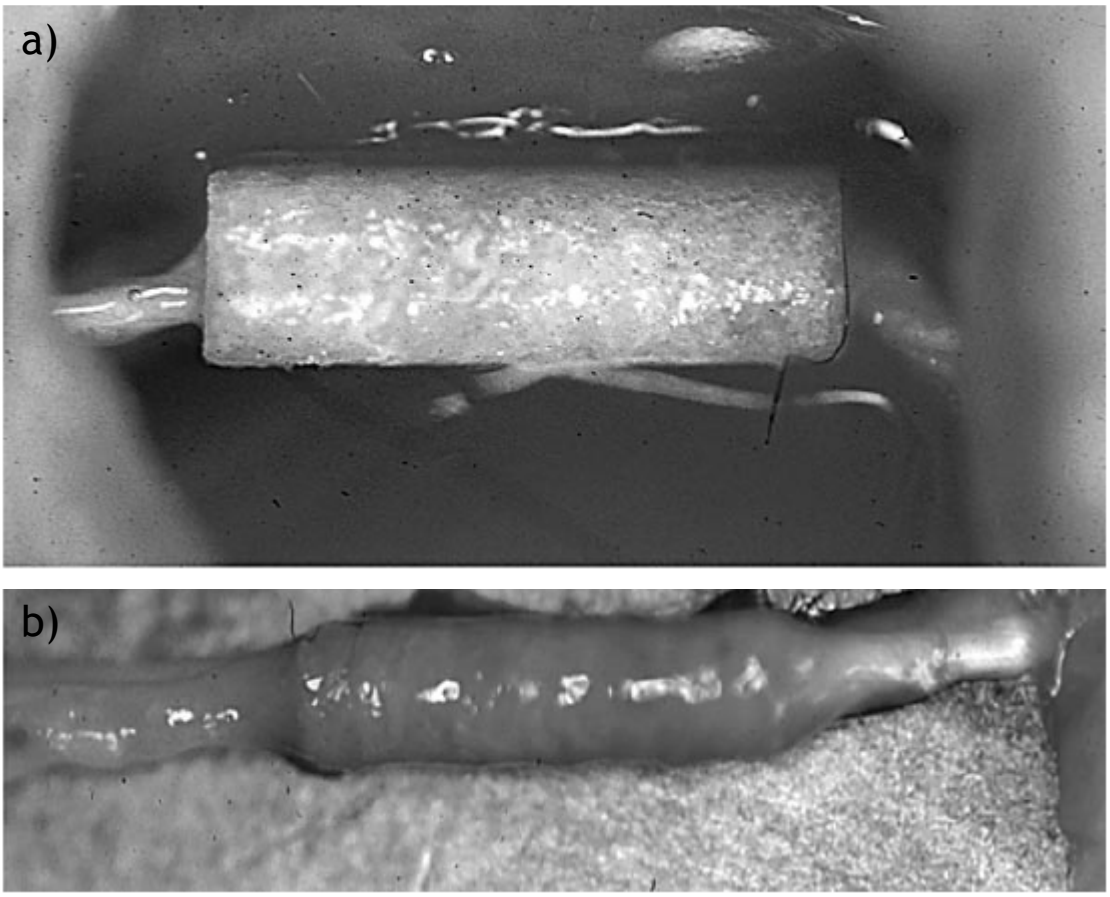

Figure 8: Poly(L-lactic acid) foam nerve guidance channels. Porous biodegradable poly(L-lactic acid) conduits were synthesized using a solvent casting, extrusion and particulate leaching technique. (a) Nerve guidance channels from 10 mm to 22 mm in lengt h were used to repair transected rat sciatic nerves. (b) After 4 months the conduits remained intact, supported tissue infiltration and vascularization (Schmidt and Leach, 2003, Evans *et al.*, 2000).

Biodegradable glass tubes have also been studied for tissue regeneration, but without satisfying results (Gilchrist *et al.*, 1998, Lenihan *et al.*, 1998). Nondegradable synthetic materials, such as silicone tubing (Dahlin and Lundborg, 2001), have also been studied for nerve repair applications. For silicone in particular, there is some insight in how this material is appropriate for nerve regeneration, as it has been studied since the 1960s. It is known that this material is able to bridge short gaps, however, it is also well known that impermeable, inert guidance channels, do not support regeneration of defects larger than 10 mm (in rats) without the presence of exogenous growth factors. Thus the development of nondegradable

scaffolds for tissue damage repair has not been very active amoung neural tissue engineering research (Schmidt and Leach, 2010).

Some other types of synthetic biodegradable materials that have been studied for neural tissue engineering applications have been described in previous sections. These have faced similar limitations as the materials described above.

In summary NSPCs have been successfully combined with various polymer scaffolds to generate 3D constructs for neural tissue repair. However, these scaffolds are only fit to repair small nerve defects. Thus there is still a great deal of work to be done in order to improve these scaffolds to repair large nerve injuries. Additionally, scaffold quality has been under-defined by capability of promoting cell survival, proliferation and neurite extension, disregarding cell-material interactions which regulate cell behavior.

Therefore this project focused in the development of an *in vitro* platform that was used for studying specific cell-material interactions, and later on be optimized towards the delivery of neuronal cells into injury sites.

3 Technical Description

3.1. Preparing PEG Hydrogels

The hydrogels were formed by a Michael-type addition of PEG-SH degradable crosslinker onto four-arm PEG-VS (Figure 3). Both polymer precursors were synthesized in-house by Silviya Zustiak, PhD, according to previously published methods (Zustiak and Leach, 2010). The reaction between the PEG-VS and the PEG-SH (cross-linker) is presented in Figure 9.

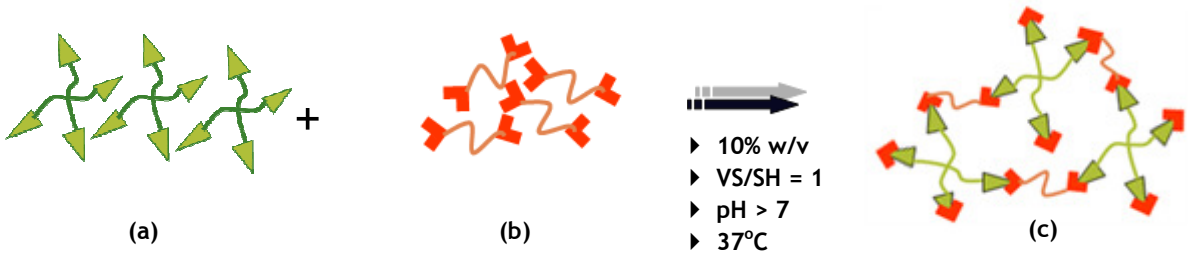

Figure 9: (a) 4 arm PEG-VS, (b) PEG-diester-dithiol cross-linker, (c) 3D hydrogel formed by mixing (a) and (b) under physiological conditions (10% w/v, VS/HS=1, meaning that the number of thiol groups should be the same as the number of vinyl sulfone groups, pH>7 and at 37°C) (Zustiak and Leach, 2010).

Furthermore, the gels were functionalized through physical incorporation of laminin (from Engelbreth-Holm-Swarm murine sarcoma basement membrane, Sigma-Aldrich, St. Louis, MO) (Figure 10) and negative controls consisted of hydrogels without laminin.

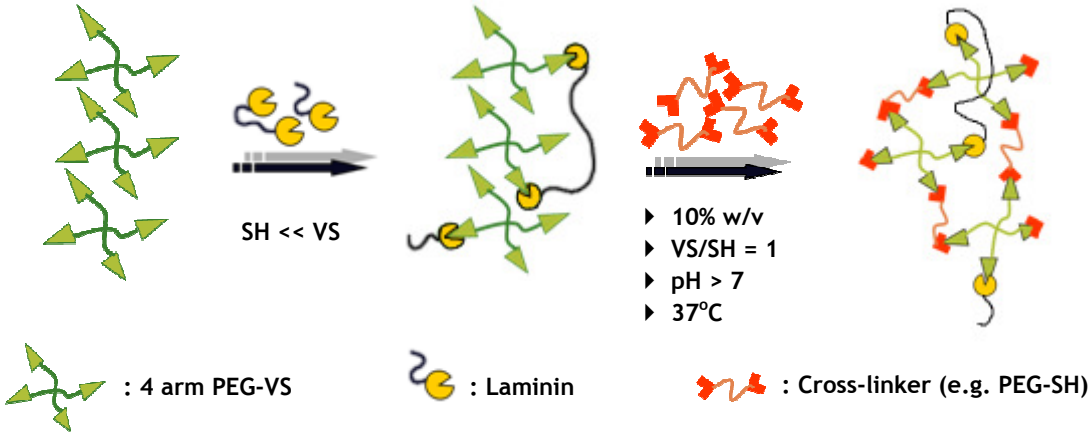

Figure 10: Schematic representation of the reaction between the 4 arm PEG-VS, laminin and the cross-linker PEG-SH.

PEG-dithioglycolate (PEG-diester-dithiol with one methylene between the ester and thiol groups) and PEG-dithiopropionate (PEG-SH with two methylenes between the ester and the thiol groups) with molecular weight 3.4 kDa (Figure 3) was used in this study as the degradable crosslinker and throughout the text will be referred to as PEG-SH 1 3.4 kDa and PEG-SH 2 3.4 kDa, respectively. Each polymer precursor was dissolved in a 0.3 M triethanolamine (TEA) solution of pH 8. To minimize weighing error, aliquots of 20% w/v PEG-VS in 0.3 M TEA were prepared in advance and stored at 4 °C until use. Laminin was added to the PEG-VS solution to achieve a final concentration of 1 and 10% v/v. The solution with PEG-SH was then added to give a final ratio of VS:SH of 1:1 for all hydrogel compositions. (Lutolf and Hubbell, 2003) Immediately after mixing, the solution was quickly vortexed and then transferred to the center of a glass slide that was treated with RainX (Sopus Products, Houston, TX) to provide a hydrophobic surface. Silicone spacers (1 mm thick cut from CoverWell perfusion chambers, Grace Bio-Laboratories, Bend, OR) were placed at the ends of the glass slide, and a second hydrophobic slide was placed on top. The two slides were clamped together over the spacers with binder clips (Figure 11) and then placed in plastic petri plates with humidified paper and transferred to an incubator and allowed to gel at 37 °C. Gelation occurred in several minutes, but the hydrogels were left in the incubator for 45 min to 1.5 hours to achieve maximum cross-linking. A >90% conversion of reactive groups was assumed for all hydrogel types (Elbert *et al.*, 2001, Metters and Hubbell, 2005, Lutolf and Hubbell, 2003).

The following sections present procedures to prepare each type of gel: 10 kDa PEG-VS and PEG-SH 2 3.4 kDa; 10 kDa PEG-VS and PEG-SH 1 3.4 kDa; and 20 kDa PEG-VS and PEG-SH 1 3.4 kDa.

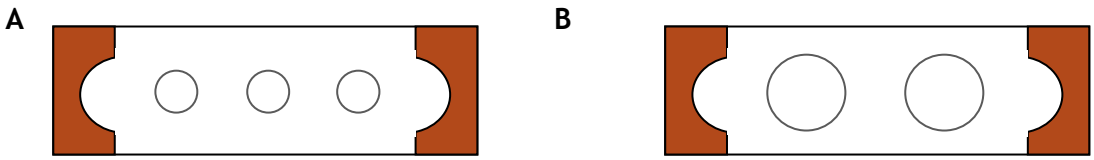

Figure 11: Placement of the hydrogels on the glass slides: (A) 50 µL hydrogels and (B) 150 µL hydrogels.

3.1.1. 10 kDa PEG-VS and PEG-SH 2 3.4 kDa

1 - Prepare an aliquot of PEG-VS: total volume of 500 µL, 20% w/v

100 mg of PEG-VS + 500 µL of 0.3 M triethanolamine pH 8.0, vortex contents.

Store at 4°C when not in use.

2 - For 100 µL of gel:

30 µL of PEG-VS

4 mg of PEG-SH – purge with nitrogen after use

70 µL TEA, pH=8.0

When using ligands, such as laminin, split the total volume of TEA between the ligand and TEA, for instance: 2 µL of ligand + 68 µL of TEA.

Note: PEG-SH must be mixed with TEA before mixing with PEG-VS and, the ligand must be added to the solution before mixing PEG-SH with TEA.

The hydrogels were prepared with 0%, 1% and 10% v/v of laminin. The gels were crosslinked, under an incubator at 37 ºC, for 45 min for the swelling experiments, 1 hour for the diffusion experiments and for 1.5 hours for the rheology experiments. The difference in crosslinking time is due to the difference in size between the gels (i.e., larger samples take longer to crosslink completely).

3.1.2. 10 kDa PEG-VS and PEG-SH 1 3.4 kDa

Gels containing PEG-SH 1 3.4 kDa crosslinker were synthesized using the methods described above. Our group previously determined that PEG-SH 1 3.4 kDa gels degrade much faster than PEG-SH 2 3.4 kDa gels (Zustiak and Leach, 2010). To account for this effect, PEG-SH 1 3.4 kDa gels were crosslinked for 25 minutes (rather than 45 min described above), which was determined to be sufficient for the gel size used in both the swelling experiments and the rheology experiments.

3.1.3. 20 kDa PEG-VS and PEG-SH 2 3.4 kDa

1 - Prepare an aliquot of PEG-VS: total volume of 500 µL, 20% w/v

100 mg of PEG-VS + 500 µL of 0.3 M triethanolamine pH 8.0, vortex contents.

Store at 4°C when not in use.

2 - For 100 µL of gel:

37.5 µL of PEG-VS

2.5 mg of PEG-SH –purge with nitrogen after use

62.5 µL TEA, pH=8.0

When using ligands, such as laminin, split the total volume of TEA between the ligand and TEA, for instance: 2 µL of ligand + 60.5 µL of TEA.

Note: PEG-SH must be mixed with TEA before mixing with PEG-VS and, the ligand must be added to the solution before mixing PEG-SH with TEA.

The hydrogels were prepared with 0%, 1% and 10% v/v of laminin. The gels were crosslinked, under an incubator at 37 ºC, for 45 min for the swelling experiments, 1 hour for the diffusion experiments and for 1.5 hours for the rheology experiments. The difference in crosslinking time is due to the difference in size between the gels (i.e., larger samples take longer to crosslink completely).

3.2. Procedure for the Swelling Experiments

Sample hydrogels of 50 µL were prepared, using PEG-VS 10 kDa, with each assay consisting of a group of three types of hydrogels (n=3): without laminin, with 1% and 10% v/v of laminin.

After crosslinking the hydrogels, prepared with PEG-SH 2 3.4 kDa, were incubated in a PBS 10 mM solution pH 7.4, at 37 ºC and were allowed to swell for 24 hours (the hydrogels prepared with PEG-SH 1 3.4 kDa were incubated 1 hour). The hydrogels were then removed and their mass after swelling was determined. The amount of time that was given for the hydrogels to swell was based on previous studies conducted in our group (Zustiak and Leach, 2010) and on their consistency after swelling. Then the hydrogels were placed in the oven at 80 ºC to dry for 24 hours and then weighed to determine their mass after drying.

3.3. Procedure for the Rheological Experiments

The hydrogels used in the rheology experiments were prepared using PEG-VS 10 kDa to yield gels with a total volume of 150 μL each; thus, after swelling, the hydrogels had a final diameter of approximately 20 mm. The diameter of 20 mm matches the diameter of the rheometer's top plate and guaranteed that the plate completely touched the gel while the experiment was being performed. In Figure 12 is a representation of the top and bottom plates of the rheometer (the bottom plate is bigger than the one represented). Pictures of the type of rheometer used and placement of the hydrogels can be found in Appendix 3.

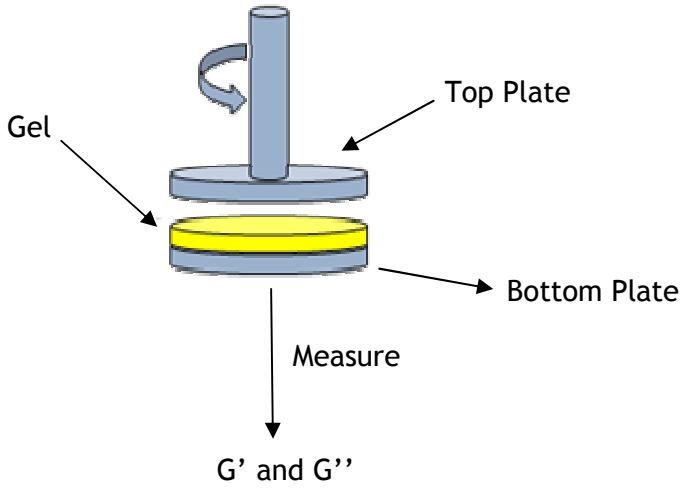

Figure 12: Representation of the top and bottom plates of the rheometer and the placement of the gel.

Each assay consisted of a group of three types of hydrogels (n=3 samples per condition): 1) without laminin, 2) with 1% v/v of laminin and 3) with 10% v/v of laminin.

The samples were allowed to swell as described in point 3.2, carefully blotted of excess water, and placed on the bottom plate of the rheometer. Then the storage modulus, G', and the loss modulus, G'', were measured for each hydrogel with an AR 2000ex rheometer (TA Instruments) in parallel plate geometry. The parameters used for measuring G' and G'' were as follows: 0.2 N of normal force, 22 ºC, angular frequency of 0.1 to 10 rad/s and 2% strain (Zustiak and Leach, 2010).

3.4. Procedure for the Diffusion Experiment

Samples with a total volume of 100 μL each were assembled. The hydrogels were prepared by incorporating laminin, with a final concentration of approximately 0.13% w/v (i.e. 0.129 mg in 100 μL of gel), in the gels solution with PEG-VS 10 kDa. For this experiment we needed a laminin solution with higher concentration than the one used in the swelling and rheological experiments in order to be within the range of the protein quantification assay. Otherwise we are not able to quantify the amount of protein diffused in solution. Since we were not able to find concentrated solutions of pure laminin we used a protein that would have both a molecular weight and size similar to that of laminin. Thus we used a solution of laminin-entactin with a concentration of 14.2 mg/mL, since it had both characteristics required (BD Biosciences, 2010).

After crosslinking the hydrogels were placed in 15 mL tubes, filled with 8 mL of 10 mM phosphate buffer saline (PBS) solution pH 7.4, and mixed end-over-end at 37 ºC. In each assay, two samples were tested. Fractions of 1 mL were collected during an 8 hour period: 4 points every 15 minutes (during a period of one hour), 4 points every 30 minutes (during the following two hours), and 5 points every hour (during the time remaining). Additional samples were taken after 13, 24 and 26 hours and after 4, 5 and 6 days (the last point corresponds to the time the hydrogels took to degrade). Each fraction collected contained a total volume of 1 mL, which was immediately replaced by the same volume of fresh PBS solution, and was later analyzed with Bio-Rad Protein Assay, following the manufacturer's microassay procedure (Bio-Rad Laboratories, Life Science Group, USA). Figure 13 represents a diagram of the diffusion experiment.

A standard curve was also determined, with solutions with concentrations of 8, 12, 16, 22 and 30 μg/mL of laminin, so that the concentration of diffused protein could be determined.

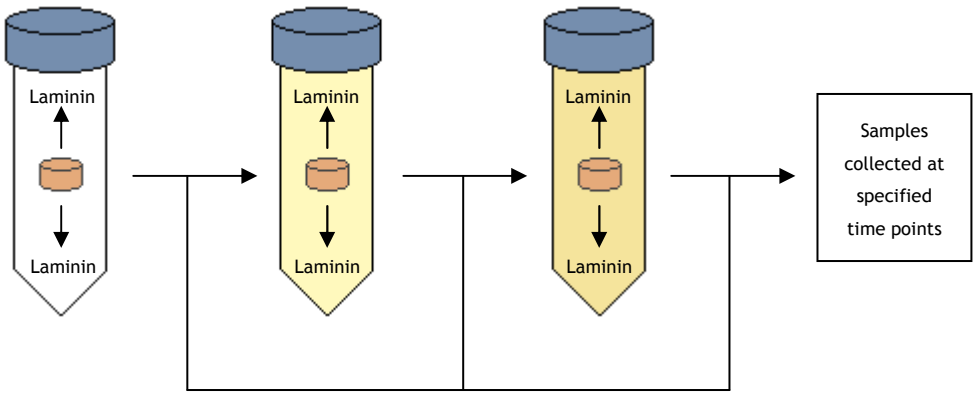

Figure 13: Scheme of data collection from diffusion experiments in PEG hydrogels.

3.5. Cell Work

3.5.1. Preparing PEG Hydrogels with NSPCs

The cells were incorporated within the hydrogels prepared with PEG-VS 10 kDa and PEG-SH 2 3.4 kDa prior to gelation. The hydrogels were prepared as described before, but this time in a sterile environment. Solutions were sterile-filtered with a 0.2 μm pore size filter before use. PEG-SH 2 3.4 kDa was UV-sterilized for 30 minutes immediately before use. The NSPCs where processed and provided by Andreia Ribeiro, one of the graduate students in our group. The procedure and quantities required to make the hydrogels are as follows:

1 - Prepare an aliquot of PEG-VS: total volume of 500 μL, 20% w/v

100 mg of PEG-VS + 500 μL of 0.3 M triethanolamine pH 8.0, vortex contents.

Filter the solution under the hood and store at 4°C when not in use.

2 - For 100 μL of gel:

30 μL of PEG-VS

4 mg of PEG-SH – left under UV light for 30 min immediately before the experiment. – purge with nitrogen after use.

42 μL TEA, pH=8.0 – filtered before usage and stored at 4 ºC when not in use.

28 μL NSPCs – from a solution prepared immediately before the experiment at a concentration of 350-500 neurospheres/ml (7-10 neurospheres per 20 μl gel).

When using ligands, such as laminin, split the total volume of TEA between the ligand and TEA, for instance: 1 μL of ligand + 41 μL of TEA. The laminin was also filtered before usage and stored at -20 ºC when not in use.

Note: PEG-SH must be mixed with TEA before mixing with PEG-VS and, the cells and ligand must be added to the solution before mixing PEG-SH with TEA and before mixing PEG-VS with PEG-SH.

The hydrogels were prepared with 0%, 1% and 10% v/v of laminin. The hydrogels were crosslinked, in a humidified incubator at 37 ºC for 45 min for the swelling experiments and for 1.5 hours for the rheology experiments. The difference in crosslinking time is due to the difference in size between the hydrogels (i.e., larger samples take longer to crosslink completely).

3.5.2. Analysis of PEG-Laminin Hydrogels as NSPCs Delivery Devices

To test the potential of the PEG-laminin hydrogels to serve as NSPCs delivery devices, NSPCs were encapsulated in PEG hydrogels with 0% and 1% v/v of laminin, prepared on top of laminin coated coverslips. As the hydrogels degraded over time, the cells were released into the surroundings and viable NSPCs attached to the laminin coated coverslips available under the gels and continued to differentiate accordingly (Figure 14). The procedure to prepare the hydrogels is described in point 3.7.1. Samples of 20 µL of hydrogel per laminin-coated coverslip were prepared (with one coverslip per well of a 12-well plate) and incubated for 30-45 min to allow complete gelation. After crosslinking the gels were covered with 2 ml of differentiation media. 2D controls were prepared by seeding cells directly into the laminin-coated coverslips. The medium was changed every 2 days of culture. All samples were incubated and then analyzed for differentiation markers.

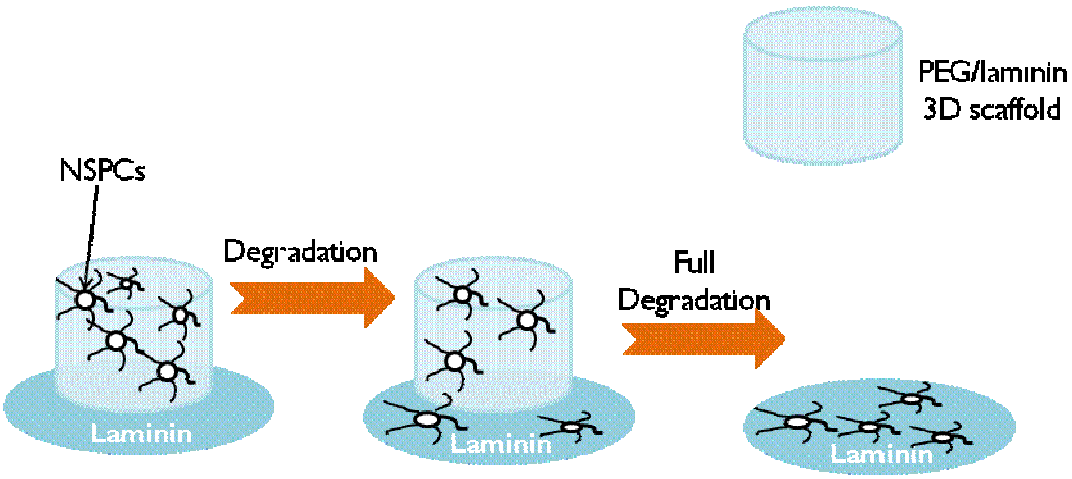

Figure 14: Representation of the migration of NSPCs as the hydrogels degrade.

3.5.3. Procedure for Swelling Experiments

Sample hydrogels of 50 μL were prepared, using PEG-VS 10 kDa and PEG-SH 2 3.4 kDa, with each trial consisting of a group of three types of gels (n=3): 0%, 1% and 10% v/v of laminin.

After crosslinking, the hydrogels were incubated in differentiation media (culture medium that promotes cellular differentiation over proliferation; prepared and provided by Andreia Ribeiro), under a sterile incubator at 37 ºC and were allowed to swell for 24 hours. The gels were then removed and their mass after swelling was determined. The amount of time that was given for the gels to swell matched the time given in previous studies conducted with gels without NSPCs (see point 3.4). Then the hydrogels were placed in the oven at 80 ºC to dry for 24 hours and then weighed to determine their mass after drying.

3.5.4. Procedure for Rheological Experiments

The hydrogels used in the rheology experiments were prepared using PEG-VS 10 kDa and PEG-SH 2 3.4 kDa to yield gels with a total volume of 150 μL each; thus, after swelling, the gels had a final diameter of approximately 20 mm (see point 3.3).

Each trial consisted of a group of three types of gels (n=3 samples per condition): 1) without laminin, 2) with 1% v/v of laminin and 3) with 10% v/v of laminin (from 1 mg/ml laminin stock from Sigma Aldrich).

The samples were allowed to swell as described in point 3.5.3, carefully blotted of excess water, and placed on the bottom plate of the rheometer. Then the storage modulus, G', and the loss modulus, G'', were determined for each hydrogel. The parameters used for measuring G' and G'' were as follows: 0.2 N of normal force, 22 ºC, angular frequency of 0.1 to 10 rad/s and 2% strain (Zustiak and Leach, 2010).

3.6. Statistical Analysis

Comparisons between two samples were performed with the two-tailed Student's t-test.

Comparisons between multiple samples can be made by following one of the two types of tests available: parametric or nonparametric. The choice of either one or the other is based on the assumption that the data either follows a Gaussian distribution, parametric tests, or not, nonparametric tests. This observation is easier when large samples are to be compared, as it is easier to determine whether a population has a Gaussian distribution or not. When small samples are to be compared it is difficult to determine if the data follows a Gaussian distribution and makes it harder to choose between the two types of tests (Motulsky, 1995).

Therefore, for the analysis of the data collected in this work, as we have small samples, both parametric and nonparametric tests were performed, in order to strengthen the results obtained from the analysis. The One-way ANOVA (parametric) and the Kruskal-Wallis (nonparametric) tests, with a Bonferroni contrast, were chosen as we had three unmatched groups to compare (Motulsky, 1995). Both tests led to the same conclusion on the statistical difference between the samples tested. For simplicity of graphical representation, the results from the One-way Anova were chosen over the ones from Kruskal-Wallis. The samples were considered statistically different when $p<0.05$ for a 95% confidence test.

4 Discussion of Results

4.1. Physical Incorporation of Laminin in PEG Hydrogels

4.1.1. Rheological Experiments

This experiment allowed us to evaluate the influence of laminin incorporation on the stiffness of the gels.

This experiment was conducted with laminin physically crosslinked within the gels. To evaluate how laminin would influence the stiffness of the gels, the storage modulus, G', was determined. A greater storage modulus indicates higher stiffness. The procedure is described in point 3.3. Gels with two different concentrations of laminin were prepared, in addition to the regular gels, to determine the effect of laminin concentration on hydrogel properties, in this case, hydrogel stiffness.

These experiments were conducted for gels with two different types of crosslinkers, PEG-SH 2 3.4 kDa and PEG-SH 1 3.4 kDa, which have the same molecular weight but different amounts of methylene groups. PEG-SH 2 3.4 kDa has 2 methylene groups and PEG-SH 1 3.4 kDa has 1 methylene group (Figure 15).

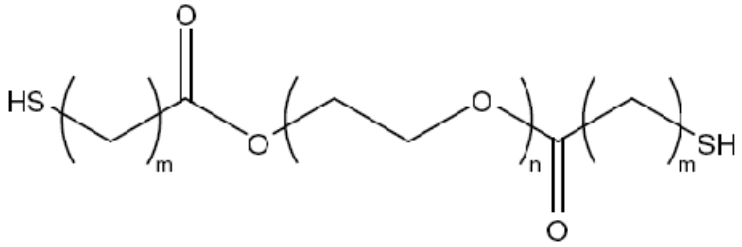

Figure 15: Structure of PEG-diester-dithiol where m equals the number of methylene groups in the polymer and n is the number of the repeat PEG unit.

Following are presented the results obtained for the hydrogels synthesized with PEG-SH 2 3.4 kDa. The results obtained for the hydrogels synthesized with PEG-SH 1 3.4 kDa are presented in Appendix 3.

4.1.1.1. Results for Hydrogels Synthesized with PEG-SH 2 3.4 kDa

This section describes the results obtained for the rheology experiments for gels synthesized with 4-arm PEG-VS 10 kDa and PEG-SH 2 3.4 kDa, with and without physically incorporated laminin. Figure 16 and Table 1 present the mean storage modulus of each of the three types of gels (0%, 1% and 10% v/v of laminin).

Appendix 4 presents a comparison of storage and loss modulus that shows that G''< G' which is indicative that all the samples were gels (Zustiak and Leach, 2010).

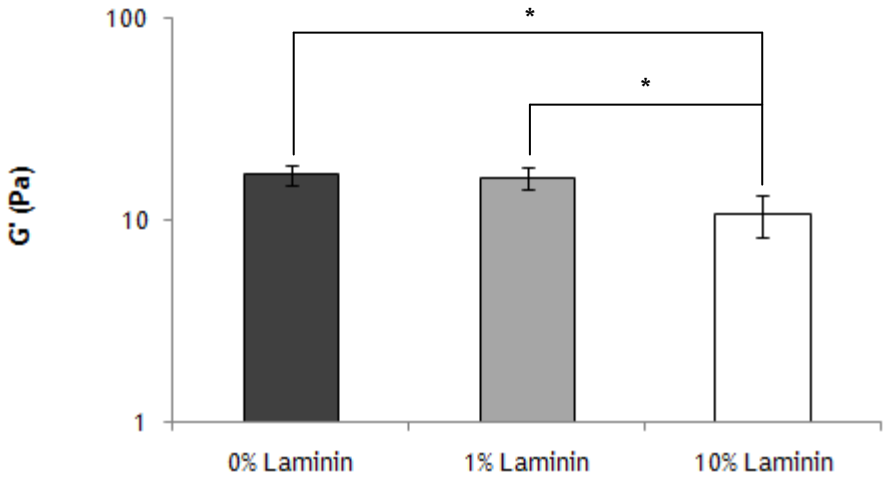

Figure 16: Representation of the storage modulus, G', of gels with 0%, 1% and 10% laminin. (*) denotes significant differences between the gels ($p<0.05$). Bars represent average ± standard deviation for $n \geq 3$ samples.

Table 1: Results obtained for storage modulus (stiffness).

Laminin Concentration	0% v/v Laminin	1% v/v Laminin	10% v/v Laminin
G' (Pa)	16.7 ± 1.7	16.2 ± 2.1	10.7 ± 2.5

Hydrogel stiffness is decreased with increased laminin concentration. Significant differences were observed between gels without laminin and 10% v/v of laminin, and between gels with 1% v/v of laminin and 10% v/v laminin. This means that incorporating higher concentrations of laminin affects the stiffness of the gels, which can be explained by the fact that the presence of laminin decreases the crosslinking density, that is a measure of the fraction of monomer units of the hydrogel that are crosslinked. This result suggests that laminin may be blocking the reactive sites of the PEG-VS backbone, decreasing the chemical bonds between VS and SH

moieties responsible for the formation of the gels, therefore the degree of crosslinking decreases thus decreasing the stiffness of the gels.

4.1.2. Swelling Experiments

The main objective of the swelling experiment was to estimate structural parameters such as mesh size. Hydrogel swelling is a function of network structure, degree of cross-linking and polymer hydrophilicity.

Similar to the rheological experiments, the swelling experiments were conducted with laminin physically crosslinked within the gels. To evaluate how laminin would influence the mesh size of the gels, the swelling ratio, Q_m, was determined, based on the mass of the gels after swelling, M_S, and their mass after drying, M_D, by the following equation:

$$Q_m = \frac{M_S}{M_D} \quad (1)$$

The procedure is described in point 3.2. Hydrogels with two different concentrations of laminin were also prepared, in addition to the regular gels, to determine the effect of its concentration on the swelling properties of the gels.

These experiments were also conducted for hydrogels with two different types of crosslinkers, PEG-SH 2 3.4 kDa and PEG-SH 1 3.4 kDa.

Following are presented the results obtained for the hydrogels synthesized with PEG-SH 2 3.4 kDa. The results obtained for the hydrogels synthesized with PEG-SH 1 3.4 kDa are presented in Appendix 3.

4.1.2.1. Results for Hydrogels Synthesized with PEG-SH 2 3.4 kDa

This section describes the results obtained for the swelling experiments for gels synthesized with 4-arm PEG-VS 10 kDa and PEG-SH 2 3.4 kDa and physically incorporated laminin. Swelling ratio and mesh size are evaluated for gels with and without laminin.

Figure 17 and Table 2 present the mean swelling ratio of the three gel types (0%, 1% and 10% v/v of laminin).

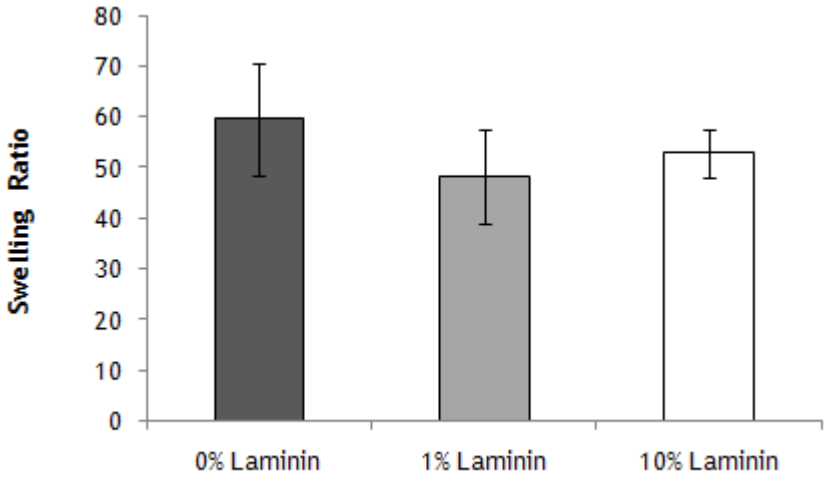

Figure 17: Representation of the swelling ratio of gels with 0%, 1% and 10% laminin. Bars represent average ± standard deviation for n ≥ 3 samples.

Table 2: Results obtained for swelling ratio.

Laminin Concentration	0% v/v Laminin	1% v/v Laminin	10% v/v Laminin
Q_m	59.6 ± 11.1	48.1 ± 9.4	52.8 ± 4.7

By analyzing Figure 17 it can be concluded that the incorporation of laminin within the gels does not affect the swelling properties of the materials, as no significant differences were observed between the different studied conditions ($p>0.05$).

Once the swelling ratio of each gel was known, the mesh size could be determined using Flory-Rehner calculations (Lu and Anseth, 2000). The molecular weight between crosslinks, $\overline{M_C}$, was calculated by Equation 2:

$$\frac{1}{\overline{M_C}} = \frac{2}{\overline{M_n}} - \frac{\frac{\bar{v}}{V_1}\left(ln(1-v_2) + v_2 + \chi_1 v_2^2\right)}{v_2^{1/3} - \frac{v_2}{2}} \qquad (2)$$

where $\overline{M_n}$ is the number-average molecular weight of the un-crosslinked hydrogel (the molecular weight (MW) of the polymer = MW PEG-VS + MW PEG-SH), V_1 is the molar volume

of the solvent (18 cm^3/mol for water), v_2 is the polymer volume fraction in equilibrium swollen hydrogel, which is equal to the reciprocal of Q_V, which is given by:

$$Q_V = 1 + \frac{\rho_s}{\rho_p}(Q_m - 1) \tag{3}$$

where ρ_p is the density of the dry polymer (1.12 g/cm^3 (Lutolf and Hubbell, 2003)) and ρ_s is the density of the solvent (1 g/cm^3 for water). From equation 2, $\bar{v}$ is the specific volume of the polymer (ρ_s / ρ_p), and χ_1 is the polymer-solvent interaction parameter (0.426 for PEG-water (Lu and Anseth, 2000 and Leach *et al.*, 2003), and assumed constant for our work because χ_1 has been found to be nearly independent of PEG v_2 for values of v_2 between 0.04-0.2 (Merrill *et al.*, 1993)).

The mesh size can then be determined as described by Equation 4 (Canal and Peppas, 1989):

$$\xi = v_2^{-1/3}\left(\overline{r_0^2}\right)^{1/2} \tag{4}$$

where $\left(\overline{r_0^2}\right)^{1/2}$ is the root-mean-square end-to-end distance of the polymer chain in the unperturbed state, and may be determined by the following equation:

$$\left(\overline{r_0^2}\right)^{1/2} = l\, C_n^{1/2}\, n^{1/2} \tag{5}$$

where l is the average bond length (0.146 nm (Cruise *et al.*, 1998 and Mellot *et al.*, 2001)), C_n is the characteristic ratio of the polymer (typically 4.0 for PEG (Merrill *et al.*, 1993 and Mellot *et al.*, 2001)), and n is the number of bonds in the crosslinks (Raeber *et al.*, 2005):

$$n = 2\frac{\overline{M}_C}{M_r} \tag{6}$$

where M_r is the molecular weight of the repeat unit (44 for PEG (Zustiak and Leach, 2010)).

These calculations relate an experimentally-determined parameter, Q_m, to a theoretical parameter, ξ, that provides insight into the hydrogel structure. Notably, because ξ is in $Q_V = \frac{1}{v_2}$ and by equations 3 and 4, $Q_m \propto \frac{1}{\xi}$.

Figure 18 and Table 3 present the mean mesh size for the gels without laminin and the gels with 1% and 10% v/v of laminin.

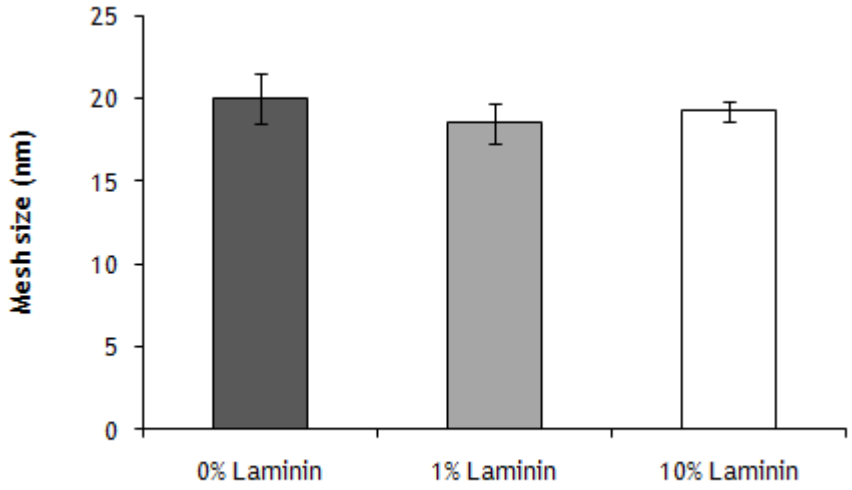

Figure 18: Representation of the mesh size of gels with 0%, 1% and 10% laminin. Bars represent average ± standard deviation for n ≥ 3 samples.

Table 3: Results obtained for mesh size.

Laminin Concentration	0% v/v Laminin	1% v/v Laminin	10% v/v Laminin
ξ, nm (average)	20.0 ± 1.5	18.5 ± 1.2	19.2 ± 0.6

As expected, from the results obtained from the swelling ratio, there are no significant differences in the mesh sizes obtained for each gel.

As mentioned in point 1.1.4, of the Introduction section, laminin is a cross-like shaped heavy protein (MW 800-900 kDa). The three identical short arms have a mean size of 37 nm, while the longest arm has a size of 75 nm (Lathia *et al.*, 2007, Rao *et al.*, 1982), so as mentioned in point 5.1 we would expect laminin to be physically entangled within the hydrogel network that is characterized by a mesh size of approximately 20 nm as shown in Figure 17 and Table 3. As a result we anticipated that the presence of laminin within the gels would have a high impact on the mechanical properties of the gels.

Through rheological measurements we concluded that the incorporation of laminin at high concentrations decreased the stiffness of the hydrogels (Figure 15 and Table 1). However, the physical crosslinking of laminin did not affect the swelling capacity of the PEG hydrogels as concluded from the results presented in Figure 16 and Table 2. As mentioned at the

rheological experiments section, both results could be explained by the fact that laminin may have occupied crosslinking sites between the VS and SH groups, reducing crosslinking density. However, the overall degree of crosslinking was not affected, as laminin may be compensating for the lack of entanglements, and the gel network remained equally packed (Figure 19). Therefore there is no measurable increase in the molecular weight between crosslinks and as a result the mesh size of the gels and their hydrophilicity are kept constant for the laminin concentrations evaluated in this study.

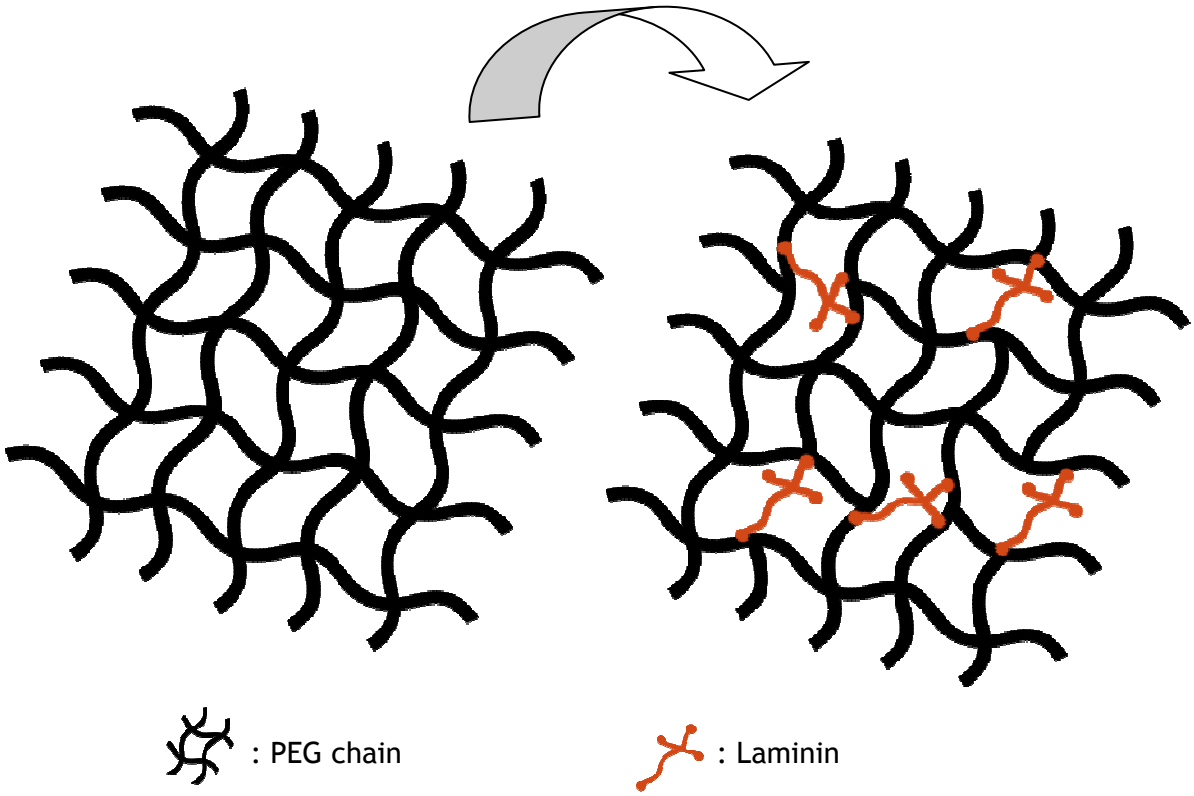

Figure 19: Representation of: (a) the hydrogel network and (b) laminin entrapped within hydrogel network.

4.1.3. Diffusion Experiments

The purpose of this experiment was to determine if laminin was being released from the hydrogels. To evaluate the diffusion of laminin throughout the gels, the effective diffusivity, D_e, was determined.

The procedure for this experiment is described in point 3.4. To analyze the data collected it was assumed that the buffer environment of the gels was a perfect sink (Park, 1997). Therefore, the concentration of solute outside the hydrogel was negligible and diffusion was the driving force for solute transport. The gels were mixed end-and-over to ensure that the concentration of solute on the surface of the gels was negligible. It was also assumed insignificant radial diffusion due to gel slab geometry (Ritger *et al.*, 1987 and Peppas *et al.*, 1987).

The PEG gels were assumed to be homogenous systems and therefore effective diffusivity, D_e, could be described by Fick's Second Law of Diffusion (Equation 7), as the diffusion process occurs in a transient regime translating the amount of laminin dissolved in PBS solution over time:

$$\frac{\partial c}{\partial t} = D_e \frac{\partial^2 c}{\partial x^2} \tag{7}$$

with the following initial condition:

$$-\delta < x < \delta, t = 0 \quad \Rightarrow \quad C = C_0 \tag{8}$$

and the following boundary conditions:

$$\begin{aligned} x = \pm \delta \,,\ t \geq 0 \quad &\Rightarrow \quad C = 0 \\ x = 0 \,,\ t \geq 0 \quad &\Rightarrow \quad \frac{\partial C}{\partial t} = 0 \end{aligned} \tag{9}$$

where c is the concentration of the solute inside the hydrogel, x and t are position and time of release, δ is half of the hydrogel thickness (1 mm gels for this study) and c_0 is the initial solute concentration inside the hydrogel. For short release times ($m_i / m_{inf} < 0.6$) Equation 7 can be solved to give:

$$\frac{m_i}{m_{inf}} = 2\left[\frac{D_e\, t}{\delta^2}\right]^{1/2}\left[\frac{1}{\sqrt{\pi}} + 2\sum_{n=1}^{\infty}(-1)^n\ i\,erfc\,\frac{n\,\delta}{\sqrt{D_e\, t}}\right] \tag{10}$$

where m_i is the mass of solute released at time i, m_{inf} is the mass of solute released at the end of the experiment and m_i / m_{inf} is the fractional mass of solute released at time i (Leach and Schmidt, 2005). Equation 10 can be further reduced by using only the first term (n=1) of the summation series:

$$\frac{m_i}{m_{inf}} = 2\left[\frac{D_e\, t}{\pi\ \delta^2}\right]^{1/2} \tag{11}$$

Since m_i / m_{inf} is directly proportional to $t^{1/2}$, a plot can be used to determine D_e. To calculate m_i, a mass balance was performed:

$$m_i = c_i\, V + \sum c_{i-1}\, V_S \tag{12}$$

where C_i is the concentration of solute in the release solution at time i, V is the total volume of the release solution (8 mL) and V_S is the sample volume (1 mL).

Figure 20 depicts representative results of the mass of solute in the release solution versus time.

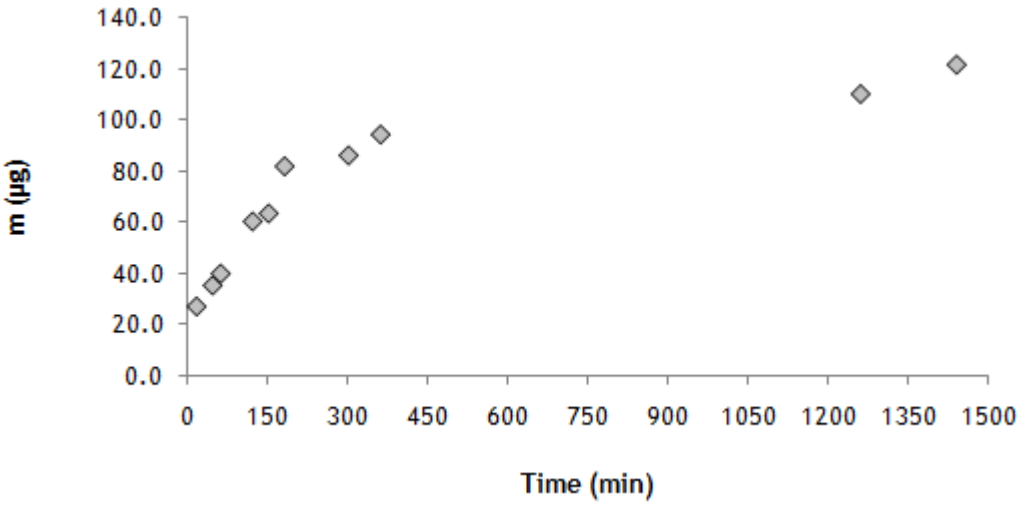

Figure 20: Mass of laminin released in solution over time in gels with ~10% v/v of Laminin.

By observing Figure 20, it can be seen that the concentration of solute in the release solution increased exponentially up to 6 hours (360 minutes) and then stabilized in the total mass of laminin initially added to the system (129 µg). As described in point 3.4, a standard curve was determined (Figure 21).

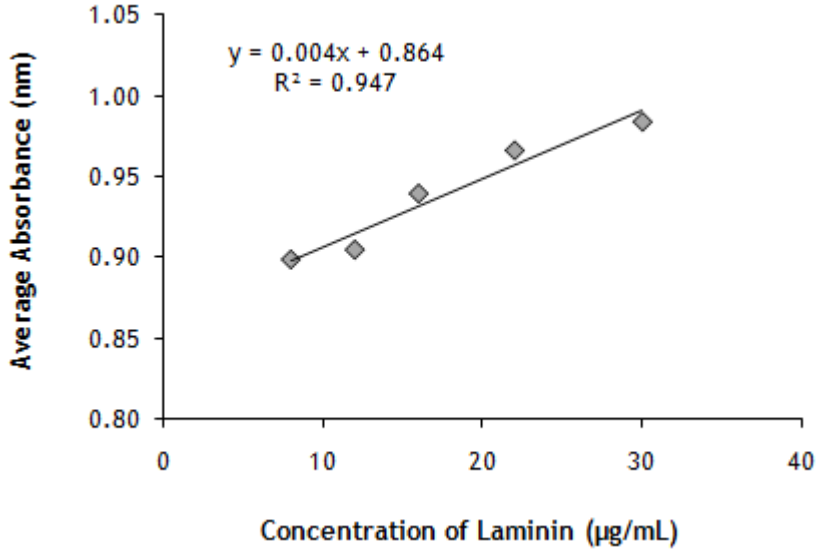

Figure 21: Standard curve used to determine the concentration of laminin in the release solution at each collection.

Using the data shown in Figures 20 and 21, Figure 22 depicts the mass fraction in the release solution versus time, which was then applied in Equation 11 to determine D_e to be 2.2 x 10^{-4} mm^2/min (3.7 x 10^{-6} mm^2/s).

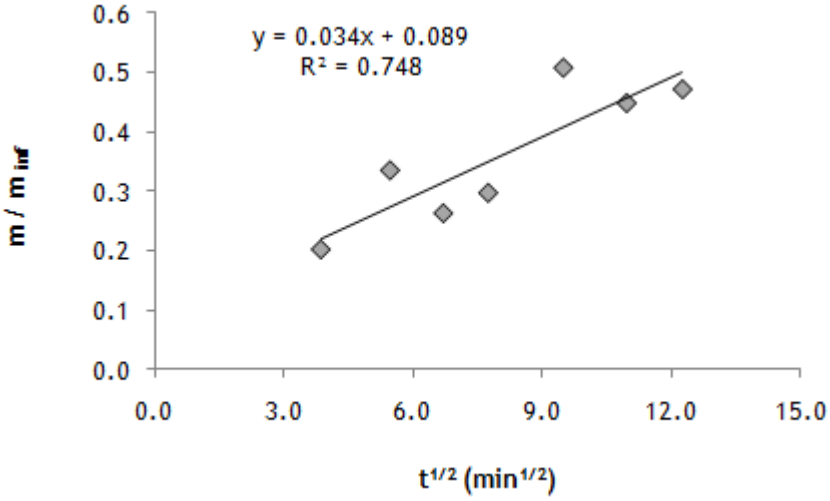

Figure 22: Fractional release of laminin versus the square root of time.

As described before, laminin is a large molecule and its size is larger than the mesh size of the hydrogels. Also, it is known that a molecule leaves a gel by diffusion if its size is smaller than the mesh size of the gel. However, the PEG hydrogels may have a mesh size distribution, as mesh size is an indirect measure determined by swelling ratio, and therefore there may be mesh sizes larger than the size of laminin. As the order of magnitude of the mesh size is the same as the size of laminin, this effect will allow laminin to slowly diffuse throughout the gel.

We assumed that for the first 6 hours the degradation of the gels was negligible, and that laminin was leaving the gels primarily by diffusion. This is supported by Figure 20 that represents a typical curve of mass release by diffusion, where it has an exponential increase in the first 24 hours and starts to stabilize in the value of total mass introduced in the system. Neglecting gel degradation in the first 6 hours was also supported by previous studies done in our group by Silviya Zustiak, where she showed that at ~75% degradation the mesh size of the hydrogels increased only by about 8% which is not significantly different from the initial mesh size (Figure 23) (Zustiak and Leach, 2010).

Molecular weight of cross-linker (kDa)	Initial mesh size (nm)	Mesh size (nm) at ~75 % degradation
3.4	13.6 ± 0.8	21.2 ± 0.2
Number of methylene groups between thiol and ester		
2 -CH_2- groups	15.0 ± 0.1	16.4 ± 0.4

Figure 23: Initial mesh size and mesh size at approximately 75 degradation for gels with molecular weight of 3.4 kDa and with 2 methylene groups (Zustiak and Leach, 2010).

Hence, although theoretically Fick's Law of Diffusion would not be appropriate for this problem, we have assumed it is a good approximation to quantify the release of laminin. Overall we have demonstrated that laminin is in fact being released of the hydrogels and that gel degradation is negligible for the release of laminin from the gels.

4.2. Incorporation of NSPCs within the PEG Hydrogels

In order to analyze the potential of the PEG-laminin scaffolds to pre-condition and deliver NSPCs, we incorporated NSPCs within the hydrogels and observed their behavior over time (see point 3.5.2).

NSPCs were encapsulated within the PEG-laminin hydrogels as aggregates; these neuronal cell aggregates are called neurospheres due to their sphere-like form. Some pictures were taken that show the behavior of neurospheres within the hydrogels (Figure 24). Cell migration was observed after 3-5 days of culture and three types of migration patterns were identified. In most cases NSPCs showed a radial migratory effect in which individual cells migrated from the center of the neurosphere to the periphery (Figure 24 (a,d)). However, in some other cases the neurospheres elongated along the hydrogels adapting an open configuration, with most of the cells located at the periphery. In this situation the cells migrated toward the center of the empty space of the neurosphere instead of away from it (Figure 24 (b,e)). Small neurospheres were also observed inside the hydrogels, and in this situation the neurospheres dissociated into individual cells randomly oriented throughout the hydrogel matrix (Figure 24 (c,f)).

The expansion of NSPCs within the hydrogels, as shown in Figure 24, suggested that inside the 3D PEG gels NSPCs favored proliferation over differentiation. To test for self-renewal capacity we analyzed the cultures for nestin-positive cells, which is a protein expressed in dividing cells during early stages of development. Figure 25 shows that the majority of the NSPCs inside the hydrogels are nestin-positive and therefore remain undifferentiated and maintain their proliferative ability.

As the hydrogels continue to degrade, cells start being released to the outside culture environment. At the bottom of the culture wells, the cells released from the PEG scaffolds were provided with an adhesive laminin surface. After approximately 2 weeks of culture few cells attached to the laminin-coated coverslips at the bottom of the wells were observed. The number of cells adhered to the laminin surface increased over time and after 3 weeks in culture the phenotype of the cells released from the PEG hydrogels was determined and compared to the 2D controls (consisting in NSPCs cultured from day 0 on laminin-coated coverslips) (Figure 26 (a-c)). The cultures were stained with antibodies against TUJ1, a neuronal marker expressed very early by the NSPCs after commitment to the neuronal lineage, and GFAP, a glial cell marker expressed in astrocytes. We observed both GFAP-positive cells and TUJ1-positive cells in all the culture conditions (Figure 26 (d-f)). The NSPCs cultured on the 2D controls differentiated predominantly into astrocytes while for the cells previously cultured in the 3D PEG gels more neuronal cells were observed (Figure 26).

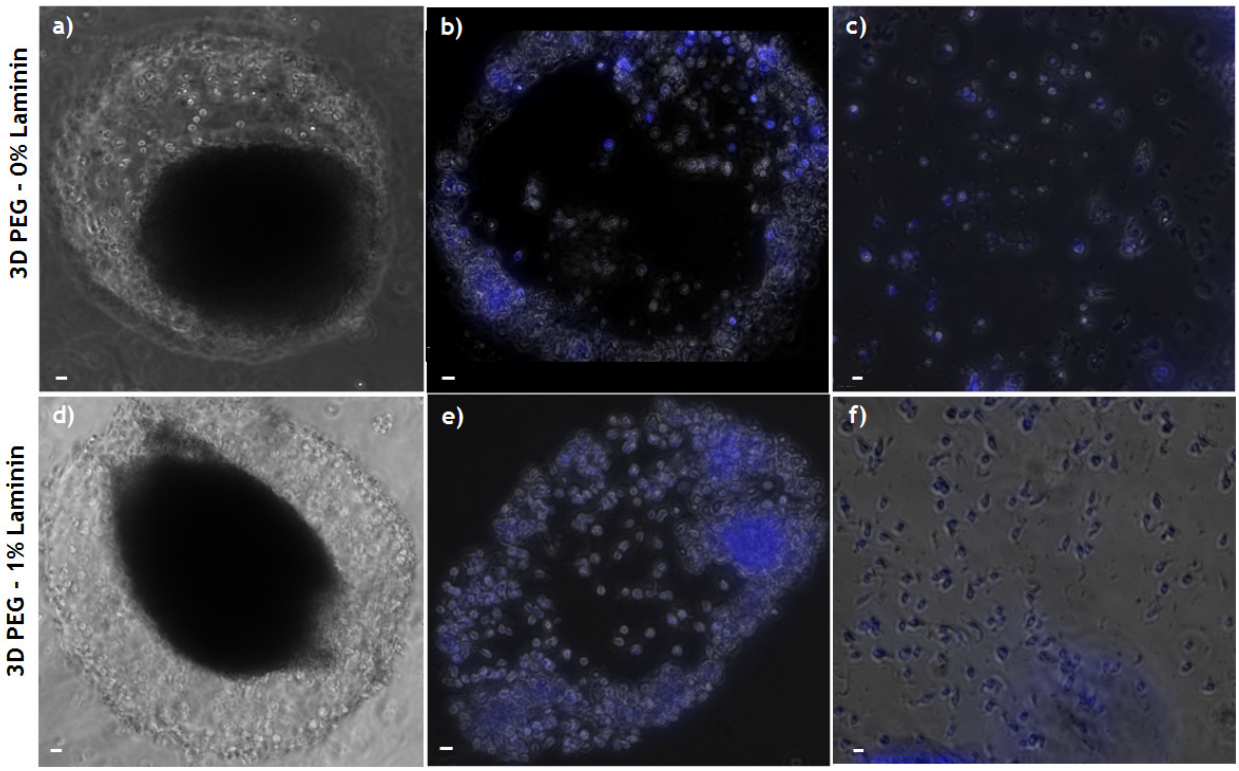

Figure 24: Phase contrast micrographs and overlay with DAPI of neural progenitor cells immobilized as neurospheres in the PEG hydrogels for 15 days: (a-c) 0% laminin PEG hydrogels and (d-f) 1% laminin PEG hydrogels. Cell nucleus is labeled with DAPI and is shown in blue. Scale bars, 10 μm.

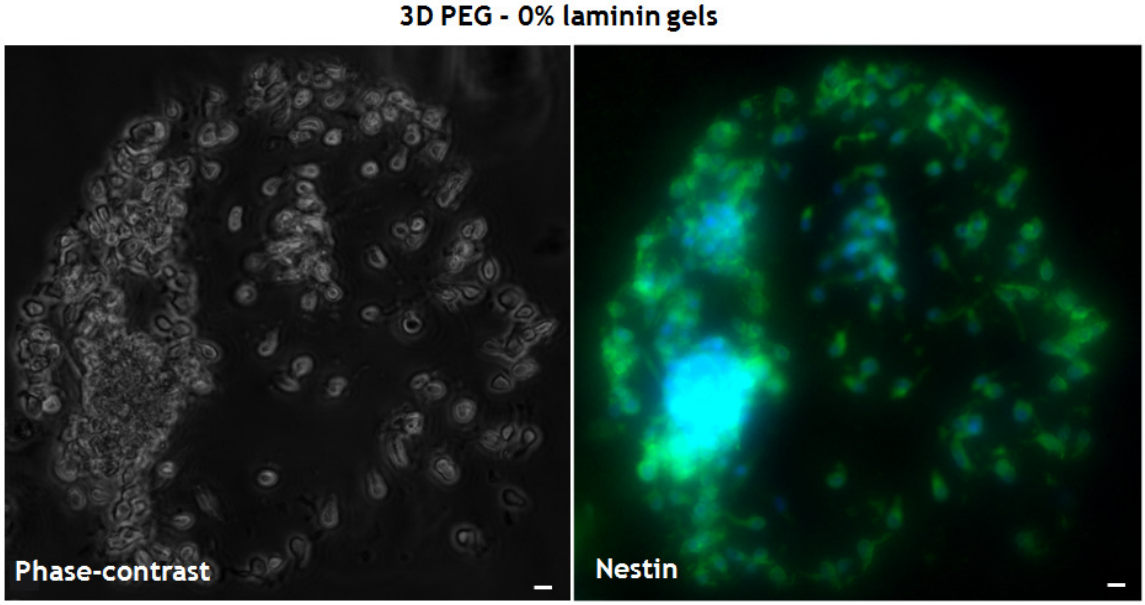

Figure 25: After 15 days in culture, NSPCs remain undifferentiated and maintain the progenitor capacity (nestin-positive). (a) Phase contrast and (b) fluorescent images of immunostained NSPCs inside 0% laminin-PEG hydrogels. Cell nucleus is labeled with DAPI and is shown in blue. Scale bars, 10 μm.

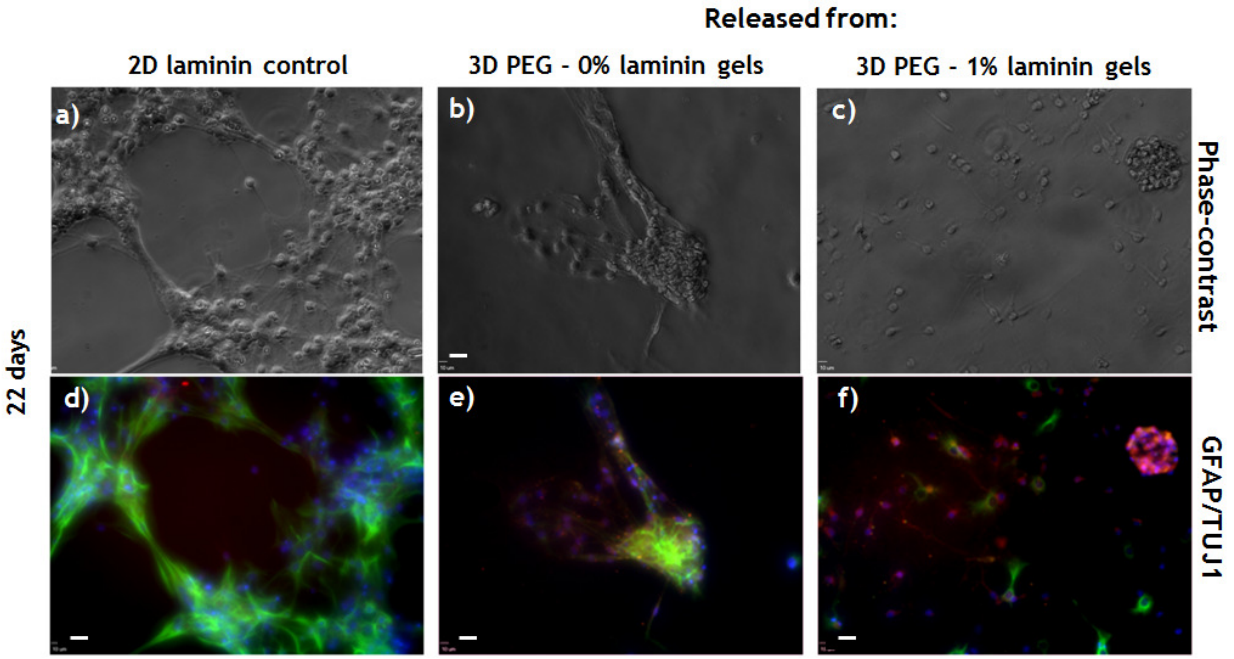

Figure 26: Differentiation of the NSPCs delivered upon gel degradation. (a-c) Phase contrast and (d-e) fluorescent micrographs. Cell nucleus is labeled with DAPI and is shown in blue. Neurons are shown in red and astrocytes are shown in green. Scale bars, 10 μm.

Quantification of the differentiated populations showed that a significant increase in neuronal population is in fact observed in the cells previously cultured in both 0 and 1 % laminin - PEG gels (41.8 ± 6.4 % and 61.6 ± 1.6 %, respectively) when compared to the 2D laminin controls (13.4 ± 2.3 %). The incorporation of laminin into the 3D PEG gels resulted in a significant enhancement of NSPCs differentiation into neurons (Figure 27).

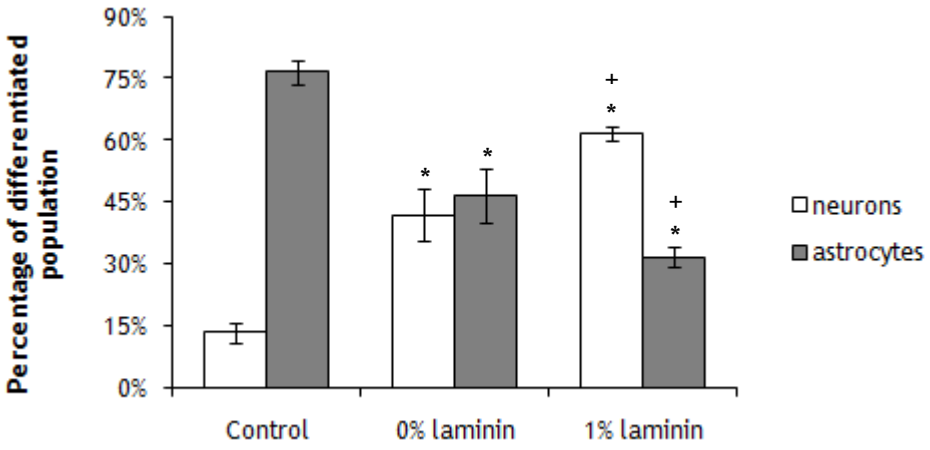

Figure 27: Percentage of differentiated NSPCs into neurons and astrocytes in the 2D laminin controls and in the laminin-coated coverslips after release from the 3D PEG-laminin constructs. Bars represent average ± standard deviation for n ≥ 3 samples. Symbols note statistical differences ($p<0.05$) between: * the 2D controls and + the 0% laminin-PEG gels.

The effect of laminin incorporation within the gels is reflected on the released NSPCs by enhancing their differentiation into neurons, as this increase is significant when compared to the NSPCs delivered from plain PEG hydrogels (Figure 27). Laminin may be playing its role in increasing neuronal differentiation in multiple ways. Although inside the gels NSPCs seem to favor proliferation over differentiation, laminin may be programming the majority of the cells to a neuronal phenotype that is activated as soon as the cells are released from the gels. Moreover, as the gels degrade, laminin is released along with the cells and this constant presence of laminin in culture can be regulating a preferential differentiation into neurons, as seen in previous studies (Raeber and Lutolf, 2005). The total release of laminin from the PEG hydrogels was measured and the results may be consulted at point 4.1.3. With this study we have confirmed that the total amount of solute added prior to gelation is released after complete degradation of the gels.

These results suggest that pre-culture of NSPCs in 3D hydrolytically degradable PEG hydrogels with a continuous and controlled release of cells is preferable to culture NSPCs directly on an adhesive substrate. This pre-conditioning 3D environment increases cellular differentiation into the neuronal phenotype following gel release, and this effect can be enhanced by the incorporation of laminin into these gels. As highly tunable scaffolds, several parameters can be customized within the PEG hydrogels in order to optimize their design towards specific clinical applications. In this study we modified the hydrogels with laminin, characterized their mechanical properties and tested the ability of the PEG-laminin constructs to deliver viable and differentiated NSPCs in an optimized scenario compared to the traditional 2D culture of cell suspensions. Our PEG hydrogels offer the possibility of modifying an array of mechanical and biological properties, through the incorporation of different biomolecules or peptide ligands in diverse concentrations (Zustiak *et al.*, 2010), or by altering the degradable cross-linker (Zustiak and Leach, 2010) and test the effect of different degradation times in NSPC delivery, which recently became a topic of interest to scientific groups working with degradable hydrogels (Lampe *et al.*, 2010). In conclusion, we have shown that our novel hydrolytically degradable PEG hydrogels are promising as transplantable materials as they have potential to be customized and used as carriers of NSPCs into injury sites.

4.2.1. Rheological Experiments

NSPCs may influence the stiffness of the hydrogels. Therefore we incorporated NSPCs within the gels and measured G', as in the tests with PEG hydrogels incorporated with laminin. The procedure to prepare the gels and the procedure for this experiment are described in points 3.5.1 and 3.5.4 respectively.

This experiment was conducted with 0%, 1% and 10% v/v laminin physically crosslinked within the hydrogels. For these studies we used PEG-SH 2 3.4 kDa as crosslinker. Figure 28 presents the mean storage modulus, G', showing both results from the experiment with NSPCs and the experiment without NSPCs (controls).

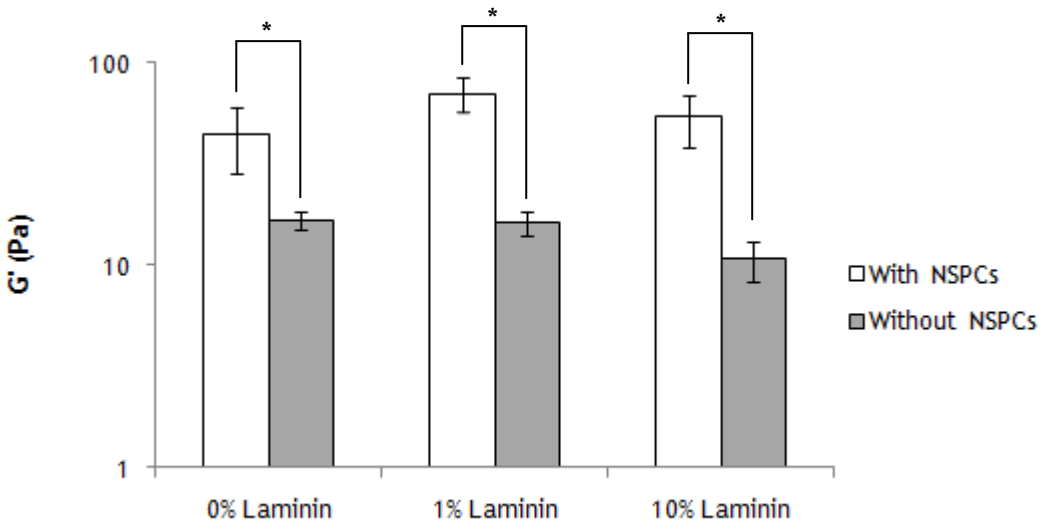

Figure 28: Representation of storage modulus of gels with 0%, 1% and 10% v/v laminin, with and without NSPCs. (*) denotes significant difference between the gels ($p<0.05$). Bars represent average ± standard deviation for $n \geq 3$ samples.

Table 4: Results obtained for storage modulus for hydrogels with NSPCs.

Laminin Concentration	0% v/v Laminin	1% v/v Laminin	10% v/v Laminin
G' (Pa)	44.1 ± 15.6	70.4 ± 13.5	54.2 ± 15.6

Encapsulation of NSPCs within the hydrogels increases hydrogel stiffness, as significant differences between the controls were observed for all types of gels (0%, 1% and 10% laminin).

4.2.2. Swelling Experiments

NSPCs may also influence the mesh size of the hydrogels. Therefore we incorporated NSPCs within the hydrogels and measured the swelling ratio, as in the tests with PEG hydrogels incorporated with laminin. The procedure to prepare the gels and the procedure for this experiment are described in points 3.5.1 and 3.5.3, respectively.

This experiment was conducted with 0%, 1% and 10% v/v laminin physically crosslinked within the hydrogels. As in the rheological experiments we used PEG-SH 2 3.4 kDa as the crosslinker. The same method of calculation of the swelling ratio and mesh size was used, as described in points 4.1.2 and 4.1.2.1, respectively. Figure 29 presents the results obtained for the swelling experiments.

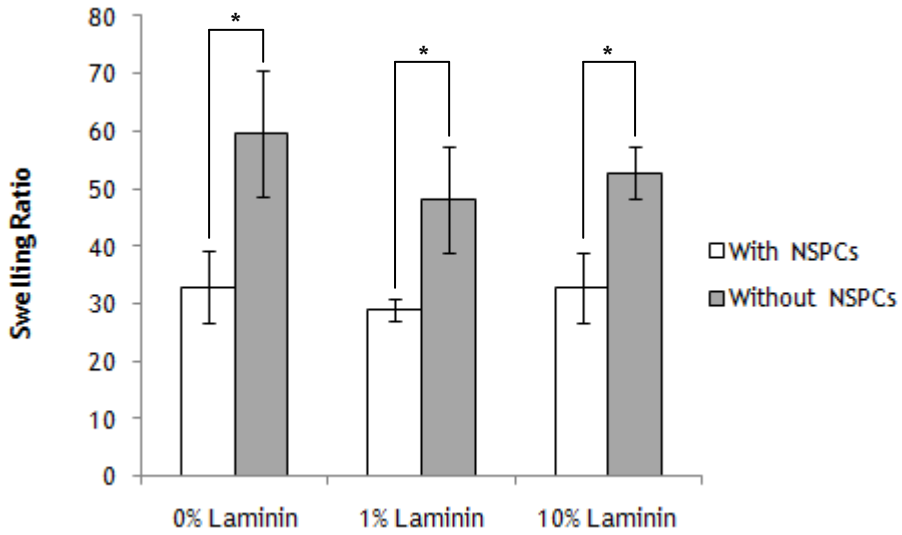

Figure 29: Representation of swelling ratio of gels with 0%, 1% and 10% v/v laminin with and without NSPCs (controls). (*) denotes significant difference between the gels ($p<0.05$). Bars represent average ± standard deviation for $n \geq 3$ samples.

Table 5: Results obtained for swelling ratio and mesh size for hydrogels with NSPCs.

Laminin Concentration	0% v/v Laminin	1% v/v Laminin	10% v/v Laminin
Q_m	32.9 ± 6.3	29.1 ± 1.9	32.8 ± 5.9
ξ (nm)	15.7 ± 1.3	15.1 ± 0.1	16.0 ± 1.4

As expected from the results obtained from the rheological experiments the swelling ratio and mesh size of the hydrogels decreases when NSPCs are added to the system.

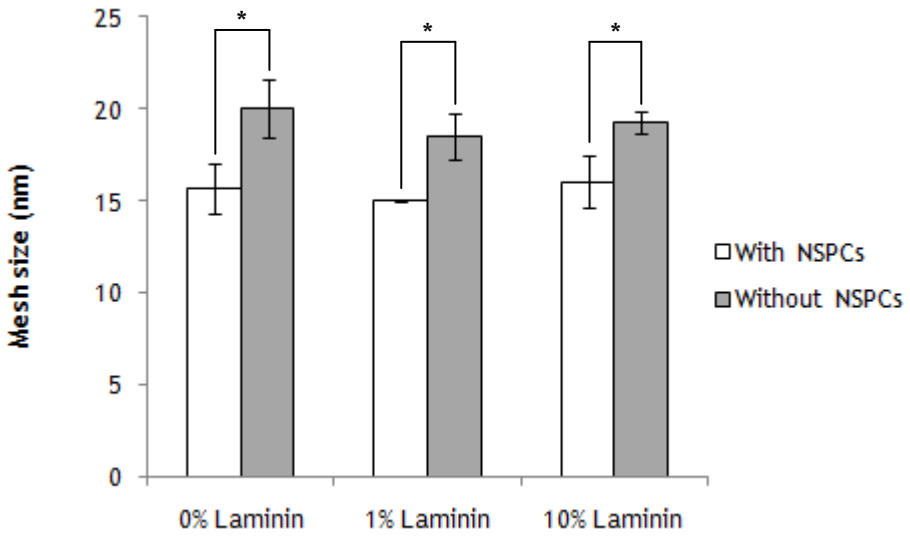

Figure 30: Representation of swelling ratio of gels with 0%, 1% and 10% v/v laminin with and without NSPCs (controls). (*) denotes significant difference between the gels ($p<0.05$). Bars represent average ± standard deviation for $n \geq 3$ samples.

As expected from the results obtained from the rheological experiments, significant differences were also observed for swelling ratio and mesh size between the controls for all types of gels (0%, 1% and 10% laminin), indicating that the addition of NSPCs within the gels affects their swelling ratio and thus their mesh size. These results suggest that the polymer density increased with the addition of NSPCs and consequently the hydrogel matrix is more packed in the presence of cells.

We have also observed a dramatic increase in the degradation time when NSPCs are incorporated within the gels which can be explained by the effect that NSPCs have on the hydrogels. As the degradation sites become less accessible due to the increase in hydrogel density and reduction in mesh size caused by the presence of the NSPCs, the degradation time went from 3 to 5 days to over three weeks. It is important to acknowledge the effect of cellular incorporation in the properties of 3D scaffolds as most studies do not evaluate this relationship and assume that the gel properties do not change when cells are incorporated in the structure. We report that this assumption cannot be made with certainty and each case should be evaluated individually as these results may be dependent on gel and cell type and cell density. Moreover, it was previously shown that NSPCs can synthesize fibronectin in a cell–collagen gel–bioreactor culture system (Ma, 2006, Lin *et al.*, 2004). It is highly likely that NSPCs cultured within our 3D PEG gels are also synthesizing their own ECM molecules as they remodel their surroundings.

5 Conclusions

We made several conclusions from this work.

From the physical incorporation of laminin within the PEG hydrogels synthesized with PEG-SH 2 3.4 kDa as crosslinker, we concluded that the properties of the hydrogels change with the addition of biomolecules. By physically incorporating laminin, the stiffness of the gels decreased, while mesh size and swelling ratio remained constant.

From the physical incorporation of laminin together with the encapsulation of NSPCs within the PEG hydrogels synthesized with PEG-SH 2 3.4 kDa as crosslinker, we concluded that the properties of the hydrogels change with the addition of cells. By encapsulating NSPCs the stiffness of the gels increased followed by a decrease in the swelling ratio and mesh size, when compared with the controls (PEG gels incorporated with laminin).

Finally, from the study of the capability of PEG-laminin hydrogels as NSPCs delivery devices, we have concluded that as the gels start to degrade, NSPCs are released and adhere to the laminin coated coverslips. Also, once they have adhered to the coverslips they started to differentiate accordingly. It was then concluded that the presence of laminin in 3D PEG constructs lead to a higher differentiation into neurons; unlike what happens with the 2D controls where NSPCs preferentially differentiate into astrocytes.

6 Evaluation of Work Conducted

6.1. Accomplished Objectives

The present work had the following objectives:

1. Incorporate laminin within PEG hydrogels and determine their mechanical properties.

When mixed with a biomolecule, the hydrogel properties will change, thus it is important to quantify these changes in order to correlate cell response and scaffold properties. We analyzed stiffness, degradation and mesh size. We have determined how the mechanical properties of the hydrogels were affected by the addition of laminin as a physically entangled molecule within the hydrogels.

2. Incorporate NSPCs within PEG-laminin hydrogels, and analyze scaffold capability for inducing NSPC differentiation and delivery.

The objective was to evaluate how cells interact with the hydrogels, with and without laminin. We measured NSPCs viability and percentage of the differentiated populations. We have also determined how the mechanical properties of the hydrogels were affected by the addition of NSPCs as a physically entangled molecule within the hydrogels.

3. Modify laminin, i.e., generate thiol groups (SH) in laminin, to incorporate within the PEG gels.

The experiment did not work as expected. We were not able to generate thiol groups in laminin structure.

4. Determine the mechanical properties of the hydrogels, with modified laminin incorporated in the hydrogels by chemical crosslinking.

These experiments were not conducted due to unsuccessful modification of laminin.

5. Incorporate NSPCs within the laminin-modified PEG gels and analyze scaffold capability for inducing NSPC differentiation and delivery.

These experiments were also not conducted due to unsuccessful modification of laminin.

6. The studies described in points 1 and 2 were tested for PEG hydrogels crosslinked with two different degradable crosslinkers, a PEG-SH 1 3.4 kDa and PEG-SH 2 3.4 kDa, where 3.4 refers to the molecular weight of the crosslinker (in kDa) and the numbers 1 and 2, refer to the number of methylene groups between the ester and thiol moieties. An increase in the number of methylene groups increased the degradation time of the gels, and previous studies in our group found that gels with PEG-SH 1 3.4 kDa as crosslinker degrade in less than one day while gels with PEG-SH 2 3.4 kDa as crosslinker degrades in about 3 days (results without proteins or cells incorporated in the gels) (Zustiak and Leach, 2010).

In this project steps 1, 2 and 6 were completed. Step 3 was also conducted but without successful results. Other steps were not conducted due to the fact that the incorporation of thiol groups in laminin did not work as expected, thus we were not able to test the behavior of both PEG hydrogels and NSPCs with the modified protein.
From point 6 only the part involving the characterization of hydrogels synthesized with PEG-SH 1 3.4 kDa and cell work was not preformed. Overall the primary objectives of the project were completed and other experiments stand for future work.

6.2. Other Work Conducted

Mechanical properties of hydrogels, synthesized with PEG-SH 1 3.4 kDa, incorporated with laminin were determined, the results can be found in Appendix 3. The results from the modification of laminin with SH groups are described in detail in Appendix 3, together with a modification experiment that was performed with Bovine Serum Albumine (BSA) to test the modification protocol.

6.3. Journal Club

During group meetings, we held a journal club, where each undergraduate student chose an article regarding their work theme. These meetings have helped us evaluate articles for their scientific merit and improve our presentation skills. In other group meetings all the members from the Leach lab group presented their work and respective future perspectives.

The article I chose for the journal club, "Characterization of poly(ethylene glycol) gels with added collagen for neural tissue engineering", was a fairly recent study that incorporated a protein within PEG-diacrylate gels and evaluated their properties (R.K. Willits, 2010). Appendix 5 presents the slides containing information depicted from the article.

In an interesting note, this article was presented in the Society for Biomaterials Conference (SFB), which was held in Seattle in April 21-24th of 2010 and to which I had the pleasure to attend. Here I was able to learn about some of the interesting work being done in the area of synthetic materials as scaffolds for tissue engineering and the recent advances in this area.

6.4. Limitations and Future Work

We have faced several limitations while conducting this work.

First the laminin modification with SH groups did not work as expected. Several attempts were made towards the success of the incorporation of SH groups within the protein but without positive results. Thus, as future work, other approaches, like the use of different protocols such as the Modification of Amines with 2-Iminothiolane (Traut's reagent) or the Modification of Amines with N-Acetyl Homocysteine Thiolactone (Hermanson, 2008), should be taken into consideration in order to obtain positive results.

We have also faced a shortage of supplies to make the PEG hydrogels. The components used to prepare the PEG hydrogels, PEG-VS and PEG-SH, are fairly hard to make and the amount of both VS and SH groups incorporated into PEG is also hard to control, thus there is some variability from batch to batch. Therefore we could only work with the amounts available in the lab and always used the same batches. Despite the shortage of those components all the experiments were able to be preformed. However, as future work, more assays should be performed in order to strengthen the results obtained in this project.

Regarding cell work we were not able to focus on how the NSPCs are keeping the gels from degrading, or even making them stiffer. With the knowledge from previous works in our group, from cell cultures in collagen-coated coverslips and collagen gels studied by the PhD student Andreia Ribeiro, we could make some assumptions on the interaction between the cells and the hydrogel. As future work, figuring out what exactly is happening within the gels, what are the cells producing and how it is affecting the properties of the gels is a matter of great importance.

Flow cytometry (Fluorescence-activated cell sorting, FACS) will be used in future studies for a more accurate determination of viability, proliferation and differentiation analysis. FACS is a technique that sorts a heterogeneous mixture of biological cells into two or more containers, one cell at a time, based upon specific fluorescent characteristics of each cell.

Finally, another important experiment that should be conducted in the future is the optimization of the concentration of laminin physically incorporated, or chemically crosslinked in the gels and in the laminin coated coverslips toward NSPCs differentiation into neurons.

6.5. Final Comment

Most of the objectives were accomplished during the timeframe of this project. While conducting the experiments the main objective of the project, which was the modification of laminin with SH groups followed by its chemical crosslinking with the PEG-VS backbone and further evaluation of the mechanical properties of the scaffolds, was changed. As the modification was not working we physically incorporated laminin within the hydrogels and after collecting all the data regarding the mechanical properties of the gels we started the encapsulation of NSPCs within the gels.

Evaluating how NSPCs influenced the mechanical proerties of the hydrogels proven to have greater importance than the previous main objective. However, the modification of laminin should not be discarded taking part of one of the future works to be conducted.

References

- Aboody, K.S., Najbauer, J. and Danks, M.K. Stem and progenitor cell-mediated tumor selective gene therapy. *Gene Therapy*, 15(10), 739-52 (2008).
- Amersham Biotechnology, 2003, Instructions: PD-10 Desalting Column: http://wolfson.huji.ac.il/purification/PDF/dialysis/AMERSHAM_PD10Desalting.pdf
- Andersson, E., Tryggvason, U., Deng, Q., Friling, S., Alekseenko, Z., Robret, B., Perlmann, T. and Ericson, J. Identification of Intrinsic Determinants of Midbrain Dopamine Neurons. *Cell*, 124, 393-405 (2006).
- Ando, T., Yamazoe, H., Moriyasu, K., Ueda, Y. and Iwata, H. Induction of dopamine-releasing cells from primate embryonic stem cells enclosed in agarose microcapsules. *Tissue Engineering*, 13, 2539-2547 (2007).
- Andressen, C., Adrian, S., Fässler, R., Arnhold, S. and Klaus, A. The contribution of $\beta 1$ integrins to neuronal migration and differentiation depends on extracellular matrix molecules. *European Journal of Cell Biology*, 84, 973-982 (2005).
- Ashton, R.S., Banerjee, A., Punyani, S., Schaffer, D.V. and Kane, R.S. Scaffolds based on degradable alginate hydrogels and poly(lactide-co-glycolide) microspheres for stem cell culture. *Biomaterials*, 28, 5518-5525 (2007).
- BD Biosciences, 2010: http://www.bdbiosciences.com/ptProduct.jsp?prodId=579485&catyId=775681&page=product&wcm_page=/cellculture/&wcm_title=Cell%20Culture&wcm_category=775681
- Bio-Rad Laboratories, Life Science Group, USA, Bio-Rad Protein Assay Protocol: http://labs.fhcrc.org/fero/Protocols/BioRad_Bradford.pdf
- Blurton-Jones, M., Kitazawa, M., Martinez-Coria, H., Castello, N.A., Müller, F-J., Loring, J.F., Yamasaki, T.R., Poon, W.W., Green, K.N. and LaFerla, F.M. Neural stem cells improve cognition via BDNF in a transgenic model of Alzheimer disease. *Procedings of the National Academy of Sciences*, 16(32), 13594-13599 (2009).
- Bryant, S.J., Nuttelman, C.R. and Anseth, K.S. Cytocompatibility of UV and visible light photoinitiating systems on cultured NIH/3T3 fibroblasts in vitro. *Journal of Biomaterials Science Polymer Ed.*, 11, 439-457 (2000).
- Canal, T. and Peppas, N.A. Correlation between mesh size and equilibrium degree of swelling of polymeric networks. *Journal of Biomedical Research*, 23(10), 1183-93 (1989).

- Ceballos, D., Navarro, X., Dubey, N., Wendelschafer-Crabb, G., Kennedy, W.R. and Tranquillo, R.T. Magnetically aligned collagen gel filling a collagen nerve guide improves peripheral nerve regeneration. *Experimental Neurology*, 158(2), 290-300 (1999).
- Cell Biology, consulted in May 2010: http://219.221.200.61/ywwy/zbsw(E)/edetail4.htm
- Chen, Y.S., Hsieh, C.L., Tsai, C.C., Chen, T.H., Cheng, W.C., Hu, C.L. and Yao, C.H. Peripheral nerve regeneration using silicone rubber chambers filled with collagen, laminin and fibronectin. *Biomaterials*, 21, 1541-47 (2000).
- Clark, P., Britland, S. and Connolly, P. Growth cone guidance and neuron morphology on micropatterned laminin surfaces. *Journal of Cell Science*, 105, 203-212 (1993).
- Copland, R. A. *ENZYMES A Practical Introduction to Structure, Mechanism, and Data Analysis*. 2nd ed. John Wiley and Sons, New York, 2000.
- Cruise, G.M., Scharp, D.S. and Hubbell, J.A. Characterization of permeability and network structure of interfacially photopolymerized poly(ethylene glycol) diacrylate hydrogels. *Biomaterials*, 19(14), 1287-94 (1998).
- Dahlin, L. and Lundborg, G. The use of silicone tubing in the late repair of the median and ulnar nerves in the forearm. *Journal of Hand Surgery [Br.]*, 26, 393-94 (2001).
- Dalton, P.D., Flynn, L. and Shoichet, M.S. Manufacture of poly(2-hydroxyethyl methacrylate-co-methyl methacrylate) hydrogel tubes for use as nerve guidance channels. *Biomaterials*, 23, 3843-51 (2002).
- Dawson, E., Mapili, G., Erickson, K., Taqvi, S. and Roy, K. Biomaterials for stem cell differentiation. *Avanced DRUG DELIVERY Reviews*, 60(2008), 215-228 (2007).
- Dubey, N., Letourneau, P.C. and Tranquillo, R.T. Guided neurite elongation and Schawnn cell invasion into magnetically aligned collagen in simulated peripheral nerve regeneration. *Experimental Neurology*, 158, 338-50 (1999).
- Elbert, D.L., Pratt, A.B., Lutolf, M.P., Halstenberg, S. and Hubbell, J.A. Self-selective Reactions in the Design of Materials for Controlled Delivery of Proteins. *Journal of Controlled Release*, 76, 11-25 (2001).
- Evans, G.R., Brandt, K., Niederbichler, A.D., Chauvin, P., Herrman, S. *et al*. Clinical long-term in vivo evaluation of poly(lactic acid) porous conduits for peripheral nerve regeneration. *Journal of Biomaterials Science. Polymer Ed.*, 11, 869-78 (2000).

- Gilchrist, T., Glasby, M.A., Healy, D.M., Kelly, G., Lenihan, D.V., McDowall, K.L., Miller, I.A. and Myles, L.M. In vitro nerve repair – *in vivo*. The reconstruction of peripheral nerves by entubulation with biodegradable glass tubes – a preliminary report. *British Journal of Plastic Surgery*, 51, 231-37 (1998).
- Grimpe, B. and Silver, J. The extracellular matrix in axon regeneration. *Progress in Brain Research*, 137, 333-49 (2002).
- Harris, J.M. Topics in Applied Chemistry – *Poly(ethylene glycol) Chemistry: Biotechnical and Biomedical Applications*., Plenum Press, New York (1992).
- Hermanson, G.T. *Bioconjugate Techniques*. 2nd ed., Academic Press, London (2008).
- Hubbell, J.A. and Lutolf, M.P. Synthesis and physicochemical characterization of end-linked poly(ethylene glycol)-co-peptide hydrogels formed by Michael-type addition. *Biomacromolecules*, 4(3), 713-22, (2003).
- Hynes, S.R., McGregor, L.M., Rauch, M.F., Lavik, E.B. Photopolymerized poly(ethylene glycol)/poly(L-lysine) hydrogels for the delivery of neural progenitor cells. *Journal of Biomaterials Science: Polymer Edition*, 18(8), 1017–1030(14) (2007).
- Iwanami, A., Kaneko, S., Nakamura, M., Kanemura, Y., Mori, H., Kobayashi, S., Yamasaki, M., Momoshima, S., Ishii, H., Ando, K., Tanioka, Y., Tamaoki, N., Nomura, T., Toyama, Y. and Okano, H. Transplantation of human neural stem cells for spinal cord injury in primates. *Journal of Neuroscience Research*, 80(2), 182-90 (2005).
- Jacques, T.S., Relvas, J.B., Nishimura, S., Pytela, R., Edwards, G.M., Streuli, C.H. and ffrench-Constant, C. Neural Percursor cell chain migration and division are regulated through different β1 integrins. *Development*, 125, 3167-3177 (1998).
- Jones, J.R. Observing cell response to biomaterials. *Materials Today*, 9(12), 34-43, 2006.
- Khademhosseini, A., Langer, R., Borenstein, J., Vacantil, J.P. Microscale technologies for tissue engineering and biology. *Procedings of the National Academy of Sciences*, 103(8), 2480-2487 (2006).
- Krsko, P. and Libera, M. Biointeractive hydrogels. *Materials Today*, 8, 36-44 (2005).
- Kulbatski, I., Mothe, A.J., Nomura, H. and Tator, C.H. Endogenous and exogenous CNS derived stem/progenitor cell approaches for neurotrauma. *Current Drug Targets*, 6(1), 111-26 (2005).
- Lampe, K.J., Bjugstad, K.B. and Mahoney, M.J. Impact of degradable macromer content in a poly(ethylene glycol) hydrogel on neural cell metabolic activity, redox state, proliferation, and differentiation. *Tissue Engineering Part A*, 16(6), 1857-66 (2010).

- Lathia, J.D., Patton, B., Eckley, D.M., Magnus, T., Mughal, M.R., Sasaki, T., Caldwell, M.A., Rao, M.S., Mattson, M.P. and FFrench-Constant, C. Patterns of Laminins and Integrins in the Embryonic Ventricular Zone of the CNS. *The Journal of Comparative Neurology*, 505, 630-643 (2007).
- Laverty, P.H., Leskovar, A., Breur, G.J., Coates, J.R., Bergman, R.L., Widmer, W.R., Toombs, J.P., Shapiro, S. and Borgens, R.B. A Preliminary Study of Intravenous Surfactants in Paraplegic Dogs: Polymer Therapy in Canine Clinical SCI. *Journal of Neurotrauma*, 21(12), 1767-1777 (2004).
- Leach, J.B., Bivens, K.A., Patrick Jr., C.W. and Schimdt, C.E. Photocrosslinked hyaluronic acid hydrogels: natural, biodegradable tissue engineering scaffolds. *Biotechnology and Bioengineering*, 82(5), 578-89 (2003).
- Leach, J.B., Schmidt, C.E. Characterization of protein release from photocrosslinkable hyaluronic acid-polyethylene glycol hydrogel tissue engineering scaffolds. *Biomaterials*, 26(2), 125-35 (2005).
- Lenihan, D.V., Carter, A.J., Gilchrist, T., Healy, D.M., Miller, I.A., Myles, L.M. and Glasby, M.A. Biodegradable controlled release glass in the repair of peripheral nerve injuries. *Journal of Hand Surgery [Br.]*, 23, 588-93 (1998).
- Lepore, A.C., Neuhuber, B., Connors, T.M., Han, S.S., Liu, Y., Daniels, M.P., Rao, M.S. and Fischer, I. Long-term fate of neural precursor cells following transplantation into developing and adult CNS. *Neuroscience*, 139(2), 513-30 (2006).
- Levenberg, S., Khademhosseini, A. and Langer, R. *Essentials of Stem Cell Biology*. 2nd ed., Chapter 63, Academic Press, 2009.
- Lim, D.W. and Park, T.G. Stereocomplex Formation between Enantiomeric PLA–PEG–PLA Triblock Copolymers: Characterization and Use as Protein-Delivery Microparticulate Carriers. *Journal of Applied Polymer Science*, 75(13), 1615-1623 (2000).
- Lin, H.J., O'Shaughnessy, T.J., Kelly, J., Ma, W. Neural stem cell differentiation in a cell-collagen-bioreactor culture system. *Brain Research. Developmental Brain Research*, 153(2), 163-73 (2004).
- Lore, A.B., Hubbell, J.A., Bobb Jr, D.S., Ballinger, M.L., Loftin, K.L., Smith, J.W., Smyers, M.E., Garcia, H.D. and Bittner, G.D. Rapid Induction of Functional and Morphological Continuity between Severed Ends of Mammalian or Earthworm Myelinated Axons. *The Journal of Neuroscience*, 19(7), 2442-2454 (1999).

- Lu, S. and Anseth, K. S. Release behavior of high molecular weight solutes from poly(ethylene glycol)-based degradable networks. *Macromolecules*, 33, 2509–2515 (2000).
- Ma, W., Fitzgerald, W., Liu, Q.Y., O'Shaughnessy, T.J., Maric, D., Lin, H.J., Alkon, D.L. and Barker, J.L. CNS stem and progenitor cell differentiation into functional neuronal circuits in three-dimensional collagen gels. *Experimental Neurology*, 190(2), 276-88 (2004).
- Ma, W., Tavakoli, T., Chen, S., Maric, D., Liu, J.L., O'Shaughnessy, T.J. and Barker, J.L. Reconstruction of functional cortical-like tissues from neural stem and progenitor cells. *Tissue Engineering Part A*, 14(10), 1673-86 (2008).
- Ma, W. inventor THE GOVERNMENT OF THE UNITED STATES OF AMERICA, as represented by THE SECRETARY OF THE NAVY, assignee. A Neural stem cell-collagen-bioreactor system to construct a functional embryonic brain-like tissue. USA. 2006.
- Mahoney, M.J. and Anseth, K.S. Three-dimensional growth and function of neural tissue in degradable polyethylene glycol hydrogels. *Biomaterials*, 27(10), 2265-74 (2006).
- Martínez-Ramos, C., Lainez, S., Sancho, F., García Esparza, M.A., Planells-Cases, R., García Verdugo, J.M., Gómez Ribelles, J.L., Salmerón Sánchez, M., Monleón Pradas, M., Barcia, J.A. and Soria, J.M. Differentiation of postnatal neural stem cells into glia and functional neurons on laminin-coated polymeric substrates. *Tissue Eng*ineering *Part A.*, 14(8), 1365-75 (2008).
- Mason, M.N., Metters, A.T., Bowman, C.N. and Anseth, K.S. Predicting Controlled-Release Behavior of Degradable PLA-*b*-PEG-*b*-PLA Hydrogels. *Macromolecules*, 34, 4630-4635 (2001).
- Mellott, M.B., Searcy, K., Pishko, M.V. Release of protein from highly crosslinked hydrogels of poly(ethylene glycol) diacrylate fabricated by UV polymerization. *Biomaterials*, 22(9), 929-41 (2001).
- Merrill, E.W., Dennison, K.A. and Sung, C. Partitioning and diffusion of solutes in hydrogels of poly(ethylene oxide). *Biomaterials*, 14(15),1117-26 (1993).
- Metters, A.T., Anseth, K.S. and Bowman, C.N. Fundamental studies of a novel, biodegradable PEG-*b*-PLA hydrogel. *Biomaterials*, 41, 3993-4004 (2000).
- Metters, A.T., Anseth, K.S. and Bowman, C.N. Fundamental studies of biodegradable hydrogels as cartilage replacement materials. *Biomedical Science Instrumentation*, 35, 33-38 (1999).

- Metters, A. and Hubbell, J. Network formation and degradation behavior of hydrogels formed by Michael-type addition reactions. *Biomacromolecules*, 6, 290-301 (2005).
- Molina, I., Li, S., Martinez, M.B. and Vert, M. Protein release from physically crosslinked hydrogels of the PLA/PEO/PLA triblock copolymer-type. *Biomaterials*, 22(4), 363-369 (2001).
- Moriyasu, K., Yamazoe, H. and Iwata, H. Induction dopamine releasing cells from mouse embryonic stem cells and their long-term culture. *Journal of Biomedical Materials Research*, 77, 136-147 (2006).
- Morpurgo, M., Veronese, F.M., Kachensky, D. and Harris, J.M. Preparation and Characterization of Poly(ethylene glycol) Vinyl Sulfone. *Bioconjugate Chemistry*, 7, 363-368 (1996).
- Motulsky, H. *Intuitive Biostatistics*., Oxford University Press, New York (1995).
  Chapter 37 – Choosing a Test, available online: http://www.graphpad.com/www/Book/Choose.htm
- Nakamura, M., Toyama, Y. and Okano, H. [Transplantation of neural stem cells for spinal cord injury]. *Rinsho Shinkeigaku*, 45(11), 874-6 (2005).
- Namba, R.M., Cole, A.A, Bjugstad, K.B. and Mahoney, M.J. Development of porous PEG hydrogels that enable efficient, uniform cell-seeding and permit early neural process extension. *Acta BIOMATERIALIA*, 5(2009), 1884-1897 (2009).
- Nicoli, A.N., Fini, M., Rocca, M., Giavaresi, G. and Giardino, R. Guided regeneration with resorbable conduits in experimental peripheral nerve injuries. *International Orthopaedics*, 24, 121-25 (2000).
- Nisbet, D.R., Crompton, K.E., Horne, M.K., Finkelstein, D.I. and Forsythe, J.S. Neural Tissue Engineering of the CNS Using Hydrogels. *Journal of Biomedical Materials Research Part B*: *Applied Biomaterials*, 87B(1), 251-263 (2008).
- Park, K. Controlled drug delivery: challenges and strategies. *An American Chemical Society Publication*, Washington, DC, 529-57 (1997).
- Peppas, N.A. and Ritger, P.L. A simple equation for description of solute release: I. Fickian and anomalous release from swellable devices. *Journal of Controlled Release*, 5, 37-42 (1987).
- Piantino, J., Burdick, J.A., Goldberg, D., Langer, R. and Benowitz, L.I. An injectable, biodegradable hydrogel for trophic factor delivery enhances axonal rewiring and improves performance after spinal cord injury. *Experimental Neurology*, 201(2), 359-67 (2006).

- Pierce Biotechnology, Inc., 4/2004, Instructions for SATA and SATP: http://www.piercenet.com/files/0126as4.pdf
- Prang, P., Muller, R., Eljaouhari, A., Heckmann, K., Kunz, W., Weber, T., Faber, C., Vroemen, M., Bogdahn, U. and Weidner, N. The promotion of oriented axonal regrowth in the injured spinal cord by alginate-based anisotropic capillary hydrogels. *Biomaterials*, 27, 3560-3569 (2006).
- Raeber, G.P., Lutolf, M.P. and Hubbell, J.A. Molecularly engineered PEG hydrogels: a novel model system for proteolytically mediated cell migration. *Biophysical Journal*, 89(2), 1374-88 (2005).
- Rao, C.N., Margulies, I.M.K., Tralka, T.S., Terranova, V.P., Madri, J.A. and Liotta, L.A. Isolation of a Subunit of Laminin and its Role in Molecular Structure and Tumor Cell Attachment. *The Journal of Biological Chemistry*, 257(16), 9740-9744 (1982).
- Ribeiro, A., Vargo, S., Powel, E.M. and Leach, J.B. Effects of microenvironment dimensionality in sensory neuron development and process outgrowth: 3D better mimics *in vivo* features. in prep., planned submission to *Proceedings of the National Academy of Sciences* (2010).
- Ritger, P.L. and Peppas, N.A. A simple equation for description of solute release: I. Fickian and non-Fickian release from non-swellable devices in form of slabs, spheres, cylinders, or disks. *Journal of Controlled Release*, 5, 23-36 (1987).
- Rutishauser, U. Adhesion molecules of the nervous system. *Current Opinion in Neurobiology*, 3, 709-15 (1993).
- Sigma-Aldrich, 2010:

  http://www.sigmaaldrich.com/life-science/metabolomics/enzyme-explorer/learning-center/structural-proteins/laminin.html
- Schmidt, C.E. and Leach, J.B. Neural Tissue Engineering: Strategies of Repair and Regeneration. *Annual Review of Biomedical Engineering*, 5, 293-347 (2003).
- Scott, C.T. *Stem Cell Now: A Brief Introduction to the Coming Medical Revolution.*, Plume, New York (2006).
- Shalaby, S.W. and Burg K.J.L. Advances in Polymeric Biomaterials Series - *Absorbable and Biodegradable Polymers.*, CRC Press LLC, (2004).
- Soldani, G., Varelli, G., Minnoci, A. and Dario, P. Manufacturing and microscopical characterization of polyurethane nerve guidance channel featuring a highly smooth internal surface. *Biomaterials*, 19, 1919-24 (1998).

- Subramanian, A., Krishnan, U.M. and Sethuraman, S. Development of biomaterial scaffold for nerve tissue engineering: Biomaterial mediated neural regeneration. *Journal of Biomedical Science*, 16:108, (2009).
- Svendsen, C.N., Caldwell, M.A., Shen, J., ter Borg, M.G., Rosser, A.E., Tyers, P., Karmiol, S. and Dunnett, S.B. Long-term survival of human central nervous system progenitor cells transplanted into a rat model of Parkinson's disease. *Experimental Neurology*, 148(1), 135-46 (1997).
- Tavakoli, T., Ma, W., Derby, E., Serebryakova, Y., Rao, M.S. and Mattson, M.P. Cell-extracellular matrix interactions regulate neural differentiation of human embryonic stem cells. *BMC Developmental Biology*, 8:90, (2008).
- Veronese, F.M. and Pasut, G. PEGylation, successful approach to drug delivery. *Drug Delivery Today*, 10(21), 1451-1458.
- Whitworth, I.H., Brown, R.A., Dore, C., Green, C.J. and Terenghi, G. Orientated mats of fibronectin as a conduit material for use in peripheral nerve repair. *Journal of Hand Surgery [Br.]*, 20, 429-36 (1995).
- Willerth, S.M., Arendas, K.J., Gottlieb, D.I. and Sakiyama-Elbert, S.E. Optimization of fibrin scaffolds for differentiation of murine embryonic stem cells into neural lineage cells. *Biomaterials*, 27, 5990-6003 (2006)
- Willerth, S.M., Faxel, T.E., Gottlieb, D.I. and Sakiyama-Elbert, S.E. The effects of soluble growth factors on embryonic stem cell differentiation inside of fibrin scaffolds. *Stem Cells (Dayton, Ohio)*, 25, 2235-2244 (2007).
- Willits, R.K., Scott, R. and Marquardt, L. Characterization of poly(ethylene glycol) gels with added collagen for neural tissue engineeting. *Journal of Biomedical Materials Research Part A*, 93(3), 817-23 (2010).
- Wnek, G.E. and Bowlin, G.L. *Encyclopedia of Biomaterials and Biomedical Engineering*. 2nd ed., Volume 4, Informa Healthcare, New York (2008).
- Yamasaki, T.R., Blurton-Jones, M., Morrissette, D.A., Kitazawa, M., Oddo, S. and LaFerla, F.M. Neural Stem Cells Improve Memory in an Inducible Mouse Model of Neuronal Loss. *The Journal of Neuroscience*, 27(44), 11925-11933 (2007).
- Yoshii, S. and Oka, M. Peripheral nerve regeneration along collagen filaments. *Brain Research*, 888, 158-62 (2001).
- Yoshii, S., Oka, M., Shima, M., Taniguchi, A. and Akagi, M. 30 mm regeneration of rat sciatic nerve along collagen filaments. *Brain Research*, 949, 202-8 (2002).

- Young, R.C., Wiberg, M. and Terenghi, G. Poly-3-hydroxybutyrate (PHB): a resorbable conduit for long-gap repair in peripheral nerves. *British Journal of Plastic Surgery*, 55, 235-40 (2002).
- Zhao, D., Najbauer, J., Garcia, E., Metz, M.Z., Gutova, M., Glackin, C.A., Kim, S.U. and Aboody, K.S. Neural stem cell tropism to glioma: critical role of tumor hypoxia. *Molecular Cancer Research (MCR)*, 6(12), 1819-29 (2008).
- Zhao, X. and Harris, J.M. Novel degradable poly(ethylene glycol) hydrogels for controlled release of protein. *Journal of Pharmaceutical Sciences*, 87, 1450-1458 (1998).
- Zigova, T., Snyder, E.Y., Sanberg, P.R. *Neural Stem Cells for Brain and Spinal Cord Repair*. Humana Press Inc., New Jersey (2003).
- Zustiak, S.P., Durbal, R. and Leach, J.B. Influence of cell-adhesive peptide ligands on poly(ethylene glycol) hydrogel physical, mechanical and transport properties. *Acta BIOMATERIALIA*, (2010).
- Zustiak, S.P. and Leach, J.B. Hydrolytically Degradable Poly(Ethylene Glycol) Hydrogel Scaffolds with Tunable Degradation and Mechanical Properties. *Biomacromolecules*, 11, 1348-1357 (2010).

Appendix 1 Additional Protocols

A1.1. Procedure for Sulfhydryl Modification of Protein

The PEG-hydrogels were formed under a controlled and specific crosslinking chemistry. We adapted the PEG functionalized with vinyl sulfone (VS) groups, depicted from J. Hubbell's work (Hubbell and Lutolf, 2003). Since PEG-VS reacts specifically with free thiols, a PEG-VS crosslinker was developed by functionalizing PEG with thiol groups (or sulfhydril, SH), to yield a fully hydrophilic and inert hydrogel with a rapid and highly specific crosslinking chemistry (Zustiak and Leach, 2010). Peptides and other biomolecules, such as laminin, can be modified to crosslink with the PEG gels. This may be done by reacting the biomolecule with SATA (N-Succinimidyl S-Acetylthioacetate) or SATP (N-Succinimidyl S-Acetylthiopropionate), which are reagents used to introduce SH groups into proteins, peptides and other molecules. The presence of the SH groups in the biomolecule will allow its crosslinking with the PEG-VS backbone of our gels. For this project we chose SATP since it provides more steric freedom for the unprotected sulfhydryl group (Figure 31).

The preparations of the various solutions needed for the following procedures can be found in Appendix 2.

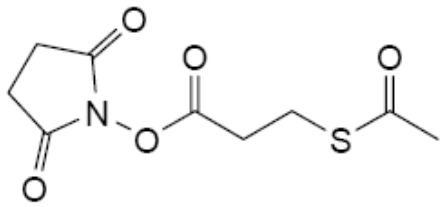

Figure 31: Molecular structure of SATP.

The steps to perform this modification, according to the manufacturer's instructions, are as follows (Pierce Biotechnology, Inc., 4/2004).

A. Reaction of Protein with SATA or SATP

1 - Immediately before reaction, dissolve 6-8 of SATA/SATP in 0.5 mL of Dimethylsulfoxide (DMSO) - resulting in ~55 mM solution.
2 - Combine 1.0 mL of Protein solution (Appendix 1) with 10 µL of the SATA/SATP solution. Mix contents and incubate at room temperature for 30 minutes.

Note: The level of sulfhydryl incorporation may be altered by using different molar ratios of SATA to protein. This default reaction uses a 9:1 molar ratio of SATA to protein. More complete acylation of all primary amino groups will occur when larger molar excesses of SATA are used; however, higher levels of acylation correspond to greater risk of protein inactivation. Increase or decrease the amount of SATA in the reaction by adding more or less than 10 µl of the SATA solution per ml of Protein Solution.

B. Desalt to Purify Acylated Protein from Excess Reagent and By-Products

1 - Equilibrate and operate a desalting column, collecting separate fractions of 1 mL each as they emerge from the column.
2 - Identify fraction(s) that contain protein by measuring for those having peak absorbance at 280 nm. Pool fractions that contain the protein.

Note: At this point, the modified protein may be stored indefinitely for later deacetylation and generation of sulfhydryl groups (Section C).

C. Deacetylate SATA-Modified Protein to Generate Sulfhydryl Groups

1 - Combine 1.0 ml of SATA-modified (acetylated) protein with 100 µl of the Deacetylation Solution.
2 - Mix contents and incubate reaction for 2 hours at room temperature.
3 - Use a desalting column to purify the sulfhydryl-modified protein from the Hydroxylamine in the Deacetylation Solution. Desalt into Reaction Buffer containing 10 mM of ethylenediaminetetraacetate (EDTA) to minimize disulfide bond formation using the same procedure as in Section B. Promptly use the prepared protein in the end application. Before or after desalting, the protein may be assayed for sulfhydryl content using Ellman's Reagent (see Related Pierce Products).

In Figures 32 and 33 is presented a schematic representation of the steps previously stated.

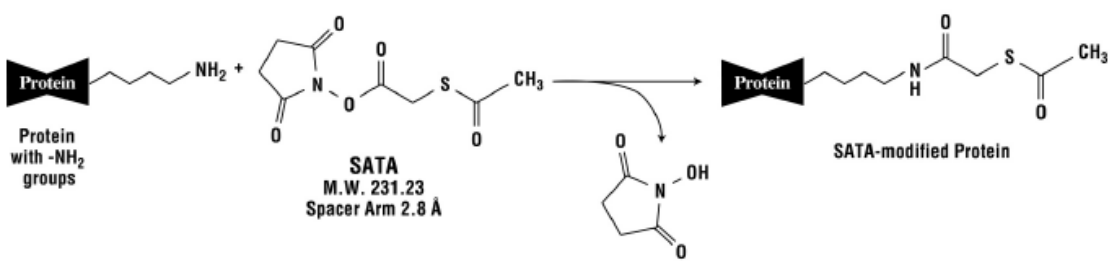

Figure 32: Step 1 – reaction of SATA with a primary amine (present in the protein) (Pierce Biotechnology, Inc., 4/2004).

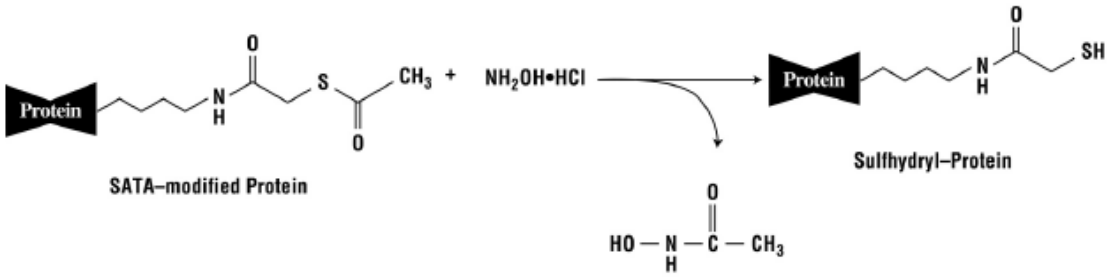

Figure 33: Step 2 – deprotection with hydroxylamine to generate free thiol groups (Pierce Biotechnology, Inc., 4/2004).

A1.2. Operate a PD-10 Desalting Column 3.5 mL

The procedure to equilibrate and operate a PD-10 desalting column of 3.5 mL, according to the manufacturer's instructions, is as follows (Amersham Biosciences, 2003):

1 . Cut off bottom tip, remove cap and pour off excess liquid.
2 . Equilibrate the column with approximately 25 mL of reaction buffer solution. Discard the flow through.
3 . Add sample of 2.5 mL (if the sample has a total volume that's less than 2.5 mL, add reaction buffer solution till a total volume of 2.5 mL is achieved). Collect flow through (this is due to the fact that some of the protein might already be leaving the column).
4 . Elute with 3.5 mL of reaction buffer solution. Collect flow through.

Appendix 2 Preparation of Solutions

A2.1. Reaction Buffer:

- Prepare 200-500 ml of PBS - 0.1 M phosphate, 0.15 M NaCl, pH 7.2-7.5

To prepare 1 L Phosphate Buffered Saline (PBS) solution with 10 mM phosphates:

8.0	G	NaCl
2.17	G	$Na_2HPO_4 \cdot 7H_2O$ (heptabasic)*
0.2	G	KCl
0.2	G	KH_2PO_4
1	L	Deionized water

(*) For instance $Na_2HPO_4 \cdot H_2O$ may be used instead of $Na_2HPO_4 \cdot 7H_2O$, as bellow.

Before completing the total volume of 1 L with deionized water, the pH of the solution should be adjusted first till it reaches a volue of 7.2-7.4. Depending of the pH value obtained before adjustment, acid or basic, NaOH or HCl solutions should be used to adjust, respectively.

So, for a PBS solution with a concentration in phosphates of 0.1 M and a 0.15 M concentration in NaCl, the quantities should be as follows:

$C_{NsCl} = \frac{n}{V} = 0.15\ M$ → 1 L total volume gives n = 0.15 mol

$m_{NsCl} = n_{NaCl} \cdot M_{NaCl} = 0.15 \cdot 58 = 8{,}7\ g$

$C_{phosphate} = 0.1\ M = \frac{n}{V = 1L} \longrightarrow n_{phosphate} = 0.1\ mol$

$n_{phosphate} = \frac{m_{1\ (Na_2HPO_4 \cdot H_2O)}}{M = 160} + \frac{m_{2\ (KH_2PO_4)}}{M = 136.1} \xrightarrow{TRIAL\ AND\ ERROR} m_1 = 13\ g\ and\ m_2 = 2.5\ g$

8.7	G	NaCl	M = 58	g/mol
13	G	$Na_2HPO_4 \cdot H_2O$	M = 160	g/mol
0.2	G	KCl		
2.5	G	KH_2PO_4	M = 136.1	g/mol
1	L	Deionized water		

- Reaction Buffer containing 10 mM EDTA – dissolve EDTA in water to give a final concentration higher than 10 mM and then dilute with PBS previously prepared to give the final concentration of 10 mM.

A2.2. Protein Solution:

- Dissolve protein to be modified in Reaction Buffer to a concentration of 60 μM (2-10 mg/ml). For an IgG with 150 kDa molecular weight, 60 μM corresponds to 9 mg/ml.

For BSA, example:

$$C_{BSA} = 60\ \mu M \quad \longrightarrow \quad \rho_{BSA} = 60 \cdot 10^{-6} \left(\frac{mol}{L}\right) \cdot\ 66\,382 \left(\frac{g}{mol}\right) = 3.98\ g/L$$

For a total volume of 5 mL of Protein Solution:

$$m_{BSA} = 3.98 \times 5 \times 10^{-3} \quad \longrightarrow \quad m_{BSA} = 0.01992\ g$$

A2.3. Deacetylation Solution:

- 0.5 M Hydroxylamine, 25 mM EDTA in PBS, pH 7.2-7.5.

For a total volume of 50 mL, and an available solution of EDTA with a concentration of 0.5 M:

$$C_{1\,EDTA} \cdot V_{EDTA} = C_{2\,EDTA} \cdot V_T$$

$$0.5 \cdot V_{EDTA} = 0.025 \cdot\ 50 \quad \longrightarrow \quad V_{EDTA} = 2.5\ mL$$

- Dissolve 1.74 g of hydroxylamine and 2.5 mL of EDTA in 40 mL of Reaction Buffer.
- Adjust pH with NaOH or HCl, depending if the solution obtained is acid or basic, respectively.
- Add ultrapure water until the final volume of 50 mL is achieved.

A2.4. 0.3 M Triethanolamine (TEA) Solution pH 8.0:

Prepare 50 ml of 0.3 M TEA solution pH 8. TEA is a biological solution that is not toxic to cells. This solution must be prepared under the fume hood!!!

- Add 40 mL of PBS buffer (10 mM, pH=7.4) to a glass bottle.
- Add 2 mL of TEA with a glass pipette. Keep in mind that the TEA solution is very viscous and so some may be lost in the pipette walls.
- Mix contents.
- Measure the pH of the solution (should be >10). Titrate with 6 M HCl solution to get it down to pH=8.0.
- Once the desired pH is achieved, add PBS till the final volume is reached. Use graduated cylinder to measure the exact volume.

Appendix 3 Other Work Conducted

A3.1. Rheological Results for Hydrogels Synthesized with PEG-SH 1 3.4 kDa

This section describes the results obtained for the rheology experiments for gels synthesized with 4-arm PEG-VS 10 kDa and PEG-SH 1 3.4 kDa, with and without physically incorporated laminin. Figure 34 and Table 6 present the mean storage modulus of each of the three types of gels (0%, 1% and 10% v/v of laminin).

Appendix 4 presents the gel loss modulus; a comparison of modulus values shows that G''< G' which is indicative that all the samples were gels (Zustiak and Leach, 2010).

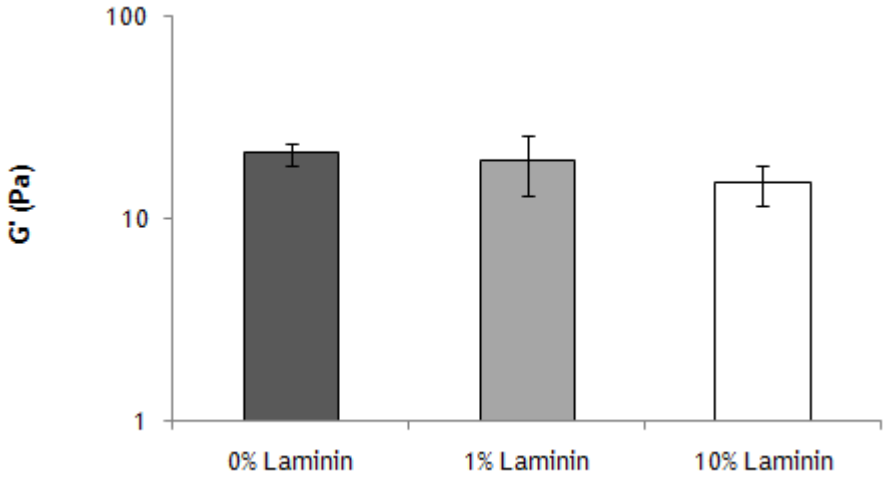

Figure 34: Representation of the storage modulus, G', of gels with 0%, 1% and 10% v/v laminin. Bars represent average ± standard deviation for n ≥ 3 samples.

Table 6: Results obtained for storage modulus (stiffness).

Laminin Concentration	0% v/v Laminin	1% v/v Laminin	10% v/v Laminin
G' (Pa)	20.8 ± 2.6	19.4 ± 6.5	14.8 ± 3.3

Unlike what happens with the PEG hydrogels prepared with PEG-SH 2 3.4 kDa, for these gels no difference was observed between them, indicating that the addition of laminin to the gels has no effect over their stiffness.

This result suggests that the gels prepared with PEG-SH 1 3.4 kDa, as they take less time to degrade, are less susceptible to the addition of laminin, thus not changing in any way their stiffness.

A3.2. Swelling Results for Hydrogels Synthesized with PEG-SH 1 3.4 kDa

This section describes the results obtained for the swelling experiments for gels synthesized with 4-arm PEG-VS 10 kDa and PEG-SH 1 3.4 kDa and physically incorporated laminin. Swelling ratio and mesh size are evaluated for gels with and without laminin.

Figure 35 and Table 7 show the results obtained for the gels without laminin and the gels with 1% and 10% v/v of laminin.

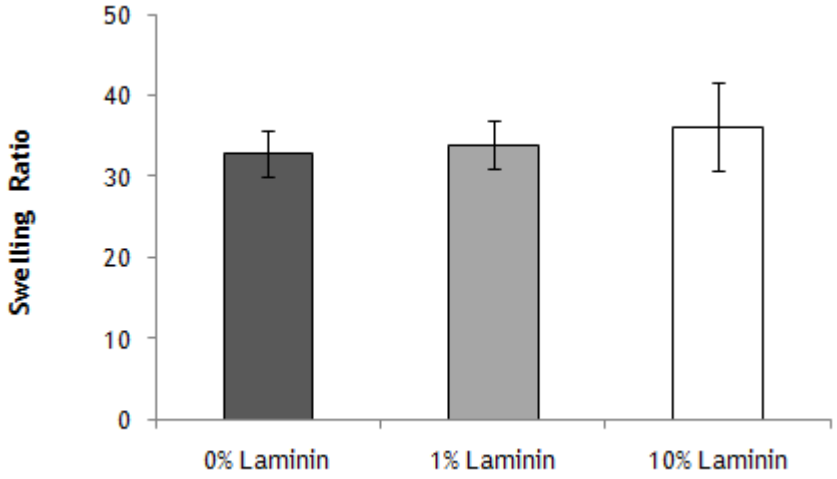

Figure 35: Representation of the swelling ratio of gels with 0%, 1% and 10% v/v laminin. Bars represent average ± standard deviation for n ≥ 3 samples.

Table 7: Results obtained for the different types of gels regarding swelling ratio.

Laminin Concentration	0% v/v Laminin	1% v/v Laminin	10% v/v Laminin
Q_m	32.9 ± 2.8	33.9 ± 3.0	36.1 ± 5.4

The mesh size was then determined using the same methods as for the gels with PEG-SH 2 3.4 kDa. Figure 36 and Table 8 present the mean mesh size for gels without laminin and the gels with 1% and 10% v/v of laminin.

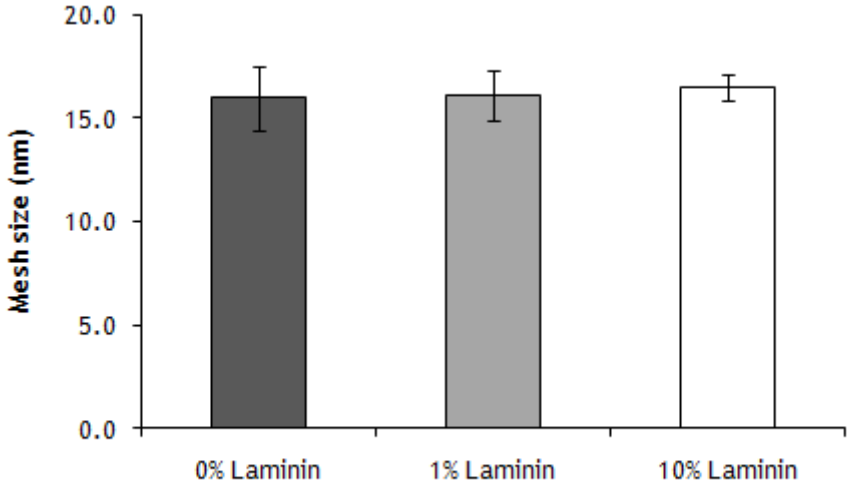

Figure 36: Representation of the mesh size of gels with 0%, 1% and 10% v/v laminin. Bars represent average ± standard deviation for n ≥ 3 samples.

Table 8: Results obtained for the different types of gels regarding mesh size.

Laminin Concentration	0% v/v Laminin	1% v/v Laminin	10% v/v Laminin
ξ (nm)	16.0 ± 0.7	16.1 ± 0.2	16.5 ± 1.1

As expected from the results obtained from the rheological experiments, there are no significant differences between the gels regarding the swelling ratio and consequently the mesh size. These results suggest that the degree of crosslinking of this type of hydrogels is not affected by the incorporation of laminin.

A3.3. Laminin Modification with SATP

We wanted to modify laminin with SH groups to then react with PEG-VS and determine the properties of the hydrogels. The protocol used is described in Appendix 1. We did some modifications to the protocol as follows. The protocol suggests a protein solution of 2-10 mg/mL should be used, which can be prepared by following the procedure presented in Appendix 2. However, since the laminin available was already in solution (in Tris-HCl buffer), with a concentration of 1 mg/mL, the protein solution was not prepared and the concentration used for the calculations was that laminin came in. The laminin amount used corresponded to 1.23 nmol which is under the amount recommended for a successful modification of protein with SH groups. In Table 9 are presented the results obtained for absorbance after the first desalting step.

Table 9: Results obtained for absorbance at 218 nm, to determine which fraction(s) contained the protein.

Fractions	Absorbance at 280 nm
1	0.9799 ± 0.0175
2	0.1086 ± 0.0006
3	2.1306 ± 0.0014
4	0.1373 ± 0.0008
5	0.1210 ± 0.0004
6	0.1324 ± 0.0000

Table 9 indicates that fractions 1 (before purging the column) and 3 (after purging the column) contained most of the protein. Since laminin is a big molecule (MW 800 – 900 kDa), it is expected to elute in the first fractions, due to the fact that smaller molecules are retained by the column. This may be explained by the fact that the resins used in desalting columns are chosen to ensure that macromolecules, such as proteins, are eluted at the void volume of the column, and so, low molecular weight molecules, such as salts, are eluted much later (Copland, 2000).

For the next steps of the experiment, the six fractions were pooled into two samples, one containing fractions 1 and 3 (sample 1), and the other one containing fractions 2, 4, 5 and 6 (sample 2). After the desalting step, the Ellman's Reagent test was performed on the fractions obtained, and then their absorbance was measured to determine which one(s) contained the modified protein.

Table 10: Results obtained for absorbance at 412 nm step, to determine which fraction(s) contained the modified protein.

Fractions (sample 1)	Absorbance at 412 nm	Fractions (sample 2)	Absorbance at 412 nm
1	0	1	0
2	0	2	0
3	0	3	0
4	0	4	0
5	0	5	0
6	0	6	0

As shown in Table 10; all absorbance values were zero, meaning that no modified protein was detected. The fact that the modified protein was not detected may be due to the buffer, Tris-HCl, contains a primary amine. These primary amines in the buffer will compete with the amines present in laminin when the reaction with SATP takes place. Another reason that the

reaction was unsuccessful may be the fact that the concentration of laminin used for the experiment was much lower than the one recommended by the manufacturer, and so it may have not been sufficient to react with the SATP.

We have also tried with higher concentrations of laminin using a synthetic laminin peptide from Millipore (Synthetic Laminin Peptide for Rat Neural Stem Cells, Millipore, Billerica, MA) without successful results. These results may be explained by the relative accessibility of the primary amines, if the amines are protected by protein chains they are more difficult to access thus decreasing the degree of modification (Hermanson, 2008).

A3.4. BSA Modification with SATP (Test)

To determine the possible causes for the reaction not being successful, the procedure was repeated with another protein, Bovine Serum Albumin (BSA, 59.96 nmol). This experiment addresses the problems observed previously as we increased the amount of protein and used a protein in powder form (e.g. no mixed buffers), as recommended in the modification protocol. The steps for the modification were the same as for the laminin.

Table 11: Results obtained for the absorbance at 218 nm step, to see which fraction(s) contained the protein.

Samples	Absorbance at 280 nm
1	0.0090 ± 0.0003
2	0
3	0
4	0
5	0.3013 ± 0.0054

Table 11 shows the results obtained for the absorbance after the first desalting step; no protein was detected in fractions 2, 3 and 4, and some was detected in fraction 5. This may indicate that some of the protein may have still remained in the desalting column, and more buffer solution should have been used to purge the column and a sixth fraction should have been collected. The main reason for assuming that some of the protein still remained at the column is because of the difference in molecular weights between laminin and BSA, 800-900 kDa and 60 kDa, respectively, and so it is a good assumption to predict that BSA will have a longer elution time than laminin.

Fraction 3 was then used in the next steps of the experiment. Even though fraction 1 had shown to have a positive value of absorbance it was discarded due to the fact that the value was very small, and it was assumed to be of little significance for the rest of the experiment. Once again, after the final desalting step, the Ellman's reagent test was performed on the fractions obtained and their absorbance at 412 nm was then measured to see, like when with laminin, which one(s) contained the modified protein.

Table 12: Results obtained for the absorbance at 412 nm step, to see which fraction(s) contained the modified protein.

Fractions	Absorbance at 412 nm
1	0.0002 ± 0.0000
2	0
3	0.0044 ± 0.0002
4	0.0017 ± 0.0000
5	0.0046 ± 0.0000
6	0.0115 ± 0.0001

The results may be consulted in Table 12; because all samples, except for sample 2, presented positive values of absorbance, the pooled fraction contained modified protein. The absorbance values were low, but may be explained by the fact that the sample used for this step contained a small amount of BSA protein.

Another assumption can be made from our results, which is the fact that previously the SATP may have indeed reacted with the amines in the Tris-HCl buffer, significantly reducing the reaction with the amines present in the laminin.

To overcome this problem, a thorough search was made to find another source of laminin such that it was more concentrated or was supplied as a dry powder. We found a promising product, consisting in an engineered synthetic peptide, supplied in a dry form, that is specifically for studies with neural stem cells and mimics the function of laminin. The next step was to modify this product with sulfhydryl groups.

Appendix 4 Additional Information

A4.1. Pictures from Rheological Experiments

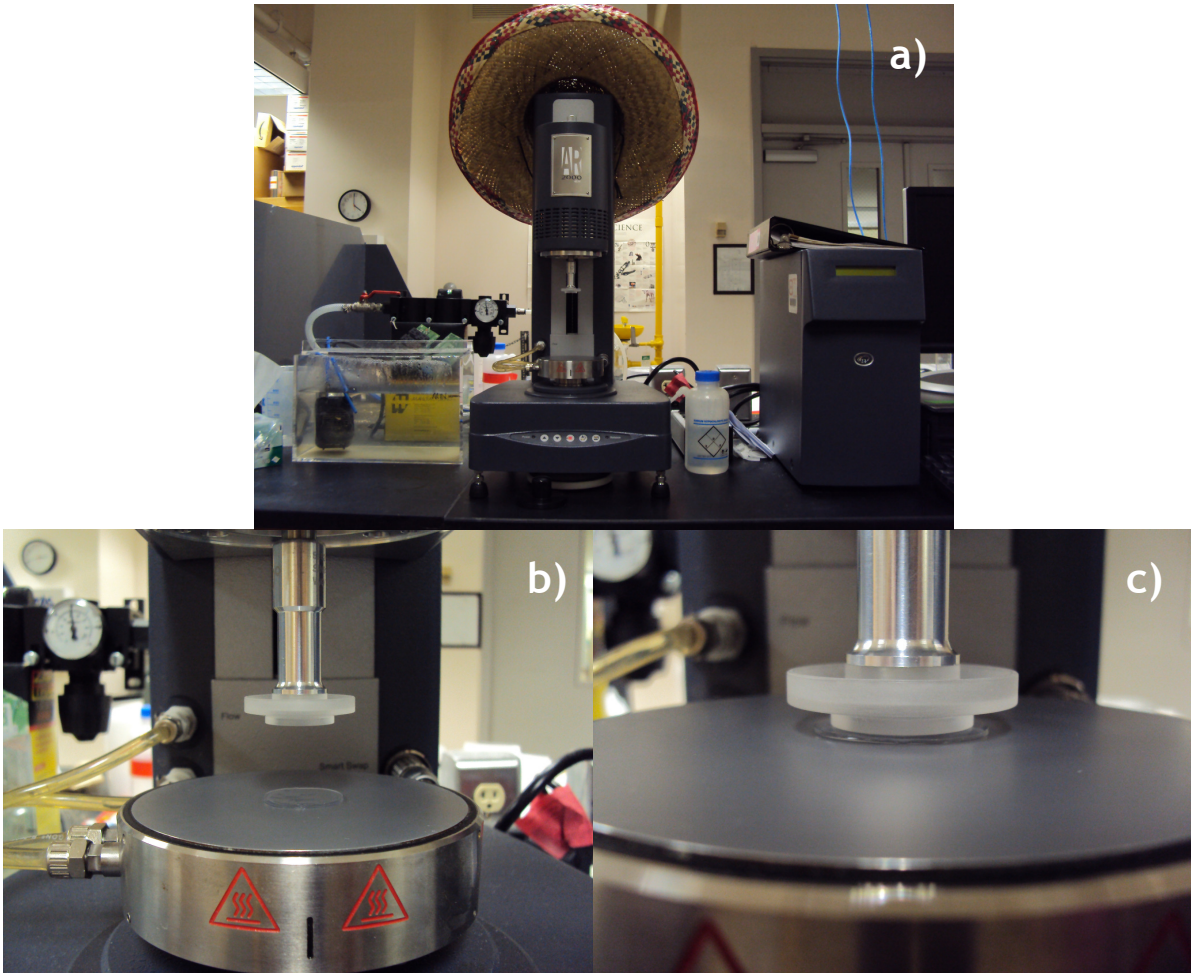

Figure 37: Pictures of (a) the type of rheometer used and (b,c) placement of the hydrogel on the bottom plate of the rheometer.

A4.2. Rheology Results: PEG-SH 2 3.4 kDa

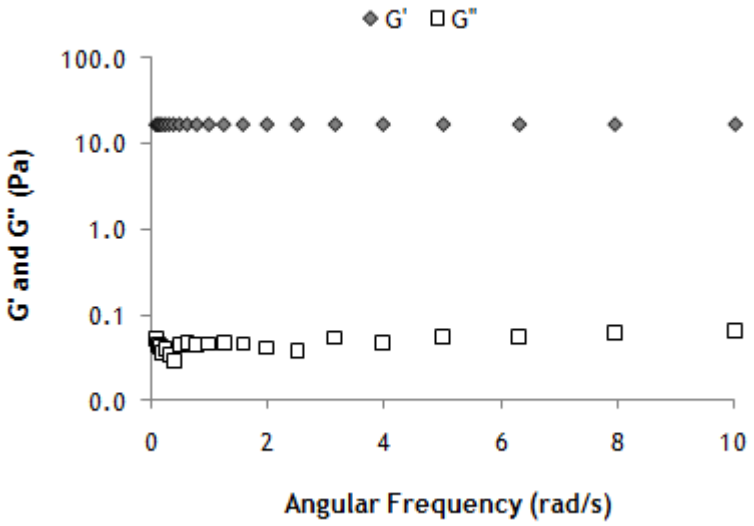

Figure 38: Representation of G' and G'' versus angular frequency, for gels without laminin.

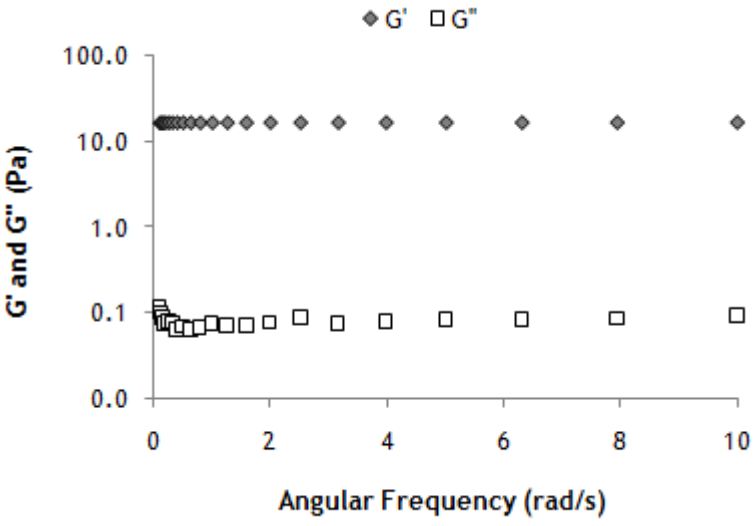

Figure 39: Representation of G' and G'' versus angular frequency, for gels with 1% v/v of laminin.

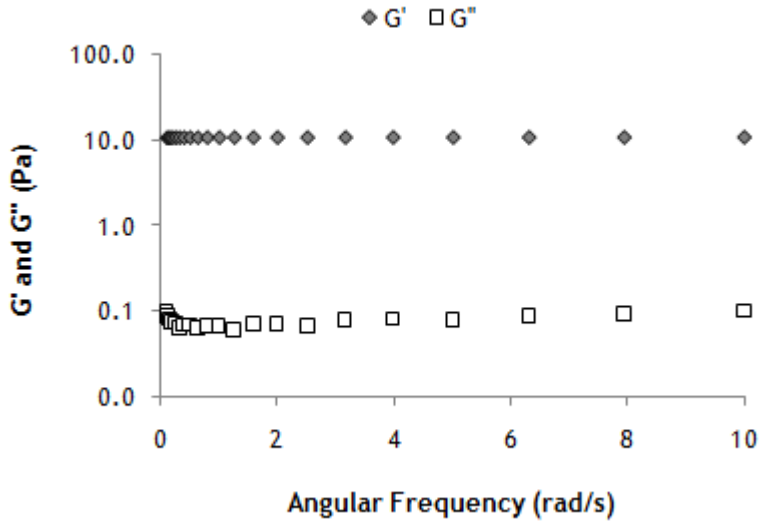

Figure 40: Representation of G' and G'' versus angular frequency, for gels with 10% v/v of laminin.

A4.3. Rheology Results: PEG-SH 1 3.4 kDa

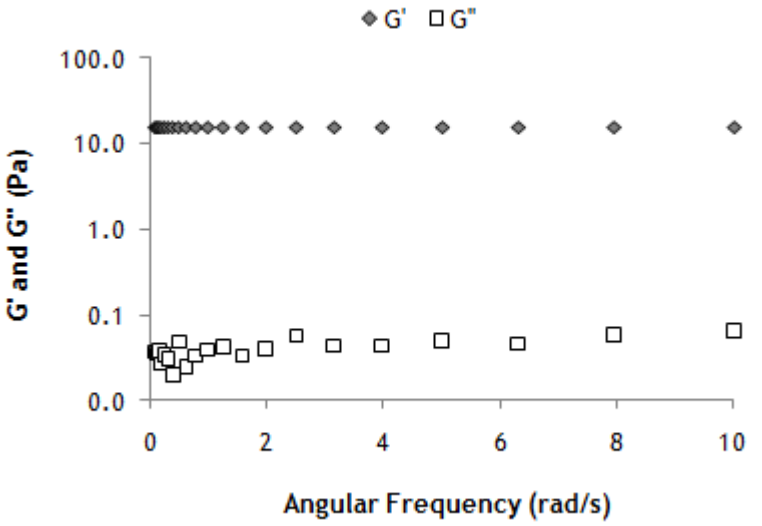

Figure 41: Representation of G' and G'' versus angular frequency, for gels without laminin.

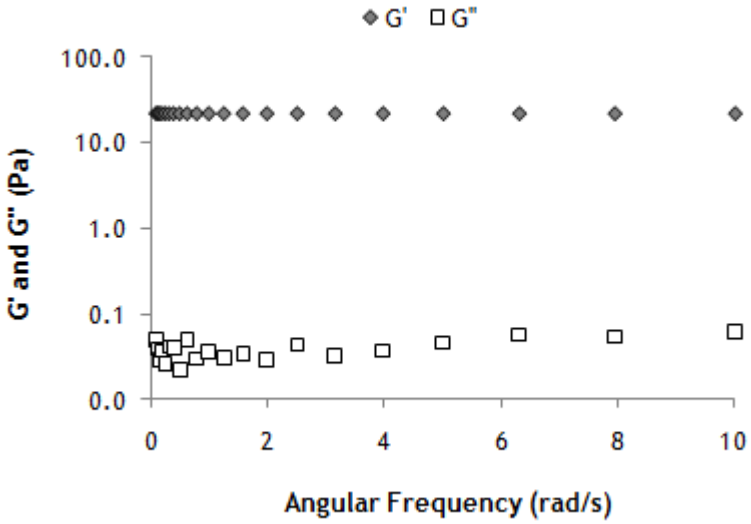

Figure 42: Representation of G' and G'' versus angular frequency, for gels with 1% v/v of laminin.

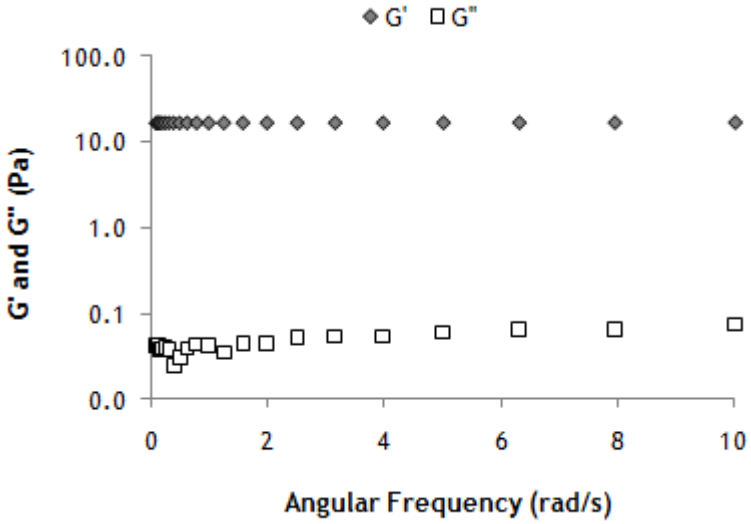

Figure 43: Representation of G' and G'' versus angular frequency, for gels with 10% v/v of laminin.

A4.4. Rheology Results: PEG-SH 2 3.4 kDa plus NSPCs

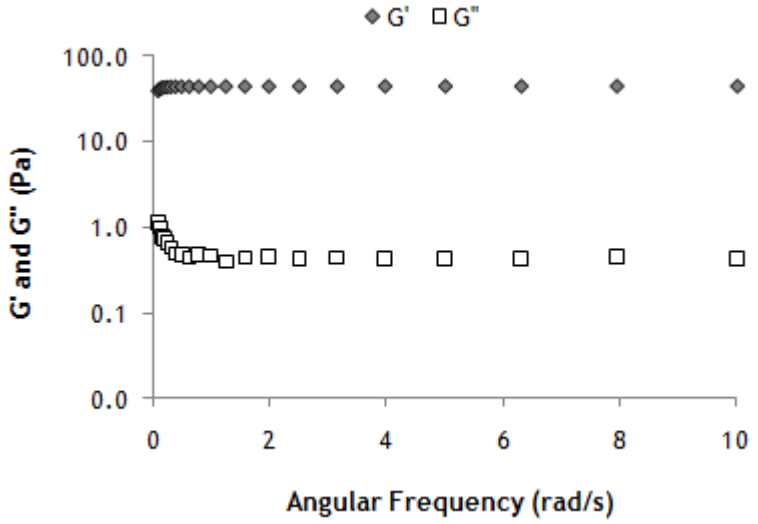

Figure 44: Representation of G' and G'' versus angular frequency, for gels without laminin.

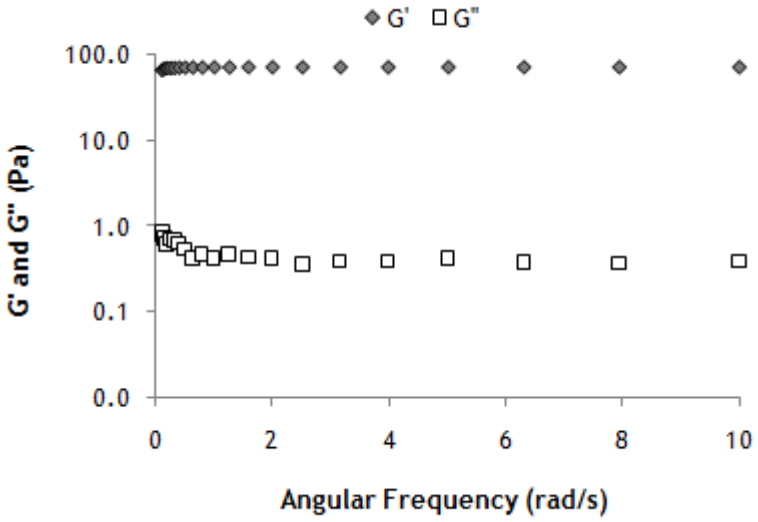

Figure 45: Representation of G' and G'' versus angular frequency, for gels with 1% v/v of laminin.

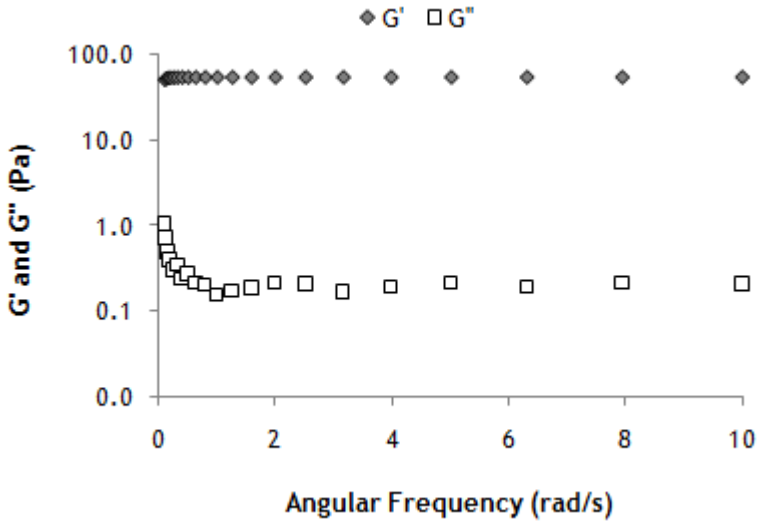

Figure 46: Representation of G' and G'' versus angular frequency, for gels with 10% v/v of laminin.

A4.5. Pictures from Analysis of PEG-Laminin Hydrogels as NSPCs Delivery Devices

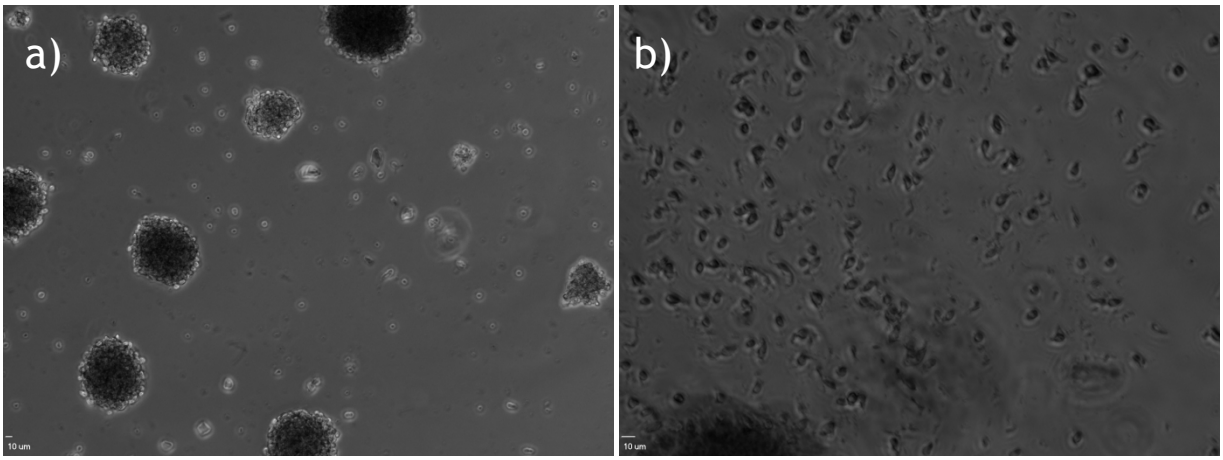

Figure 47: Pictures of (a) neurospheres inside PEG hydrogels with 1% v/v laminin and (b) NSPCs leaving a neurospehere inside PEG hydrogels with 1% laminin.

Appendix 5 Journal Club Presentation

Characterization of Poly(ethylene glycol) Gels With Added Collagen for Neural Tissue Engineering

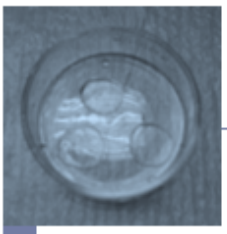

Journal Club Presentation - UMBC

BS/MS in Chemical Engineering

Presented By: Helena Gaifem 04/12/10

Index

- Introduction
- Materials and Methods
- Results
- Conclusions

2

Introduction

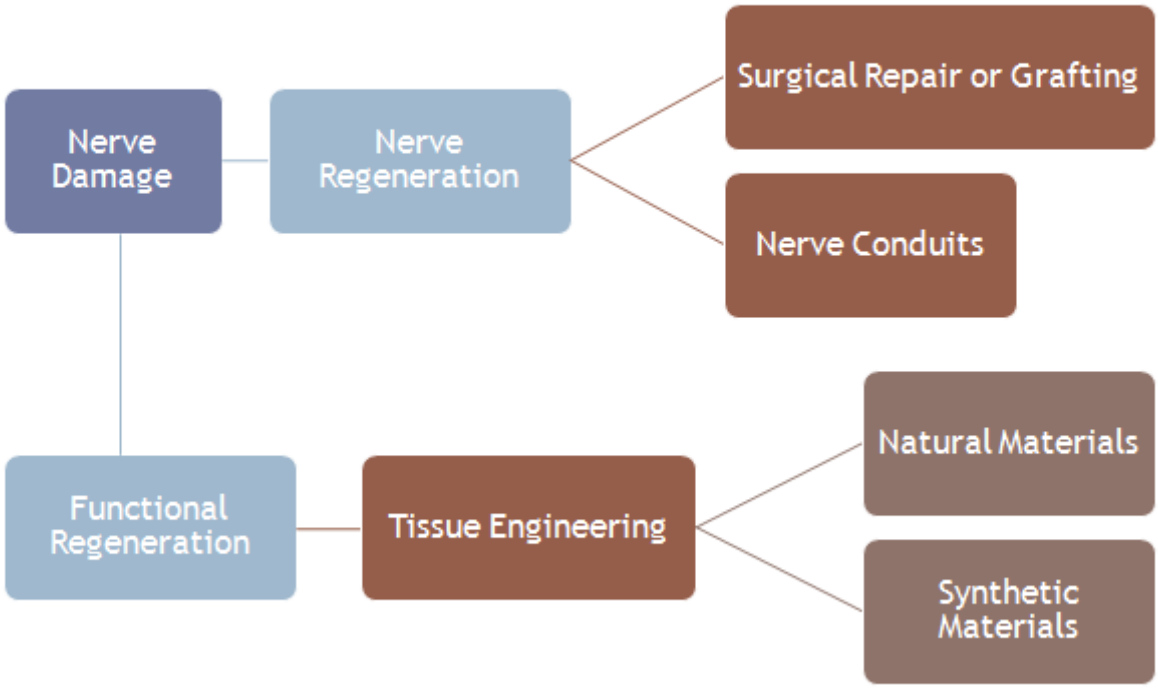

3

Materials and Methods

Materials:

- PEG-collagen conjugate - covalently biding NHS groups (in acryl-PEG-NHS) to amines in collagen (4 NHS: 1 collagen).

Mechanical testing of PEG-collagen conjugate gels:

- PEG gels made with 3%, 4% and 5% w/w PEG-DA, Irgacure 2959 and DI H_2O.
- PEG-conjugate gels made with varying concentrations of PEG-DA (3%, 4% and 5% w/w) and PEG-protein conjugate (0.1, 1 and 10 µg/mL).
- G* (mechanical stiffness) ⟹ rheology $|G^*| = \sqrt{(G')^2 + (G'')^2}$

4

Materials and Methods

- Mechanical testing of PEG-NHS conjugate gels:
  - Acryl-PEG-NHS was added to the gels in the same molar amount as the collagen conjugate, for example:

1 µg of collagen conjugate (~12.4 mmoles) added per mL of gel

then 12.4 mmoles of Acryl-PEG-NHS was added for this testing

- Swelling of PEG-collagen conjugate gels:
  - Swelling capacity calculated by: $\%C = \frac{W_{wet} - W_{dry}}{W_{wet}} \times 100$

5

Materials and Methods

- Spatial distribution of protein conjugate:
  - To label the protein calculated amounts of PEG-NHS and collagen were mixed with fluorescent dye.
  - PEG-protein conjugate solutions: 5% w/w PEG-DA, fluorescently labeled protein conjugate (0.1, 1 and 10 µg/mL), Irgacure and F12K.
  - Gels were imaged at top, middle and bottom at three separate locations of each gel.
  - 5% PEG gels used as controls to set the exposure level.

6

Materials and Methods

- PC12 neurite expression on PEG collagen or PEG-collagen conjugate gels:
  - PEG-DA (3, 4 and 5%), Irgacure and F12K.
  - Collagen or PEG-collagen conjugate was added to the gels at concentrations of 0, 10, 100 or 500 µg/mL. All solutions (except 500 µg/mL) crosslinked for 360 s (6 min.) under UV light.
  - 500 µg/mL did not permit gelation ⟹ concentration too high
  - PC12 cells cultured with NGF.

7

Materials and Methods

- Neurite extension of partially dissociated DRG on PEG collagen or PEG-collagen conjugate:
  - PEG gels made the same way as for the PC12 cells.
  - DRG partially dissociated with 1x trypsin for 10 min.
  - 3 partially dissociated DRG seeded per gel with NGF.
  - Percent of DRG extending compared to total number of DRG examined.

8

Results

Mechanical Testing of PEG-gels

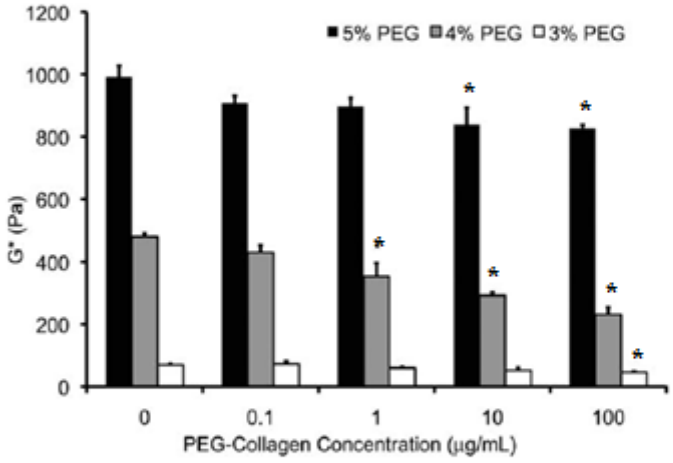

Figure 1. Stiffness (as represented by G*) of the PEG-collagen conjugate gels. The G* was determined for each gel at 10 rad/s and averaged. Error bars represent standard error and * represents statistical difference from plain gels.

- G' > G'' ⟹ gels
- Difference between 3, 4 and 5% PEG-DA
- > Concentration of conjugate < G*
- PEG-NHS gels - no significant difference when compared with PEG-collagen conjugate gels.

9

Results

Swelling of PEG-gels

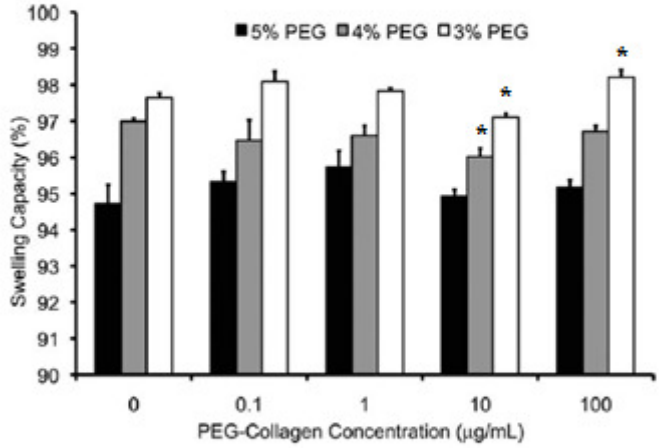

Figure 2. Swelling capacity of PEG-collagen conjugate gels. Error bars represent standard error and * represents statistical difference from plain gels.

- < PEG-DA concentration
  > Swelling capacity

10

Results

Spatial Distribution of Protein Conjugate

Table 1. Average Fluorescence Levels of PEG-Collagen Conjugate Gels.

	5% PEG-DA		
Location in Gel	100 μg/mL PEG-Collagen	10 μg/mL PEG-Collagen	0 μg/mL PEG-Collagen
Top	0.129 ± 0.013	0.023 ± 0.004	0.002 ± 0.002
Middle	0.112 ± 0.016	0.020 ± 0.003	0.004 ± 0.002
Bottom	0.087 ± 0.014	0.020 ± 0.004	0.002 ± 0.002

- Collagen molecules positioned homogeneously throughout the gel
- > Concentration of PEG-collagen conjugate > Average fluorescence level
- No difference between average fluorescence levels at top, middle or bottom.

11

Results

PC12 Neurite Expression

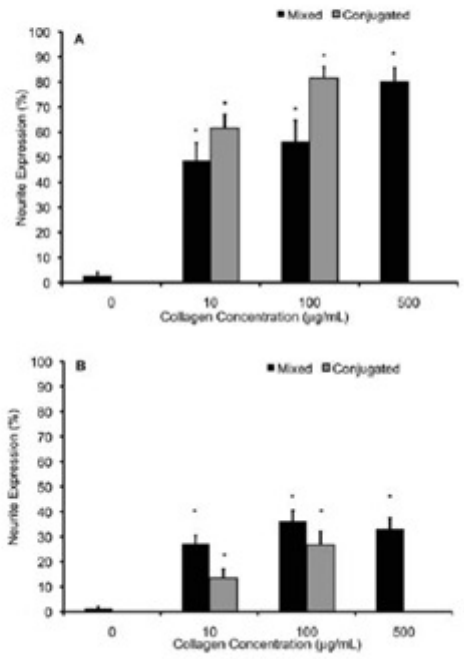

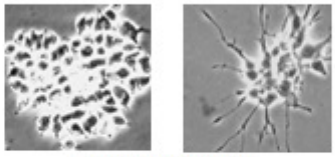

www.roberts.ca/smeskin/

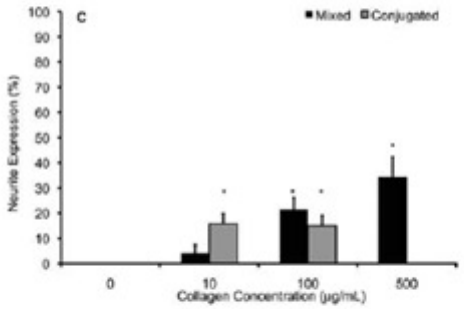

Figure 3. Percent neurite expression of PC12 cells in (A) 3%, (B) 4%, and (C) 5% PEG gels with added collagen or PEG-collagen conjugate. No expression was found on any 5% plain gels. Error bars represent standard error and * represents statistical difference from plain gels.

12

Results

Partially Dissociated DRG Extension

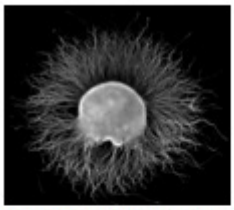

http://en.wikipedia.org/wiki/Dorsal_root_ganglion

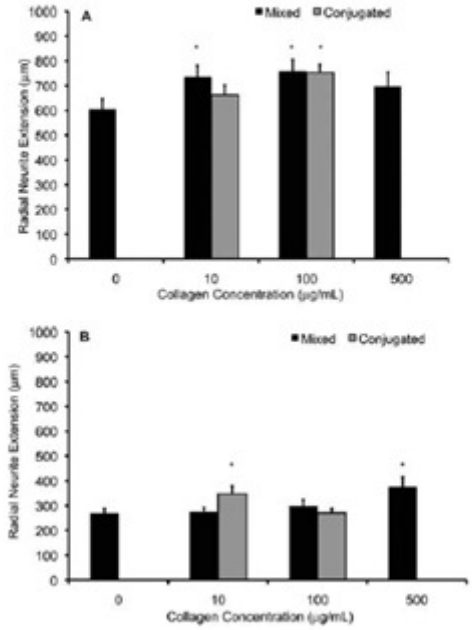

Figure 4. Radial neurite extension of partially dissociated DRG (A) 3%, (B) 4% and (C) 5% PEG gels with added collagen or PEG-collagen conjugate. Error bars represent standard error and * represents statistical difference from plain PEG gels.

13

Conclusions

- > concentration of PEG-DA > gel stiffness
- Addition of protein conjugate < gel stiffness

  protein conjugate terminates the growing PEG chain
- Storage modulus compared with molecular weight between entanglements (M_e):

$$G' = \frac{p R T}{M_e}$$

- Mesh size calculated by:

$$\xi = l C_n^{0.5} n^{0.5} V_{2,S}^{0.33}$$

Table 2. Storage modulus, molecular weight between entanglements, and mesh size of PEG-gels.

[PEG-DA]	G' (Pa)	$M_e \times 10^6$ (g/mol)	ξ (μm)
5%	992.24	3.02	0.19
4%	479.97	6.25	0.30
3%	63.96	46.90	0.92

14

Conclusions

- Both collagen concentration and PEG-DA concentration influenced overall neurite expression.
- Although increased expression was noted at 100 µg/mL in 3% PEG-DA, it was not seen at other concentrations - not the primary mechanism for neurite expression.
- Neurite expression higher at lower concentrations of PEG-DA - lower concentrations better promote neurite expression.

15